A WATER CHANNEL (AQP9) IN RETINAL GANGLION CELL APOPTOSIS AND GLAUCOMA

by

MING-HUI YANG

Bachelor of Science, 2000
University of Central Oklahoma
Edmond, Oklahoma

Master of Science, 2003
University of Texas at Dallas
Dallas, Texas

Submitted to the Graduate Faculty of the
College of Science and Engineering
Texas Christian University
in partial fulfillment of the requirements
for the degree of

Doctor of Philosophy

May 2007

ACKNOWLEDGMENTS

TABLE OF CONTAINS

iv

VITA

ABSTRACT

LIST OF FIGURES

LIST OF TABLES

INTRODUCTION

Water transport

Water is the best solvent and the main component of living cells. Water transport through tissue barriers and plasma membranes was assumed to be by simple diffusion until water channels were discovered. Diffusion happens in all biological membranes, but water channels exist in a subset of epithelia with higher water permeation capacity than can be produced by diffusion. Diffusion and water transport through water channels (aquaporins, AQPs) are bi-directional and driven by osmotic gradients.

Osmotic gradients allow water molecules to pass through water channels in the membrane to equalize the osmotic pressure. All channel proteins control the membrane permeability by one of these methods: (1). Regulation of the open probability, which is the fraction of time the channel spends in the open state; (2). Regulation of the channel permeability by affecting open/ close state gating, which is the most common method for ion channel protein actions as all or none; (3). Regulation of the number of channel-forming proteins in the plasma membrane by affecting exocytosis or endocytosis, a method associated with AQP2 changes in the kidney (Borgnia et al., 1999). The water permeability of AQP0 in lens is regulated by either gating the pore or by alteration of the open-pore water permeability (Varadaraj et al., 2005). In addition, water channels, such as AQP1 in thymocytes, may have post-translational modifications because these channels were found on the cell surface without the ability to function (Jablonski et al., 2004). At the present time, it is difficult to generalize how aquaporins regulate membrane permeability to alter cellular function. In particular, do they participate in cell survival and/or cell death mechanisms?

Discovery of water channels

The lipid bilayer structure was discovered in the 1920s. Then ion channels, exchangers and co-transporters were discovered in the 1950s. After decades of exploring cell membranes and solute transmembrane movements, a water transporter was reported and renamed as aquaporin-1 by Preston et al. (1992).

The identification of water channels allowed for a better understanding of water transport in tissues. The first aquaporin was discovered during the study of the red blood cell Rh group antigens (Agre et al., 1987). A 28-kDa polypeptide was found as part of a tetrameric integral membrane protein (homotetramer) and was abundant in red blood cells and renal proximal tubules (Denker et al., 1988). It was named "CHIP28" as "channel-like integral protein of 28 kDa" before being officially named "aquaporin-1" (AQP1) in 1997 (Agre et al., 1993, 1997). This protein's cRNA was injected into Xenopus laevis oocytes, which do not express any water channel and are water impermeable, in order to express the water channel in this cell. Under hypotonic conditions, the oocytes expressing AQP1 swelled and exploded while control oocytes showed no effect (Preston et al., 1992). This demonstrated that the protein AQP1 was transporting water.

Water channels have been reported in vertebrates, invertebrates, plants, eubacteria and archebacteria (Agre et al., 2002). Aquaporins appear to play important roles in normal physiology and pathophysiology. However, Tanghe (2006) reported that aquaporins are more abundant in eukaryotes (67 % of 33 species) than in prokaryotes (26 % of 193 species). Interestingly, the only major intrinsic protein (MIP), a membrane protein, expressed in *Schizosaccharomyces pombe*, a species of yeast, does not function as an aquaporin (Tanghe et al., 2006). Aquaporins, therefore, may not be essential for basic cellular function for

microbial survival. So far, thirteen human aquaporins have been reported (Castle, 2005), although not all their functions are known.

Structure of water channels

Due to the difficulties in collecting pure water channel proteins in large quantities, X-ray crystal structures are only available for AQP1 (Sui et al., 2001), AQP0 (Harries et al., 2004), and the bacterial glycerol-transporting Glpf channel (Fu et al., 2000). The structure of AQP1 is widely discussed as the common structure for aquaporins. AQPs are hydrophobic membrane proteins and AQP1 contains two tandem repeats, each formed from three transmembrane domains with a highly conserved loop containing an asparagine-proline-alanine (NPA) motif (Yamamoto et al., 2001). These repeats orient to each other with point symmetry. The molecular structure of each AQP1 subunit has been likened to "the hour glass model" because loops B and E fold and touch each other midway through the bilayer (Jung et al., 1994). This is shown in Fig. 1. Each monomeric aquaporin unit has a functional pore, but monomers are assembled in membranes as tetramers as shown in Fig. 2 (Verkman, 2005). This characteristic is very different from tetrameric ion channels, which form a central functional pore.

The narrowest diameter of the pore of aquaporins is 2.8 Å (Murata et al., 2000). This can barely fit a water molecule. In addition, the transmembrane domains are mostly hydrophobic with NPA (Asparagine-Proline-Alanine) regions. These two polar asparagines (N76 and N192) form hydrogen bonding with water molecules while other residues repel protons. Water molecules pass through the pore in a single file as hydrogen bonds formed between water molecules are broken and reformed with asparagines, and broken again to

reform with water molecules. Thus, aquaporins use space, electrostatic interactions, and hydrogen bonding to control water movement through the pore. This explains the highly effective water transport function.

Water channel classification and distribution in eyes

Researchers used homology cloning technology to identify members of the aquaporin family. There are two classes of aquaporins. AQP1, AQP2, AQP4, AQP5, and AQP8 are mainly for water-selective transport. Aquaglyceroporin is another name for other water channels having the ability to transport small solutes (e.g. glycerol) in addition to water. This class includes AQP3, AQP7, AQP9, and AQP10. AQP0 and AQP6 have low water permeability and are not permeable to glycerol. The degree of water and glycerol permeability of AQP11 and AQP12 are unknown (Castle, 2005). Five aquaporins have been reported in human eyes. (Agre et al., 2002): (1). AQP0, lens major intrinsic protein (MIP), may be a cell-to-cell adhesion protein, but its linkage to cataracts has been identified (Berry et al., 2000). (2). AQP1 protein was found in tissues with secretory roles including cornea, ciliary body, trabecular meshwork, lens, non-pigment epithelium, retinal photoreceptor cells, choroid plexus, and corneal endothelium (Verkman, 2005). Corneal transparency is controlled by the corneal endothelium's salt and water movements. Thus, AQP1 may be involved in corneal edema (Thiagarajah and Verkman, 2002). (3). AQP3 is localized in conjunctiva and corneal epithelium (Levin and Verkman, 2004). (4). AQP4 is abundant in ciliary epithelium and astroglial cells of retina (Nagelhus et al., 1998). (5). AQP5 is in conjunctiva, cornea and lacrimal gland epithelia and may be linked to dry eye (Oen, 2006; Nagelhus, 1998; Delporte and Steinfeld, 2006). Fig. 3 shows the distribution of aquaporins in

the human eye. In addition to these aquaporins, our results show that AQP9 is also expressed in retina.

Water channel physiology and pathophysiology

Aquaporins appear to be involved in normal and abnormal mammalian physiology. AQP0 appears to be only expressed in eyes, but AQP1 is expressed in red blood cells, lung, kidney, brain, eye, and vascular endothelium. AQP1 null individuals appear to function normally under regular conditions. Such patients may be protected against acute onset pulmonary edema (Agre et al., 2002), but under thirsting and chronic fluid overload, AQP1 null humans do not have the full capability to efficiently generate concentrated urine and would have difficulty to rapidly dissipate edema by returning fluid to the vascular space (King et al., 2001). AQP1 is also proposed to play an important role in lung water clearance at birth (Zelenina et al., 2005). That may explain the difficulties in finding AQP1-null human subjects. AQP1 knockout mice have reduced intraocular pressure (IOP) (Zhang et al., 2002) and impaired corneal transparency after swelling (Thiagarajah and Verkman, 2002). Using primary cultures of corneal endothelial cells lacking AQP1, it was shown that these cells have reduced water permeability and impaired cell volume regulation (Kuang et al., 2004). AQP-1 deficient mice, however, have a better survival rate following implantion of a tumor (Saddoun et al., 2005)

AQP2 is only expressed in kidney. Individuals having mutations in AQP2 are patients with hereditary genetic disorder nephrogenic diabetes insipidus (NDI) (Nguyen et al. 2003). AQP2 expression is controlled by vasopressin. As a result, these patients produce dilute urine (up to 20 L per day) (Nguyen et al., 2003). AQP2 upregulation is found to be related to

secondary water retention causes, such as pregnancy, cardiac failure, and liver cirrhosis (Schrier et al., 1998).

AQP3 is expressed in kidney, lung, eye, skin, and gastrointestinal tract (Ecelbarger et al., 1995; Nielsen et al., 1997a; Hamann et al., 1998; Hurley et al., 2001; Nejsum et al., 2002) and is also an aquaglyceroporin. Its water permeability can be reduced with high acidity (Zeuthen et al., 1999) while its glycerol transport function may work on skin hydration, skin barrier (Ma et al., 2002) and wound healing (Hara et al., 2002). In addition, both AQP3 and cystic fibrosis transmembrane regulator (CFTR) may have a role in the regulatory defect in cystic fibrosis (Schreiber et al., 1999).

AQP4 is expressed in kidney, brain, retina, lung, and muscle (Jung et al., 1994; Ma et al., 1997; Nagelhus et al., 1998; Frigeri et al., 1998; borok and Verkman, 2002). AQP4 is abundant in osmosensory regions of brain and retina, and their importance will be discussed in detail in another section. AQP4 null mice have a mild urinary concentrating defect (Chou et al., 1998) and AQP4 may play a minor role in airway humidification (Song et al., 2001). AQP4 abnormal expression in mdx mice may be related to muscular dystrophy (Frigeri et al., 2001).

AQP5 is expressed in salivary, lacrimal, and sweat glands, lung, and eye (Delporte and Steinfeld, 2006; Nielsen et al., 1997a; Verkman, 2003). The symptom of Sjögren's syndrome, deficiency of fluid secretion, maybe due to abnormal distribution of AQP5 expression (Steinfeld et al., 2001). AQP5-null mice have reduced secretion from submucosal gland, and AQP5 may help regulate the viscous fluid secretions in cystic fibrosis (Song and Verkman 2001). Borok and Verkman (2002) proposed a therapeutic strategy that uses AQP5 activation to reduce fluid secretion in bronchitis and rhinitis.

AQP6 is expressed in kidney exclusively (Agre et al., 2002; Agre, 2004). AQP6 is a very interesting water channel protein; when other aquaporins are inhibited by mercuric chloride (e.g. AQP1, AQP2 and AQP5), low concentrations of $HgCl_2$ can increase the water permeability of AQP6 (Yusui et al., 1999a). In addition, AQP6 is believed to participate in acid-base mechanisms (Promeneur et al., 2000). AQP6 knockout mice are available now, but no data are reported yet (Verkman, 2005).

AQP7 has high water permeability as well as being permeable to glycerol, similar to AQP3. AQP7 is expressed in kidney, testis, and adipose tissue (Ishibashi et al., 1994, 1997; Kuriyama et al., 1997). Its importance in kidney and testis is unknown. AQP7 can transfer glycerol from adipose tissue to the plasma (Kuriyama et al., 2002), so individuals with AQP7 genetic defects are unable to elevate plasma glycerol during exercise (Kondo et al., 2002). In addition, AQP7-null mice had a remarkable elevated fat mass (Hara-Chikuma et al., 2005). Both findings support a rationale that upregulation of AQP7 expression may be useful in obesity therapy.

AQP8 is expressed in kidney, liver, pancreas, testis, gastrointestinal tract, and salivary gland (Elkjaer et al., 2001; Koyama, 1997; Wellner et al., 2006). No important physiology of AQP8 expression is known, and no impairment was found in AQP8 knockout mice (Yang et al., 2005).

AQP9 is expressed in liver, leukocytes, brain, testis, spleen and osteoclast (Tsukaguchi et al., 1998; Amiry-Moghaddam et al., 2003; Loitto et al., 2002; Cho et al., 2003; Elkjaer et al., 2000; Aharon and Bar-Shavit, 2006). Recently, AQP9 expression in brain was found in astrocytes, endothelial cells, and catecholaminergic neurons (Badaut et al., 2004). AQP9 is a neutral channel, permeable to water, glycerol, and a number of solutes (Carbrey et al., 2003)

including mannitol, purines (adenine), pyrimidines (uracil), and monocarboxylates (lactate), but it is impermeable to cyclic sugars (D-glucose), glutamine, and glycine (Tsukaguchi et al., 1998, 1999). In addition, AQP9 may be involved in mucus secretion (Badaut et al., 2004) whereas AQP9 in catecholaminergic neurons may be more important in energy balance than osmotic pressure regulation (Badaut and Regli, 2004). AQP9 may also be involved in glucose metabolism and insulin resistance (Kuriyama et al., 2002). AQP9 expression in hepatocytes appears to work with AQP7 expression in adipose tissue for gluconeogenesis (Carbrey et al., 2003). Another cooperation for AQP7 and AQP9 is in the transport of arsenite, $As(OH)_3$. Since AQP9 may have a role in cell migration due to its high expression in white blood cells, this may be a potential method for leukemia (Liu et al., 2002). In addition, AQP9-null mice had a normal phenotype under unstressed conditions (Rojet et al., 2005).

AQP10 has a low permeability to water and is permeable to glycerol. AQP10 is expressed in the gastrointestinal tract (Hatakeyama et al., 2001). AQP11 is expressed in brain, liver and kidney (Gorelick et al., 2006). AQP12 is expressed in pancreatic acinar cells and is localized in intracellular membrane vesicles similar to AQP6 (Itoh et al., 2005). This suggested a role in the secretion of digestive fluid (Itoh et al., 2005). The detailed physiological functions of AQP10, AQP11, and AQP12 are unresolved.

Water channels and cellular osmolarity

Cellular volume homeostasis is critical for cells to survive. Changes in intracellular solute content or extracellular osmolarity can cause cells to swell or shrink. Cells can activate volume regulatory mechanisms by gaining solutes (regulatory volume increase, RVI) or

losing solutes (regulatory volume decrease, RVD) (Strange, 2004). These solutes can be inorganic ions (Na$^+$, K$^+$ or Cl$^-$) or small organic molecules called organic osmolytes (amino acids, polyols, or methylamines). Volume regulatory electrolyte movements are controlled by membrane transporters. This pathway can be activated within seconds to minutes after elevation of stimulating factors and may complete the task quickly because these transporters/channels are continuously expressed in the plasma membrane or stored in cytoplasmic vesicles. On the other hand, organic osmolyte regulation tends to be slow because the process involves transcriptional and translational events. Synthesis of organic osmolytes requires several hours, while downregulation of syntheses takes hours to days.

Another mechanism for cell volume regulation includes water movement across membranes as proposed by Krane et al. (2001). Fischbarg and coworkers have suggested that AQP1 contributes to cell volume regulation (Fischbarg, 2003; Fischbarg and Diecke, 2005). Additional observations are needed to support this hypothesis. However, there is no doubt that aquaporins participate in cell volume regulation when the osmolarity changes. A role for aquaporins may be more important during cellular changes in osmolarity than during normal cellular volume homeostasis.

A human kidney can filter up to 180 liters of water a day (Zelenina et al., 2005). It is not surprising that kidneys express several aquaporins. AQP1 is expressed in the proximal tube, the thin desending limb of henle (TDLH), and the outer medullary descending vasa recta (OMDVR). AQP2 is expressed in collecting ducts and is also trafficked by vasopressin moving from an intracellular vesicular compartment to the cell plasma membrane. AQP3 and AQP4 are co-expressed in the collecting duct, but AQP3 is mainly in the proximal segments while AQP4 is in the inner medullary collecting duct. AQP6 is expressed in collecting duct

intercalated cells. AQP7 is expressed in the proximal tubule (Verkman, 2005). These aquaporins may be critical for rapid, osmotically driven water transport because it was shown that salt and urea are actively transported to produce osmotic gradients, and this mild hypertonicity drives water across membranes through aquaporins (Verkman, 2006).

Similar mechanisms using active salt transport are found in secretion of near-isosmolar fluid such as saliva secretion. AQP5 is involved because AQP5 knockout mice secreted 50 per cent less saliva fluid (Ma et al., 1999). Similarly, choroid plexus secretion of cerebrospinal fluid (CSF) and aqueous fluid secretion of ciliary epithelium are AQP1-dependent (Oshio et al., 2005; Zhang et al., 2002).

Lung is another organ expressing several aquaporins. AQP1 is expressed in capillary endothelium while AQP3, AQP4, and AQP5 are co-expressed in the airway epithelial cells (Castle, 2005). These aquaporins may be involved in water clearance at birth and in maintaining airway surface liquid composition after birth (Zelenina et al., 2005). However, experiments in knockout animals showed these aquaporins are not involved in normal physiological lung functions as these animals exhibit a normal phenotype (Bai et al., 1999; Ma et al., 2000; Song et al., 2000). Perhaps, as in other tissues, they become important during pathology.

Water channels and ocular cells

Human eyes are similar to those of other mammals. They function in judging distance and determining object shapes and colors. The eye can be divided into three layers (Csillag, 2005). The cornea has the contact with air in the front and gradually changes to sclera in the back. The intermediate layer has the iris, ciliary body, and choroids. The inner layer is the

retina. Other basic structures include anterior/posterior chambers, lens, vitreous, and optic nerve.

Lens fibers express AQP0, whose point mutations can cause congenital cataracts, and such patients lose vision when they are young (Berry et al., 2000; Francis et al., 2000). The lens also expresses AQP1 from lens epithelial cells, but the physiological importance of AQP1 in these cells is still not understood (Verkman, 2003). Epithelial cells exist in most tissues with a variety of characteristics. Corneal epithelium expresses AQP3 and AQP5 (Levin and Verkman, 2004), and its basal layer cells proliferate continually and then migrate to the surface to be washed away by the lacrimal fluid. Unlike most epithelial cells, corneal epithelial cells are non-keratinizing. This characteristic is expected because these cells are at the surface of the eye where functions of cell hydration, corneal transparency, and corneal wound healing are critical. Using primary cultures of corneal epithelial cells from wild-type and AQP3-null mice, Levin and Verkman (2006) demonstrated that AQP3 may play a role in corneal epithelial cell migration and proliferation. Also, AQP5 is important in maintaining the proper corneal hydration level (Hamann, 2002). The cell layer of the cornea facing the anterior chamber (touching aqueous fluid) is the endothelium. It is a layer of flattened cells that cannot proliferate because the corneal endothelium is the medium between the matrix and the aqueous. It is not surprising that they express AQP1. The water permeability of AQP1 is high, and the amount of water (and other solutes) has to be carefully regulated. Indeed, AQP1-null mice had reduced corneal thickness under normal conditions and delayed recovery of transparency and thickness after the exposure of the corneal surface to distilled water (Thiagarajah and Verkman, 2002).

The conjunctiva has several layers of cells including epithelium, goblet, fornical, and palpebral. AQP3 and AQP5 are expressed in epithelial cells (Levin and Verkman, 2004; Oen et al., 2006). Levin and Verkman (2004) reported that the cell water permeability in AQP3-null mice was not lowered in a rate-limiting way. They concluded that the function of the glycerol transport of AQP3 may play a role, although they could not prove it. Oen and colleagues (2006) reported the finding of AQP5 in the same kind of cells, and this may explain the results from Levin and Verkman because their data was based only on AQP3 knockout mice instead of AQP3/AQP5 knockout mice. The functions of AQP3 and AQP5 in conjunctiva are still inconclusive because Oen and coworkers only identified the expression of AQP5 without examining its function.

The non-pigmented ciliary epithelium (NPE) is part of the ciliary body and functions in the secretion and composition of the aqueous humor. The expression of AQP1 in NPE is expected to have the same physiological importance as AQP1 in corneal endothelium. Additionally, NPE forms tight junctions, and this may provide an extra pathway for movements of water or solutes. AQP4 is also expressed in NPE. This suggests that a rapid regulation of water movement may be critical in cell physiology. Because the secretion of aqueous humor may determine the level of intraocular pressure (IOP), Zhang and colleagues (2002) used AQP1-null and AQP1/AQP4-null mice to examine the relationship of AQPs and IOP. They reported that aqueous fluid production was reduced in these mice, and lowered IOP values were recorded. Furthermore, the outflow of aqueous liquid was not impaired in AQP1-null mice even though AQP1 is normally expressed in the trabecular meshwork.

Trabecular meshwork (TM) expresses AQP1 only. Because the outflow of aqueous humor is through TM, whose physiology is not fully understood, but its cytoskeleton

architecture is believed to regulate aqueous humor outflow rate. However, TM has been proposed as a new target for glaucoma treatment (Ferrer, 2006). Zhang and coworkers (2002) reported no changes in IOP using AQP1-null mice. Stamer and coworkers (2001) found AQP1 expression increased TM cell volume. They hypothesized that the intracellular volume changes influence outflow facility. Specifically, they proposed that increased TM cell volume decreased outflow, and decreased cell volume can increase outflow. Indeed, Xiong and coworkers (2005) reported that inhibition of AQP1 expression in bovine TM cells may reduce outflow; Peng and coworkers (2006) had similar findings using human TM cells. Perhaps disagreements are due to the systems being used, such as *in vivo* versus *in vitro*, different species, and different stimulants.

The retina is like a "miniature brain" with excitable and non-excitable neurons and neuron supportive cells. The structure of the retina is much more complicated than other tissues of the eye and is usually viewed as composed of ten layers – the pigment epithelium (RPE), the neuroepithelial layer [rods and cones, outer and inner segments (OS, IS)], the external limiting membrane (ELM), the outer nuclear layer (ONL), the outer plexiform layer (OPL), the inner plexiform layer (IPL), the ganglion cell layer (GCL), the optic nerve fiber layer (OFL), and the internal limiting membrane (ILM).

The retinal pigment epithelium (RPE) consists of closely packed cells that separate the retina from the capillaries of the choroid. The RPE is important in photoreception because these cells can phagocytize debris from rod and cone outer segments, recycle used retinal molecules from outer segments, and control the substances between the choriocapillaries and retina (Csillag, 2005). RPE cells have tight junctions to limit the passage of substrates to the retina. These cells, however, also express AQP9 (our observation). The existence of AQP1

in RPE is still in debate. Stamer and coworkers (2003) reported AQP1 in human RPE, and Ruiz and Rok (1996) reported AQP1 in cultured fetal RPE. On the other hand, Hamann and coworkers (1998) failed to prove the presence of AQP1 in rat and human RPE. AQP1 has also been reported to be expressed in photoreceptors, amacrine, and Müller cells, although its functions remain unknown (Kim et al., 1998, 2002; Ianiev et al., 2005). Currently, our lab is studying the effects of water channel expression in RPE under disturbed osmolarity (unpublished data). These channels may function to regulate cell volume under stressed conditions.

Müller cells are one kind of glial cells. They express AQP4 strongly (Nagelhus et al., 1998) and are supportive cells in the retina by controlling solute availability to neurons. Astrocytes are the major type of glial cells in the optic nerve head, where retinal ganglion cell (RGC) axons exit the eye toward the central nervous system. Astrocytes also express AQP4 and are supportive cells to RGCs through structural support, extracellular matrix maintenance, and solute regulation (Vizuete et al., 1999). However, activated astrocytes may damage RGCs because the astrocye channel regulation is abnormal.

Retinal ganglion cells can generate action potentials that travel along the optic fibers (Csillag, 2005). RGCs are larger than other retinal neurons. In general, RGCs are a mixture of more than 20 cell subtypes. They have energy-dependent axonal transport functions - orthograde and retrograde transports (Rodieck, 1998). Retrograde axonal transport is responsible for supplying trophic factors to RGCs (Schwartz et al., 1977) while afferent axons are considered as optic fibers. RGCs can be categorized as M cells, if projecting to magnocellular layers, and P cells, if projecting to parvocellular layers (Csillag, 2005). These terminal projection areas are in the lateral geniculate body. RGCs can be sub-divided by their

morphology and physiology, but they are usually discussed without classifications. In our observation, RGCs express AQP9 in primary and secondary cultured cells. As mentioned before, AQP9 can transport water, glycerol, and a number of solutes. This increases the difficulties of analyzing its functional roles. Furthermore, RGCs also express AQP9 in mitochondrial membranes in addition to the plasma membrane (our observation). There are no reported AQP9 functions in RGCs in the literature, so our group will be the first to describe its actions. Fig. 4 shows the proposed model of RGC apoptosis in glaucoma.

Aquaporins and apoptosis

Cells have two ways to die. They can go through necrosis, which includes a cell volume increase involving swelling of intracellular organelles and cell membrane budding that ultimately results in a broken cell membrane. This may cause damage to surrounding areas and produce inflammation. The other way is through programmed cell death or apoptosis. Apoptosis is characterized by a series of morphological, biochemical, and molecular events including cell surface and volume changes, protein cleavages, and DNA fragmentation (Yorio and Dibas, 2004). It starts with the mitochondrial inner membrane where changes in the mitochondrial membrane potential causes increased release of calcium ions from the endoplasmic reticulum. Next cytochrome c is released from mitochondria into the cytosol where caspases are activated. DNAs are cut into pieces and released from the nucleus. At the end, the dying cell will be phagocytized by neighboring cells or macrophages. There usually is limited damage to neighboring tissues.

An early prerequisite for apoptosis is cell shrinkage, which is termed an apoptotic volume decrease (AVD, Maeno et al., 2000). AVD is induced by an osmotic gradient caused

by potassium ion efflux (Bortner et al., 2001). This imbalance of ion levels may be the activator of apoptosis (Bortner et al., 1997), but the water movement response to the osmotic gradient was never discussed. Because the speed of cell shrinkage is faster than that of simple diffusion, aquaporins may be involved. Jablonski and coworkers (2004) demonstrated that aquaporin activities affect the apoptosis process following AVD. When the water permeability of AQP1 was inhibited, cell shrinkage, caspase-3-like activity, and mitochondrial membrane depolarization were blocked. These studies were done using two kinds of cells, ovarian granulose cells and thymocytes, and two different stimuli of apoptosis, growth factor withdrawal and reagents (thapsigargin and C_6-ceramide), to determine that the results were neither cell-specific nor signal-specific. As expected, experiments on over-expression of AQP1 in Chinese hamster ovary cells showed that the rate of apoptosis increased (Jablonski et al., 2004).

Similar ideas were tested by various methods including inhibition of potassium and chloride ion channels, blockage of caspase activities, and usage of a high potassium medium (Hortelano et al., 2003; Vu et al., 2001; Hughes et al., 1997). Results from those studies also showed a blockage of downstream apoptotic events. Hortelano and colleagues (2002) used macrophages but did not detect AVD in apoptosis. Although neutrophil leukocytes were reported to express AQP9 (Loitto et al. 2002), macrophages may not express any aquaporins.

Recent reports showed that AQP8 and AQP9 are expressed in the inner mitochondrial membrane (IMM) (Calamita et al., 2005; Amiry-Moghaddam et al., 2005; our observation). The IMM only allows O_2, CO_2 and NH_3 to pass through without using any transporter, but the outer mitochondrial membrane (OMM) is highly permeable and nonselective. This suggests that aquaporins may regulate the volume of the mitochondrial matrix. Mitochondria

are the power plants of the cell. They function in calcium ion homeostasis, respiration, and

ATP production. The IMM is especially important for maintaining an electrochemical

gradient and extrusion of protons during respiration process. In addition, apoptosis can be

linked to dysfunctional mitochondria (Kronemer, 2003; Wang, 2001). Thus, the expression

of aquaporins of IMM may have a physiological and/or pathophysiological role.

Interestingly, AQP8 expression in mitochondria differs among the various sized

mitochondria: larger ones express more, but there appear to be subpopulations and not all

mitochondria express AQP8 (Calamita et al., 2005). Even though liver expresses AQP8,

Calamita and coworkers (2005) found that immortalized hepatocytes do not express AQP8.

The apoptotic role of aquaporins expressed in mitochondria is not clear but its involvement is

expected.

The relationship between AQPs and optic nerve damage

Aquaporins are involved in the homeostasis of ions, osmolarity, and volume inside a

nerve cell and in the extracellular matrix (ECM). These functions are fundamental in brain

and spinal cord. Any imbalance can dramatically change neuronal signaling and even

damage the brain. Dysfunctional water channel proteins can cause excess water accumulation

in the brain, which affects the mortality of cells during stoke and brain damage, such as

tumor, trauma, and infection. For example, AQP4 is well known to be expressed at the

blood-brain barrier (BBB) (Rash et al., 1998). Brain edema can be a result of upregulation of

AQP4 in astrocytes with or without disturbance of the BBB because AQP4 has an

exceptionally high water permeability (Solenov et al., 2004; Yang and Verkman, 1997).

Indeed, studies using rodents showed upregulated AQP4 expression of astrocytes in brain

injury and brain ischemia that results in brain edema (Vizuete et al., 1999; Ke et al., 2001; Taniguchi et al., 2000). Therefore, it was expected that there would be increased mortality of AQP4 knockout mice during brain edema. However, both positive and negative results were shown with AQP4 knockout mice experiments. When the cytotoxic (cellular) edema was caused by acute water intoxication, ischemic stroke, and meningitis, AQP4-null mice had reduced brain swelling (Manley et al., 2000; Papadopoulos and Verkman, 2005). The protective effects can be explained by the findings in wild-type mice. In cytotoxic edema studies, wild-type mice had greater and widespread pericapillary astrocyte foot process swelling and greater hemispheric enlargement and midline shift (Manley et al., 2000).

Nevertheless, when the brain swelling was caused by intraparencymal fluid infusion, cortical freeze injury, brain tumor, or abscess, the outcome was worse (Papadopoulos et al., 2004; Bloch et al., 2005). Overall, the improved outcome of AQP4-null mice can be explained by slowed brain water accumulation, but in vasogenic (noncellular) edema studies AQP4-deleted mice had higher intracranial pressure and brain water content (Papadopoulos et al., 2004). This impaired water clearance result was surprising and indicated that AQP4, a pure water channel, may provide a low resistance route for removing edema fluid. Extracellular fluid movement requires a bulk flow mechanism, which does not need water channels (Verkman, 2005).

Astrocytes also express AQP9, which was upregulated after transient brain ischemia (Badaut et al., 2001). Because AQP9 is permeable to water and a number of solutes, the function of AQP9 in the brain remains unclear.

In addition to the expression in choroid plexus for cerebrospinal fluid production, AQP1 expression was also reported in glioblastoma and metastatic brain cancer (Endo et al.,

1999), but not in normal brain endothelium (Market et al., 2001). This AQP1 expression may be tumor-specific, not brain-specific, because AQP1 is heavily involved in tumor angiogenesis and AQP1 deficiency did reduce tumor growth (Saadoun et al., 2005)

Although neurons do not express AQP4, AQP4 still may affect neuronal signal transduction. AQP4-null mice had hearing problems and became deaf (Li and Verkman, 2001) and also had abnormalities in electroretinograms (ERG) (Li et al., 2002). Because AQP4 expression is polarized in brain astrocytes as they make contact with endothelial cells and neurons (Saadoun et al., 2002; Nicchia et al., 2002), there was no surprise when Da and Verkman (2004) showed that AQP4-null mice had better retinal structure and larger cell number than the wild-type mice after ischemia. AQP1 is another aquaporin that may be involved in neural signal transduction. AQP1-null mice had reduced pain sensation (Oshio et al., 2001). All these findings were hypothesized in relationship to a K^+ channel, Kir4.1 (Bringmann et al., 2005). Glial cell membranes co-expresses AQP4 and Kir4.1, and these cells are responsible for the ECM of neurons. Besides, Dalloz and coworkers (2003) reported that RGCs in mice with mis-located Kir4.1 protein in Müller cells had enhanced vulnerability of ischemia reperfusion injury.

Badaut and coworkers (2004) were the first group to report water channels in neurons. Because catecholaminergic neurons respond to energy balance rather than osmotic pressure (Grill and Kaplan, 2002; Rilter, 1998) and are located in the brain with other fuel sensing neurons (Ainscow et al., 2002), AQP9 was expected to function in an energy-related role instead of a water-related role. In addition, both lactate and glycerol can be transported by AQP9, and both substances can be used as fuel by neurons (Magistretti et al., 1999; Nguyen

et al., 2003). Thus, the functional role of AQP9 in catecholaminergic and retinal ganglion cells is still not clear.

Glaucoma

Glaucoma affects more than 60 million people worldwide (Quigley, 1996) and will affect 79.6 million people in 2010 (Quigley and Broman, 2006). Glaucoma is a group of slow progressive vision disorders affecting the trabecular meshwork, the optic nerve head, and retinal ganglion cells (RGCs). Vision impairment in glaucoma is irreversible, but progression of the disease is treatable. Glaucoma is classified as primary if evidenced by optic neuropathy and as secondary if evidenced by elevated intraocular pressure (IOP) caused by other pathological processes (Foster et al., 2002). Primary open angle glaucoma is characterized by changes in the drainage system. There are primary open angle glaucoma (POAG) and primary angle closure glaucoma. Secondary glaucoma pathology is divided by the stimulating pathology.

The majority of glaucoma patients in the United States have primary open angle glaucoma (POAG), which is related to elevated intraocular pressure (IOP) (Castle, 2005; Clark, 1999). Other risk factors for glaucoma are increasing age (Mitchell et al., 1996), being African-American (Tielsch et al., 1991), visual field abnormalities in visual field examinations (Gordon et al., 2002), high myopia, family history of glaucoma (Wolfs et al., 1998), thin cornea, and a cup-to-disk ratio greater than 0.4 (Gordon et al., 2002). Knowing the risk factors is very important for early detection because the disease progression can be slowed. There are several methods for assessment of the optic disc. Examination of the optic disk is preferred over that of the visual field loss because a certain number of retinal ganglion

cells must be damaged or lost before the vision loss is detectable. The examination method uses a magnified stereoscopic view. Scanning laser polarimetry can assess the thickness of the retinal nerve fiber layer (Zangwill et al., 2000). Confocal scanning laser ophthalmoscopy shows images by layers for topography measurements (Zangwill et al., 2000). Optical coherence tomography can measure the retinal nerve fiber layer thickness and the optic disc topography (Greenfield et al., 2003). These methods are reliable for distinguishing glaucoma patterns from normal ones.

Glaucoma patients have slow, progressive degeneration of retinal ganglion cells. Factors contributing to RGC death may include local ischemia-hypoxia (Weinreb et al., 1997), excess glutamate (Lipton, 2003), low functional cellular pumps and glutamate transporters (Hama et al., 2006), oxidative stress and free radical formation (Liu and Neufeld, 2001), inflammatory cytokines such as tumor necrosis factor (TNF) (Yan et al., 2000), abnormal immunity and secondary neurodegeneration by neuronal environmental changes (Schwartz, 2003). In addition, Osborne (2006) proposed light as a risk factor when RGCs are in a low energy state. Even though glaucoma disease factors are not fully characterized, elevated IOP is the main factor without question. Although some patients with controlled IOP developed glaucoma, the current primary therapy still is to lower the IOP. The pressure in the eye is the balance between aqueous humor (AH) secretion from ciliary body and drainage via trabecular meshwork and the canal of Schlemm. Thus, the focus for treatment has been either decreasing AH formation or increasing AH outflow. The current treatments are drugs, laser surgery, incisional surgery, and glaucoma tube implants. Chemical agents used to reduce IOP by suppressing aqueous inflow are β adrenergic blockers, α2 adrenergic agonists, and carbonic anhydrase inhibitors (Villumsen et al., 1989;

Weinreb et al., 2002; Einarson et al., 2000). Drugs that increase aqueous outflow are prostaglandin analogues and cholinergic agonists (Brubaker, 2001). Those chemicals have different degrees of side-effects. The second kind of treatment is laser trabeculoplasty (Weinreb et al., 1995), which acts by reducing the aqueous humor outflow resistance of the trabecular meshwork (Bradley et al., 2000). However, the effect typically is gradually lost and additional surgery is necessary. The third kind of treatment is trabeculectomy, which involves the excision of a portion of the trabecular meshwork and/ or its surrounding area. This will increase the aqueous humor outflow, but the complications, such as development of cataract and hypotony, are not easily accepted by patients (Edmunds et al., 2002). The latest and last treatment available involves glaucoma tube implants. These tubes direct aqueous humor to a reservoir that is sutured to the sclera (Wilson et al., 2003). However, control of the IOP is difficult with this procedure, and scaring limits its efficacy.

The mechanisms responsible for the pathophysiology of glaucoma are poorly understood, but early detection is very crucial because elevated IOP may cause optic nerve changes (cupping) that eventually lead to retinal ganglion cell death and glaucoma (Dan et al., 2002).

Hypothesis:

Optic nerve degeneration in glaucoma can be mimicked in a rat model by elevated intraocular pressure (IOP) and ischemia. Astrocytes, expressing AQP3, 4, 5, 8, and 9 play an important role in optic nerve degeneration and are supportive cells to RGCs. RGCs are the neurons responsible for vision and are expected to have neuronal aquaporin-9. Elevated IOP/ischemia should change AQP9 expression in RGCs and optic nerve head astrocytes

(ONAs). These changes may contribute to optic nerve damage in glaucoma. Fig. 5 shows a proposed role of AQP9 in RGC apoptosis in glaucoma. Fig. 6 shows a proposed route of lactate among a neuron, an astrocyte, and a small blood vessel.

Specific aims:

1) Identify and confirm the presence of AQP9 in RGCs.

2) Determine whether experimentally elevated IOP in an animal model of glaucoma can change AQP9 expression in RGCs and ONAs.

3) Determine the role of AQP9 (expressed in RGCs) in apoptotic volume decrease (AVD) in experimental hypoxia to mimic glaucoma conditions.

METHODS

Tissue culture

Primary retinal ganglion cells (RGCs) were isolated from rat retinas. Retinas were dissected and incubated for 30 min in papain solution, which was a mixture of low glucose Dulbecco's modified Eagle's medium (DMEM)(Gibco, Grand Island, NY, 11995-040), papain (165 units/mL)(Sigma, P4762), DL-cysteine (0.2 mg/mL) (Sigma, C4022) and bovine serum albumin (BSA, 0.2 %)(Sigma, A7906). Then retinas were washed three times with trophic factor medium (TF), containing brain-derived neurotrophic factor (BDNF) (50 ng/mL, Biosource, PHC7074), ciliary neurotrophic factor (CNTF) (10 ng/mL, Biosource, PRC7014), insulin (5 μg/mL, Sigma, I6634), forskolin (5 μM, Sigma, F6886), and fetal bovine serum (FBS). Retinas were triturated using a pipette in TF medium until no large clumps were observed. Cell populations were plated on collagen-coated coverslips in neurobasal media (Gibco, 10888-022) with TF. Collagen-coated coverslips were prepared with poly D-lysine (Sigma, P6407) and merosin (Gibco, 12162-012). Every three days, half of the medium was replaced with fresh neurobasal medium until ready to use; only RGCs can benefit from this medium. RGCs were identified by labeling with Brn-3C (polyclonal antibodies, Convance Inc.) and Thy-1 (monoclonal antibodies, Chemicon,).

The secondary cell culture, RGC-5 cells, is a transformed rat retinal ganglion cell-line developed and obtained from Krishnamoorthy et al. (2001). RGC-5 cells were maintained in low glucose DMEM in T-150 culture flasks (Gibco, Grand Island, NY, USA) supplemented with 44 mM $NaHCO_3$, 10 % fetal bovine serum (FBS) (Hyclone Laboratories, Logan, UT) and penicillin and streptomycin (Gibco) as described by Krishnamoorthy et al. (2001). Cell passages 7-40 were used. For volume measurements and immunocytochemistry studies,

cells were subcultured onto 25-mm glass coverslips 1-2 days prior to experimentation. For immunoblotting and polymerase chain reaction (PCR) analyses, cells were subcultured in 100-mm plastic dishes 2-3 days prior to experimentation. The culture media was changed to serum-free (SF) DMEM before any treatment.

Differentiated RGC-5 cells were obtained by using HNPE conditioned medium, which consisted of low glucose DMEM incubated with human non-pigmented ciliary epithelial cells (HNPE). HNPE are SV-40 transformed and were a gift from Dr. Miguel Coca-Prados (Yale University). HNPE was maintained in DMEM supplemented with 10 % FBS and antibiotics; this medium was collected after HNPE cells had reached confluency in 150-mm dishes (about 4 days). For every 50 mL of HNPE conditioned medium, 1 mL of fresh DMEM with 10 % FBS and antibiotics was added to enrich growth factors. The medium for RGC-5 cells was changed every day until cells were differentiated. This process usually took three to four days when cells were ready for experimentation.

Primary cultures of human optic nerve head astrocytes (hONAs) originally isolated from donor eyes (92-year-old donor) were provided by Dr. Abbot Clark (Alcon Research, Fort Worth, TX). These cells were isolated as described previously with some modifications (Hernandez et al., 1988; Lambert et al., 2001). Cultured hONAs were maintained in DMEM plus 10 % FBS. Additionally, human U373MG astrocytoma cells (human glioblastoma) (ATCC, Manassas, VA) were also used. All cultures were maintained in 5 % CO_2-95 % O_2 at 37 °C and medium was changed every 2-3 days. Nearly 100 % confluency was reached after approximately 4 weeks for primary culture and 1 week for secondary culture. These hONAs were confirmed as Type 1b astrocytes by detecting the presence of glial fibrillary acidic protein (GFAP) and neural cell adhesion molecule (NCAM) (Hernandez et al., 1988;

Lambert et al., 2001). The hONAs were grown in collagen Type I-coated 100-mm culture

dishes (Becton– Dickinson Labware, Bedford, MA) or T-75 culture flasks and were

maintained at 37 °C in DMEM supplemented with 44 mM NaHCO$_3$, 10 % fetal bovine

serum (Hyclone Laboratories, Logan, UT), and antibiotics (Gibco). Cell passages used for

hONAs were between 7 and 12 in this study.

ARPE-19, spontaneously transformed human retinal pigmented cells (ATCC,

Manassas, VA), were maintained in DMEM (high glucose): F12 medium in T-150 culture

flasks (Gibco) supplemented with 44 mmol/L NaHCO$_3$, 10 % fetal bovine serum (Hyclone

Laboratories, Logan, UT), and antibiotics (Gibco). Cell passages used were between 18-34.

Intracellular volume measurements

All measurements were conducted using a Nikon Diaphot microscope (Tokyo, Japan),

utilizing a dynamic single-cell video imaging technique with image-1FL Quantitative

Fluorescence System (Universal Imaging, West Chester, PA). RGC-5 cells were loaded with

fura-2/AM (4 μM) in a modified Krebs-Ringer solution (Krebs: 115 mM NaCl, 2.5 mM

CaCl$_2$, 1.2 mM MgCl$_2$, 24 mM NaHCO$_3$, 5 mM KCl and 25 mM HEPES, pH 7.4) for 30

minutes at 37 °C. Cells were washed with 3 mL of Krebs to remove excess probe, and

volume measurements were determined by monitoring the fluorescence of fura-2 at

excitation wavelengths of 360 nm (isosbestic point where fura fluorescence is insensitive to

intracellular changes in cytosolic Ca^{2+} but sensitive to volume changes) as described by

Grynkiewicz et al. (1985) and Altamirano et al. (1998). For cellular swelling rate

measurement, Mg132 (10 μM) and dimethyl sulfoxide (DMSO) were used.

Isolation of plasma membrane and Western blotting

A. Cells

Cell plasma membrane proteins were isolated as previously described (Dibas et al., 2005). Briefly, cells grown to confluency in 100-mm culture dishes were washed twice in 1X phosphate buffered saline (PBS), briefly centrifuged and resuspended in 1 mL of homogenization buffer (50 mM Tris-HCl, 100 mM NaCl, 1 mM EGTA, 1 mM EDTA, 2mM Na-Orthovanadate, 50 mM NaF, 10 mM Na-pyrophosphate, 10 mM NaH_2PO_4, 10 mM Na_2HPO_4, 10 mM Na_3PO_4, 10 mM Na-molybdate, 10 mM Na-tartarate, 50 mM β-glycerophosphate, pH 7.38) with protease inhibitors: 20 µg/mL leupeptin, 10 µg/mL aprotonin, 20 µg/mL soybean trypsin, and 40 µg/mL PMSF. The sample was quickly homogenized by 5 strokes in sonication and placed on ice. Then the homogenate was centrifuged at 3,000 g for 5 min. The same procedure was repeated once to remove most unbroken cells and nuclei. The supernatant was centrifuged at 100,000 g for 35 minutes at 4 °C. Portions of the supernatant [cytosolic fraction (C)] were removed for (a) sodium dodecyl sulfate-polyacrylamide gel electrophoresis (SDS-PAGE) where it was mixed with 1/4 volume of SDS-sample buffer [4X: 62±5 mM Tris-HCl, pH 6.8, 0.1 % (v/v) glycerol, 2 % SDS, 0.05 % 2-β mercaptoethanol and 0.005 % (w/v) bromophenol blue] and (b) protein concentration assay. The remaining pellet (stored on ice) was sonicated in fresh homogenization buffer containing NP-40, and then was centrifuged. The resulting supernatant (plasma membrane fraction) was removed and mixed with SDS-sample buffer (4X: 62.5 mM Tris, pH 6.8, 0.1 % (v/v) glycerol, 2 % SDS, 0.05 % 2-β-mercaptoethanol and 0.005 % (w/v) bromophenol blue) for gel electrophoresis.

Protein concentrations were determined using bicinchoninic acid protein assay (BCA).

Briefly, bicinchoninic acid solution (Sigma, St. Louis, MO, B9643) and copper sulfate solution [Sigma, C2284: 4 %(w/v)] $CuSO_4 \cdot 5H_2O$ were mixed by adding 1 volume copper sulfate solution to 50 volumes of bicinchoninic acid solution as a working solution. Each one volume of protein sample was mixed with 20 volumes of the working solution and incubated at 37 °C for 30 min (Alternatively 2 hours at room temperature, or 15 minutes at 60 °C). The absorbance at 562 nm was measured after cooling the samples to room temperature. The sample concentration was calculated according to the standard curve.

B. Retina

For retinas, Western blotting was performed on either total retinal lysates or enriched plasma membrane and cytosolic fractions. To prepare total retinal lysate, retinas were dissected from eyes, and solubilized into 250 μL of a solution containing 20 mM Tris (pH 7.4), 10 % sucrose, 2 mM EDTA, 2 mM EGTA, 50 mM NaF, 1 % Triton X-100, 0.1 % sodium dodecyl sulfate and protease inhibitors at 4 °C. Retinal lysates were incubated for 30 min on ice and then briefly sonicated before centrifugation at 14,000 g for 15 min. The supernatant was collected, and the protein concentration was measured using a bicinchoninic acid (BCA) protein assay kit (Sigma, St. Louis, MO) with bovine serum albumin (BSA) as the standard. To enrich plasma membrane fractions, retinas were dissected from eyes, and homogenized into 700 μL of a solution containing 20 mM Tris (pH 7.4), 10 % sucrose, 2 mM EDTA, 2 mM EGTA, 50 mM NaF, and protease inhibitors at 4 °C using a Potter homogenizer (60 strokes) followed by centrifugation at 3,000 g for 5 min. The unbroken tissue was sonicated 7x, and then centrifugation was repeated. The retinal supernatant was then centrifuged for 30 min at 100,000g at 4 °C. The resultant supernatant (cytosol) and pellet (PM) were collected for protein measurement using the BCA protein assay. Proteins

were separated by 10 % SDS-PAGE, with 20-30 μg (enriched fraction) or 100 μg (total retinal extract) of protein loaded in each lane. Gels were equilibrated in transfer buffer (192 mM glycine, 20 % methanol and 25 mM Tris-HCl, pH 8.3) for 10 minutes at room temperature and electroblotted on nitrocellulose membranes for 75 minutes at 100 volts using a Bio-Rad electroblotting unit. The membranes were dried at room temperature. Western blotting was performed using an Amersham Chemiluminescent Kit (Bedford, MA). Membranes were incubated with primary antibodies for 60 minutes (1 μg/mL) and with the secondary antibody for 30 minutes (1:10,000). Membranes were then exposed to an X-ray film for 30 seconds, 1 minute, and 3-5 minutes, and the film was later developed. Membranes were stripped and probed with anti-α-tubulin antibodies for normalization. Experiments were repeated three times. Band densities were quantified with image-analysis software (Scion) and the intensity of AQP4/9/Thy-1/GFAP/XIAP/caspase-3 bands was normalized for every sample relative to the intensity of the respective tubulin bands.

Isolation of total RNA and synthesis of cDNA

Total RNA was extracted with Trizol (Life Technology, Rockville, MD) as described in the manufacturer's instructions. Briefly, after cells grown in 100-mm dishes reached confluency, cells were scraped and dissolved in Trizol B reagent and then mixed with chloroform. Total RNA was purified by isopropanol and 70 % ethanol. In this study, 10 μg of total RNA was reverse transcribed using the iScript select cDNA synthesis kit (Bio-Rad, 170-8897) according to manufacturer's instructions. The protocol can be found in Bio-Rad website: http://www.biorad.com/cmc_upload/Literature/204560/10001023.PDF.

Briefly, RNA sample (10 μg total RNA), oligo (dT) 20 primer and nuclease-free water

were mixed and incubated at 65 °C for 5 minutes. After snap-chill reaction on ice for approximately 60 seconds, master mix (5x iScript select reaction mix 4 μL and iScript reverse transcriptase 1 μL) was added, and the mixture was incubated for 90 minutes at 42 °C followed by incubation at 85 °C for 5 minutes. Samples (complementary DNA, cDNA) were stored at -20 °C until ready to use.

Quantitative polymerase chain reaction and sequencing

Q-PCR was performed as described by Zhang et al. (2003). Q-PCR amplification of each sequence was performed with 2.5 μL of cDNA sample in a total volume of 25 μL using SYBR Green PCR Core regents (PE Applied Biosystems, Foster City, CA, USA). Q-PCR reactions were performed in a Cepheid Smart Cycler (Cepheid, Sunnyvale, CA, USA). Immediately after the real-time PCR run, the melting curves were generated to detect the melting temperatures of the specific products for purity (data not shown). The Q-PCR product purity was also confirmed by 1.5 % agarose gel electrophoresis. The authenticity of Q-PCR products were confirmed by DNA sequencing and a BLAST search of the sequence through NCBI (http://www.ncbi.nim.nih.gov) (data not shown). Quantification of relative RNA level was achieved by using the comparative C_T method (as described in Applied Biosystems, *Product and Service Literature*; Available at http://docs.appliedbiosystems.com/pebiodocs/04304965.pdf.). Q-PCR data are presented as the value with its corresponding untreated control in at least three experiments. The details of primer sequences and running temperatures are in Tables 1 and 2. All samples started with a pre-heating period of 50 °C for 2 min and 95 °C for 10 min before denaturation. Control Q-PCR reactions were performed in the absence of cDNA templates. The constitutively

30

expressed "housekeeping" gene S15, a small ribosomal subunit protein, and β-actin, a cytoskeletal protein, served as internal controls. β-actin and S15 were used as the housekeeping gene. Q-PCR products were run on 1.5 % agarose gels, and bands were cut and sequenced to verify identity. See Tables 1 and 2 for primer sequences and conditions.

Immunocytochemistry

RGCs were grown on glass coverslips for 1-2 days prior to experimentation. Coverslips were rinsed with PBS three times and then were fixed in 4 % paraformaldehyde for 30 min. These cells were washed with PBS before being permeabilized in 0.1 % Triton X-100 for 15 min, washed with PBS, and blocked with 5 % bovine serum albumin for 60 min. After rinsing with PBS, the cells were incubated with a mixture of Thy-1 (monoclonal antibodies, Chemicon, Temecula, CA, 1:200) and AQP9 (rabbit antibodies, Santa Cruz Inc, Santa Cruz, CA, 1:1000) or Brn-3C (polyclonal antibodies, Convance Inc, Princeton, NJ, 1:1000) and AQP9 (goat antibodies, Santa Cruz Inc, 1:1000) or Cytochrome C (polyclonal antibodies, BD Biosciences, San Jose, CA, 1:400) and AQP9 (goat antibodies, Santa Cruz Inc, 1:1000) for 1.5 hrs at room temperature and subsequently incubated with a combination of secondary antibodies of Alexa Fluor 633 donkey anti-goat conjugated IgG (Molecular Probes, Eugene, Oregon, USA) + Alexa Fluor 488 donkey anti-mouse conjugated IgG or Alexa Fluor 633 goat anti-rabbit conjugated IgG + Alexa Fluor 488 goat anti-mouse conjugated IgG for 1 h in the dark. After PBS rinses, these cells were incubated for 10 min in the dark with 300 nM 4',6-diamidino-2-phenylindole (DAPI) to stain nuclear regions. Cover-slides were mounted on glass slides in anti-fade medium (FluorSave; Calbiochem, La Jolla, CA) and allowed to dry for 20 minutes in the dark. Cells were visualized and images were taken using a Zeiss

31

LSM-410 Confocal Scanning Laser Microscope System. Controls were performed by omitting primary antibodies.

Immunohistochemistry

Rat eyes were enucleated, dissected, fixed in formalin, embedded in paraffin, and five-micron sections were obtained using a microtome. Retina sections were deparaffinized in xylenes, rehydrated using ethanol washes and washed with PBS. After permeabilization using Triton X-100 (0.1 %) and PBS washes, non-specific binding was blocked by 5 % BSA in PBS. The sections were incubated with a mixture of primary antibodies (Thy-1 monoclonal antibodies, Chemicon, 1:400), AQP9 (goat or rabbit antibodies, Santa Cruz Inc, 1:100), glutamine synthetase (monoclonal antibodies, Chemicon, 1:400), AQP4 (mouse or rabbit antibodies, Santa Cruz Inc, 1:100), glial fibrillary acidic protein (GFAP, monoclonal antibodies, Neomarkers, Fremont, CA, 1:100), and RPE65 (monoclonal antibodies, Novus Biologicals, Littleton, CO, 1:100) for 2 hrs at room temperature. Sections were rinsed with PBS three times and incubated in a mixture of secondary antibodies [a combination of donkey anti-goat conjugated Alexa 488 + donkey anti-mouse conjugated Alexa 633 or goat anti-rabbit conjugated Alexa 633 + goat anti-mouse conjugated Alexa 488 (2 µg/mL)] for 1 hour in the dark at room temperature followed by 3 washes in PBS and one final wash in deionized water. Coverslips were mounted on glass slides in antifade medium (FluorSave; Calbiochem, La Jolla, CA) and allowed to dry for 20 minutes in the dark. Retinal and optic nerve sections were viewed, and images were taken with Zeiss LSM 410 confocal microscope. Controls were performed by omitting primary antibodies.

Animal model of glaucoma

Intravitreous injection of endothelin-1 (ET-1): HEPES-buffered ET-1 or HEPES vehicle buffer alone were injected intravitreally as described (Stokely et al., 2002). Rats were anesthetized and 4 µL of HEPES-buffered ET-1 (2 nmol) or HEPES, vehicle, was injected into the vitreous of the left eye with a 30-gauge needle attached to a syringe (microliter 710, 22s gauge; Hamilton Co., Reno, NV) by polyethylene tubing (PE-20, Clay Adams Brand; BD Biosciences, Sparks, MD). During intravitreous injections, retinas were observed through the pupil with a surgical microscope (model Stiffuss S; Carl Zeiss, Thornwood, NY). During introduction of solution into the vitreous, a transient blanching of the retina was observed in all animals. One minute after injection, all retinas appeared normal in color. All studies were conducted in accordance with NIH guidelines and the ARVO Statement for the Use of Animals in Ophthalmic and Vision Research. All rats were euthanised by an intraperitoneal injection of pentobarbital (100 mg·kg^{-1}) (Sigma, P3761) after 48 hours, 72 hours or 7 days post ET-1 injection, and eyes were dissected and processed for Western blotting or for Q-RT-PCR.

The Morrison glaucoma model: Male Brown Norway retired breeder rats weighing between 200 and 300 g were used and fed standard chow. The animals were housed individually in rat gang cages in an environmentally controlled room and maintained on a 12-hour light/dark cycle with tap water ad libitum prior to experimentation. Intraocular pressure (IOP) was elevated in one eye as described by Morrison et al. (1997) where 50 µL of 1.8 M saline was injected into the episcleral veins of one eye of anesthetized rats such that blanching was observed. This procedure produces scarring of the TM with a resultant rise in IOP and damage to the optic nerve (Johnson et al., 1999). Rats were housed post-surgically

in constant low light (< 90 lux) to minimize effects of circadian influences on IOP. After

stabilization, IOP measurements were taken with a Tonolab rebound tonometer (Colonial

Medical Supply, Franconia, NH) on conscious animals in the presence of the topical

anesthetic, proparacaine (0.1 %) (Falco pharmaceuticals, Alcon, Fort Worth, TX). Animals

were weighed periodically. IOP was initially monitored twice a week for up to 10-14 days

and subsequently monitored on a weekly basis, once IOP was greater than 25 % of baseline

IOP values. IOP values at each time were recorded as an average of nine consecutive

Tonolab measurements for each eye. IOP exposure for each animal was calculated as mmHg

days as previously described by McKinnon et al. (2002). Accordingly, IOP exposure for each

rat was calculated by performing separate area-under curve (AUC) integration of IOP over

the days of exposure for the treated and control eyes. The integral value of the control eye

was subtracted from that of the experimental treated eye to yield the "IOP-integral

difference" and was expressed as mmHg days. As inclusion criteria, only rats with elevated

IOP that was 25-50 % over baseline IOP (of 21 mmHg), which was maintained for at least

200 mmHg days were included in this study. Rats with elevated IOP were maintained for

500-800 mmHg days post-surgery. All procedures involving rats adhered to the ARVO

resolution on the Use of Animals in Research and to the guidelines of the UNTHSC

Committee on Animal Welfare. Following the experimentation period, all rats were

euthanised by an i.p. injection of pentobarbital (100 mg·kg^{-1}). Comparisons between groups

of various mmHg days of IOP elevation were made using one-way ANOVA and multiple

comparison tests at $P < 0.05$. Rats ($n = 3$) were also injected with isotonic saline (sham) into

one eye and kept under the same conditions as those that received hypertonic saline for 90

days. Rat eyes were dissected and either fixed in formalin for immunohistochemistry (IH),

processed for Western blotting or Q-PCR. The contralateral eye served as the control.

Extraction of DNA and DNA laddering

DNA extraction was done as described by the manufacturer's protocol. (Invitrogen, Carlsbad, CA, K1800-01, http://www.invitrogen.com/content/sfs/manuals/easydna_man.pdf) Briefly, cells were pelleted and resuspend in PBS before adding solution A (reagent from the kit, composition unknown). Cells were incubated at 65 °C for 10 minutes before adding solution B (reagent from the kit, composition unknown). Then chloroform was added and then centrifuged at 4 °C to separate phases. The upper phase was collected and added 1 mL of cold 100 % ethanol before incubating on ice for 30 minutes followed by centrifuging. Then cold 80 % ethanol was added followed by centrifuging. The pellet was air dried and then resuspended in 100 μL TE buffer. Last, RNase was added and incubated at 37 °C for 30 minutes. DNA was stored at 4 °C and was ready to use. DNA concentration was measured by detecting the absorbance at 280 nm. Then 1.5 % gels were run with each lane having 10 μg DNA.

Apoptotic analysis

This test was performed as previously described (Yamamoto et al., 2001). Briefly, RGC-5 cells were subcultured in 100-mm culture dishes in DMEM containing 10 % FBS. The culture dishes were placed in a controlled atmosphere culture chamber (Bellco), a humidified airtight apparatus with inflow and outflow valves, into which a mixture of 95 % N_2 and 5 % CO_2 was flushed for 15 min at a flow rate of 4 L/min. The chamber was sealed to maintain the gas composition and kept at 37 °C. After exposure to hypoxia for the indicated

periods (from 1 to 4 h), the cells were processed for Western blotting, Q-PCR and IH as described in previous sections. To evaluate the effect of hypotonic shock on AQP9 mRNA, cells were exposed to media that was diluted 1:1 in sterile water. Hypertonic shock was induced by adding additional 50 mM NaCl.

Flow cytometry

Cells were grown in 100-mm dishes until confluency. Medium was collected in separate tubes before rinsing cells twice with room temperature PBS. Cells were collected by trypsin digestion (Sigma, T9935) in 10-mL tubes and centrifuged and rinsed with PBS before resuspending in 1 mL 1X PBS. Cell pellets were fixed in 3 volumes of cold 100 % ethanol for at least 30 minutes. After removing ethanol, the cell pellets were resuspended in PBS before treating with ribonuclease (final concentration 100 µg/ mL) for 30 min at 37 °C. Propidium iodide (final concentration 20 µg/mL) was added to stain cells for 30 min at room temperature. Flow cytometry analyses were done by Cytomics FC 500 Series Flow Cytometry Systems with CXP software (Beckman Coulter, Fullerton, CA). Analyses by flow cytometry were conducted within one hour.

Statistical analysis

All experiments were repeated at least twice with up to 3-4 replicates per condition each time. Statistical significance was determined by using one-way analysis of variance (ANOVA) and the Tukey multiple comparison tests at $P < 0.05$.

RESULTS

Project 1

In order to identify the existence of any water channels in retinal ganglion cells, a technique of detecting cell volume changes was used. Fura-2 is an intracellular fluorescent dye with an emission at 510 nm. When the concentration of calcium increases fura-2 fluorescence increases, the absorbance at excitation wavelength at 340 nm increases along with decreasing absorbance at 380 nm. This characteristic fluorescent response to increasing calcium concentrations of fura-2 results in a calcium independent absorbance at 360 nm, called the isosbestic point. At the isosbestic point, the absorbance is independent of the concentration of calcium but sensitive to cell volume changes. Thus, when the cell volume decreases, the intensity of fluorescence increases, so the concentration of dye increases; therefore, the baseline of the isosbestic point will increase. As a result, the fluorescence change is directly responding to the cell volume (Muallem et al., 1992). Fig. 7a and b show the fluorescent responses when cells were in isotonic and hypotonic (20%) solutions. During this experiment, no cellular lysis observed. In addition, the fluorescence intensity lessened slowly after the low osmolarity medium replaced the isotonic solution (Fig. 8a). Although the rate of fluorescence intensity change was slow, it cannot be explained by simple diffusion, whose response is passive and extremely slow. Fig. 8b and c show the results using AQP9 inhibitors, phloretin (40 μM) and α-cyano-4-hydroxycinnamic acid (CIN, 60 μM). Cells were treated with phloretin or CIN for 8 min prior to the hypotonic shock, which prevented the decrease of fluorescence intensity by preventing swelling. These observations infer the possible role of a water channel in osmoregulation of RGC-5 cells.

To confirm the presence of an AQP9 water channel, both techniques of PCR and Western blotting were used. Fig. 9 shows the bands obtained from PCR using RGC-5 cells and differentiated RGC-5 cells. Fig. 10 shows the presence of a doublet of 35 and 50 kDa proteins of a Western blot using RGC-5 cells; these molecular weights correspond are at what has been reported for AQP9. In addition, when AQP9 competing antigenic peptides were used, no labeling was shown (Fig. 10b). Differentiated RGC-5 plasma membrane fractions also showed the same bands in Western blotting (data not shown). Moreover, PCR products were sequenced and matched AQP9 in the BLAST database.

After identifying the presence of AQP9 in retina ganglion cells, it remained to be determined if AQP9 was also expressed in organelles other than the plasma membrane. Immunocytochemistry and immunohistochemistry are good techniques for localization of molecules within cells. Fig. 11 shows the co-localization of AQP9 and Thy-1, an RGC marker, obtained from primary RGC cultures. Fig. 12 shows the co-localization of AQP9 and Thy-1 obtained from the retinal ganglion cell layer of the rat retina. Fig. 13 shows the co-localization of AQP9 and cytochrome c in RGC-5 cells. Fig. 14 shows the co-localization of AQP9 and adenine nucleotide translocator (ANT), an inner mitochondrial membrane (IMM) marker. These findings suggest that AQP9 is expressed on both IMM and PM of RGCs.

Project 2

Glaucoma patients have a high level of endothelin-1 in their aqueous fluid, and indeed, the high level of ET-1 appears to damage the optic nerve head and causes axonal loss. Rats administered intravitreous injection of ET-1 can be used as a "quick" glaucoma model since the optic nerve head is damaged similarly to a glaucoma model but the ganglion cell loss

occurs more quickly (Taniguchi et. al., 2006). For this model, 23 rats were sacrificed: 8 for mRNA studies, 11 for protein studies and 4 for protein distribution studies. Results were obtained after 48 hrs post ET-1 injections.

Fig. 15 shows the effect of intravitreal injection of ET-1 on AQP4 mRNA expression in the retina by Q-PCR. A significant reduction was observed in five out of seven rates (71 %) when compared with HEPES-injected (vehicle) samples. The protein analysis had a similar finding as shown in Fig. 16c. Nine out of 11 rats (82 %) had a decreased expression. Fig. 16a shows the data from three rats where C is the control sample and T is the treated one. All of the AQP4 isoforms (~30, 37, 87 and 100 kDa) had a significant reduction of protein expression after normalization with α-tubulin protein expression (Fig. 16b).

When analyzing AQP9 mRNA expression, six out of seven rats (86 %) had a reduction in mRNA expression compared with HEPES-injected samples following ET-1 administration as shown in Fig. 17. Although changes in AQP9 mRNA expression were observed, there were no apparent differences in AQP9 protein expression.

GFAP, glial fibrillary acidic protein, is a marker of astrocytes and increases in expression are an indication of astrogliosis. Fig. 18a shows the up-regulation of GFAP protein expression. Caspase-3 is an apoptosis indicator; its protein expression was up-regulated as shown in Fig. 18b. Both protein expression data were from six rats, and all six rats had an increased expression (100 %). Thy-1 is a marker for retinal ganglion cells; its protein expression was down-regulated as shown in Fig. 18c. XIAP, X-linked inhibitor of apoptosis protein, is a blocker of caspase-3; it also was down-regulated from the protein expression as shown in Fig. 18d. Both protein expression data were from three rats, and all three rats had decreased expression (100 %).

A widely accepted animal glaucoma model is the Morrison glaucoma model. These rats develop an elevated IOP after administration of hypertonic saline into the aqueous vein of the rat eye. Rats' IOP were monitored, and they were sacrificed when the elevated IOP reached > 200 mmHg days (the pressure over certain days). This process can take 30 to 90 days. For this model, 19 rats were sacrificed: 8 for mRNA studies, 7 for protein studies and 4 for protein distribution studies.

A slowly developing elevated IOP is characteristic of the Morrison model. Fig. 19a and 19b are examples of the intraocular pressure measurement of rats. The average baseline IOP for treated and untreated eyes was 21 mmHg before the surgery. The average IOP of the treated eyes was 30 mmHg. Each rat IOP was reported as mmHg days by calculating the area-under curve (AUC, the pressure measurement), which is the IOP-integral difference of IOP elevation over days of exposure between the treated and untreated eyes. All eyes in the Morrison model were grouped as either low IOP, corresponding to 264±68 mmHg days (un-treated eyes) or high IOP, corresponding to 694±130 mmHg days (treated eyes) as shown in Fig. 20. In addition, rats with isotonic saline injection (sham) showed no increase in IOP (maintained for up to 90 days after surgery).

Although eight rats were used in mRNA studies (most literature use n=3), the data was inconclusive for AQP4. A clear animal variation was observed with four rats showing an up-regulation and four rats showing down-regulation. A possible explanation is timing of the activation of astrocytes. AQP4 expressed in astrocytes is the main AQP4 expression in the retina, and activated astrocytes have a remarkable up-regulation of AQP. Interestingly, when analyzing AQP4 protein expression, different isoforms responded differently to elevated IOP. Fig. 21 shows the Western blot of AQP4 using α-tubulin for normalization. The smaller

isoform of AQP4 showed a decreased expression whereas the higher molecular weight isoform (ubiquitinated forms) had increased expression. Both results were concluded from five of seven rats (71 %). In addition, the high IOP group had a more profound effect than the low IOP group.

With contradistinction of ET-injection, AQP9 expression was up-regulated in eyes with elevated IOP. Fig. 22 shows that AQP9 mRNA expression was up-regulated significantly in five out of eight rats (63 %). AQP9 protein levels had a similar increase in six out of seven rats (86 %) as shown in Fig. 23. Again, higher IOP causes a greater effect on expression when comparing the high and low IOP groups. GFAP protein expression and Thy-1 protein expression showed increases following IOP elevation, similar to that seen with ET-1 administrations; six out of six rats (100 %) had increased expression (Fig. 24). The expression of caspase-3 mRNA was increased in agreement with the caspase-3 protein expression pattern seen in the ET-treated group (Fig. 25).

Immunohistochemistry using confocal technology also can demonstrate protein expression patterns using co-localization of two different proteins. The current instrument can qualitatively distinguish up- or down-regulation. Fig. 26 shows the co-localization of AQP9 and RPE65 (RPE cell marker). The upper panel used goat anti-AQP9 whereas the lower one used rabbit anti-AQP9 demonstrating that both antibodies localizing to the same area. As expected, AQP9 was also detected in the retinal ganglion cell layer as shown in Fig. 27 using antibodies of AQP9 and Thy-1, a RGC marker. The effect of elevated IOP on the RPE layer was not clear, but less labeling for both AQP9 and Thy-1 was observed. This is reasonable, because elevated IOP primarily damages the RGC layer.

The rat optic nerve head (ONH) has similarities to the human ONH and are classified into 3 regions (Morrison et al., 1997). (1). The neck region: located at the level of the sclera. (2). The transition region: an extension zone below the neck region. (3). The posterior region: characterized by myelinated axons. Astrogliosis is characterized by increased labeling of GFAP and altered extracellular matrix (ECM) protein expression is observed in glaucomatous ONH (Hernandez, 2000; Varela and Hernandez, 1997).

Fig. 28 shows the co-localization of AQP4 and GFAP. This co-localization was observed in all three regions of the ONH with more cells stained following elevated IOP samples. A similar observation was found in co-localization studies of AQP9 and GFAP as shown in Fig. 29. Moreover, when analyzing AQP4 and AQP9 distribution in ONH, both AQPs were expressed in the same regions with enhanced expression upon the elevation of IOP as shown in Fig. 30. However, it is not certain if AQP4 or AQP9 expression is augmented in ONH astrocytes exposed to IOP elevation.

Glutamine synthetase (GS) is a Müller cell marker and the expression increases upon an elevation of IOP (Carter-Dawson et al., 2004; Woldemussie et al., 2004). Fig. 31 shows the co-localization of AQP4 and GS with more stained Müller cells and stronger staining of AQP4 following elevation of the IOP. This suggests an increased AQP4 expression in Müller cells. Combined with Western blotting data, this increase may represent ubiquitinated AQP4. This suggests that the elevation of IOP causes an activation of the proteasomal system in Müller cells.

Project 3

Hypoxia /ischemia damages retinal ganglion cells similar to what is seen in glaucoma. The response of RGC-5 cells to hypoxia was primarily examined using methods of Q-PCR and Western blotting.

When examining the hypoxia effect using immunoblotting, RGC-5 AQP9 protein expression was up-regulated following a three and four hour hypoxia treatment while one and two hour treatments had no significant effect (Fig. 10). Next, the quantitative reverse-transcript PCR technique was employed to observe if the hypoxia-induced stress had the same effect on AQP9 mRNA expression as seen with protein expression. This will indicate if transcriptional regulation was involved. As shown in Fig. 32, hypoxia induced an up-regulation of AQP9 mRNA by ~ 70 % after one to three hour hypoxia. Hence, hypoxia increased both AQP9 mRNA and protein expression.

A semi-quantitative apoptotic detection method was used to asses cell death and involves the process of extracting low-molecular-weight DNA for DNA fragmentation patterning. This method worked well when the majority of cells went through apoptosis. Fig. 33 shows the DNA fragmentation patterns after hypoxia treatment for several time points. However, it is possible that DNA degradation may not proceed to internucleosomal regions but stops at 50-300 kb fragments (Oberhammer et al., 1993). When this happens, the amount of extracted DNA fragment is not proportional to the apoptotic cells. Fig. 34 shows the DNA fragmentation patterns with various treatments including channel inhibitors with or without hypoxia. There was no noticeable difference between the two AQP9 inhibitors.

One common technique to assess cell apoptosis is flow cytometric analysis (FCM) with DNA dyes. Two characteristics of apoptosis are cell shrinkage and an increase in granularity,

and FCM can detect and quantify these properties. The membrane integrity of nonviable cells is lost, and this causes cells to become permeable to dyes. Propidium iodide (PI) is a popular DNA-binding dye. PI is relatively inexpensive and easy to use, but its DNA-intercalating reaction is reversible causing leakage of dye. Thus, it is advisable to start FCM analysis right after the 30-min incubation of PI. Apoptotic cells have reduced DNA stainability because of the partial loss of DNA due to the activation of endogenous endonucleases and the diffusion of low molecular weight DNA products. Thus, cells with lower DNA stainability than that of normal phase cells (G_0/G_1, S, and G_2/M) are considered as a marker of cell death by apoptosis, as sub-G_0 (Darzynkiewicz et al., 1992). Fig. 35 shows FCM diagrams of RGC-5 cell profiles after 24-hour treatments with AQP9 inhibitors, CIN, phloretin, and vehicle (methanol). Fig. 36 shows RGC-5 cell populations after 24-hour hypoxia treatment. Interestingly, FBS combined with hypoxia treatment caused more damage than the hypoxia treatment alone. Mercuric chloride ($HgCl_2$) is commonly used as an aquaporin inhibitor. Fig. 37 (a) shows no significant difference among treatments. In Fig. 37 (b), mercuric chloride may be protective under the hypoxia condition.

Project 4

U373MG, an astrocytoma cell-line, can be used to study astrocyte responses *in vitro*. AQP4 is predominantly expressed in astrocyte plasma membrane (Ma et al., 1997; Nicchia et al., 2000) but absent from neurons (Ma et al, 1997; Frigeri et al., 1995). Results from AQP4 knockout mice suggest that AQP4 is the main water channel for water transport in astrocytes (Manley et al., 2000; Papadopoulos et al., 2004); such a suggestion was verified by RNA interference (RNAi) (Nicchia et al., 2003). AQP4 may play an important role in brain edema

(Wen et al., 1999), but the regulation of AQP4 has not been fully understood. Degradation of misfolded and damaged proteins through ubiquitination is known for some channel proteins, such as Cl⁻ channel and aquaporin-1 (Zheng et al., 2002; Leitch et al., 2001). In order to confirm that AQP4 is targeted in an ubiquitin-proteasomal degradation pathway, cell swelling measurement, Q-RT-PCR, immunoblotting and immunocytostaining were used.

Fig. 38 shows the isoforms of AQP4 (32, 37, 87, and 100 kDa) by Western blotting. Mg132 and lactacystin are proteasomal inhibitors and caused increased expression of the 32 kDa isoform (Fig. 38a). Fig. 38b shows the normalization data using α-tubulin antibodies. Ubiquitinated proteins can be purified by an S5a affinity column, and Fig. 38c shows the result. AQP4 isoforms of 87 and 100 kDa were recognized after the cellular lysate was treated with an S5a affinity column. In agreement with protein data, AQP4 immunoreactivity after Mg132 treatment was up-regulated in the area around the nuclei (stained by DAPI) (Fig. 39). However, Q-RT-PCR shows no significant increase in AQP4 mRNA expression by Mg132 treatment (Fig. 40). Fig. 40 also shows the up-regulation of AQP4 mRNA by hypotonic shock at 4 hours.

To test the effect of Mg132 (10 μM) on cellular volume, U373MG cells were treated with inhibitor or vehicle (dimethyl sulfoxide, DMSO). The rate of swelling was calculated by measuring the difference in fluorescence readings divided by time. Fig. 41 shows the effects of Mg132 and DMSO on cellular swelling rates. Although DMSO caused a small degree of swelling, the effects of Mg132 were significant after 1.5, 4, and 18 hours of hypoxia treatment.

Project 5

Osmolarity plays an important role in keeping cells alive. Studies of cell response to hypotonic stock may provide hints of cell survival mechanisms. Retinal pigment epithelium (RPE) is a protective layer for the retina. When RPE cells were treated under hypotonic shock for 0.5, 1, 2, 3, or 4.5 hours, their AQP9 mRNA expression responded differently (Fig. 42). At the 0.5 and 3 hour periods, mRNA expression was up-regulated while there were no changes at the 1 and 2 hour periods. Interestingly, mRNA expression was down-regulated at the 4.5 hour period. As shown in Fig. 43, RPE cells responded strongly to hypoxia by up-regulation of mRNA. RGC5 cells responded to hypotonic shock by up-regulation of AQP9 mRNA (Fig. 44).

DISCUSSION

Project 1

Neurons normally maintain a constant volume in isosmotic media and balance their volume during release of neurotransmitters and hormones following nerve impulses (Serve et al., 1988; Alvarez-Leefmans et al., 1992). Retinal ganglion cells (RGCs) are no exception. It was proposed that RGCs utilize a water channel to regulate the cell volume in addition to other responsive mechanisms (e.g. ion transport systems) for regulatory volume decreases (RVD) or increases (RVI). In order to monitor cell volume changes, various techniques have been employed including the use of a water channel inhibitor.

There are several techniques developed for cell volume measurements. Light scattering is sensitive but requires complement techniques. Cells are kept in a perfusion chamber and monitored by a photomultiplier. The volume changes must be calculated using a series of formuli (Echevarria and Verkman, 1992; Kuang et al., 2006). The use of radioisotopes to detect total volume has a poor detection limit, as an osmotic change must be greater than 5 % before detection is noted (Parker, 1993). Coulter counter methods require cells to be in suspension without aggregation. Cells are suspended in an electrolyte solution drawn through an aperture. This process momentarily increases the impedance of the aperture and produces a pulse, which is directly proportional to the three-dimensional volume of the cell (Civan et al., 1992). Electrophysiological methods need membrane permeabilization for loading of an impermeable ion (Adorante, 1995). The method of fluorescence quenching has a good signal-to-noise ratio of 25, but it has a dependency on chloride ions. The lifetime of the fluorescent dye (SPQ) is reduced by seven-fold without chloride ions. The analog of SPQ, which is chloride ion insensitive, has a rapid dye leakage problem (Spinvias and Bonanno,

1997). The method chosen for our studies was adapted from the method based on dye dilution from Muallem et al. (1992). It utilizes a calcium florescent dye, Fura-2/AM (acetoxymethyl ester), which is a dual wavelength excitation fluorescent calcium probe that has an isobestic point at 360 nm. That is the excitation wavelength that is independent of calcium concentration. Changes in absorbance at this wavelength are independent of changes in cell calcium but reflect changes in cell volume.

The time for the half maximal swelling in RGC-5 cells was 4.6±0.5 minutes, which is higher than other known aquaporin-dependent half-times (seconds) reported by Srinivas and Bonanno (1997), using a fluorescence quenching method (fluorescent dye, SPQ, and intracellular quenchers, ICQs) in cultured bovine corneal endothelial cells (CBCECs), and by Kuang et al. (2006) using a light scattering technique in CBCECs. However, data from Jakab et al. (2006) had a half maximal swelling of ~ 2 minutes in GH4/C1 pituitary tumor cells using a video imaging system (CCD camera) measuring the cell's diameter. Additionally, reports from Altamirano et al. (1998) showed a half maximal swelling of 2.2 and 2.5 minutes using calcein and Fura-2/AM, respectively, in murine neuroblastoma cells. Thus, the difference between our results and others' may be due to different cell types, different assay methods and/or different instrument sensitivities.

Phloretin, a sap-soluble pigment extracted from the root bark of apple trees, was used to inhibit the water channel during the cell volume changing experiment (Seshadri, 1951). Phloretin was used as an AQP9-specific inhibitor in different concentrations among different cells. Cheung et al. (2003) used 100 μM on Xenopus oocytes (AQP9 cloned from rat epididymis) and Tsukaguchi et al. (1998) also used 100 μM on Xenopus oocytes (AQP9 cloned from rat liver). Similarly, Ford et al. (2000) used 100 μM phloretin on rat proestrus

oocytes, which express AQP9 naturally. Whereas, Aharon and Bar-Shavit (2006) used only

50 μM on bone marrow macrophages, but cells were incubated with phloretin for 48 hours.

Satisfactory inhibition of osmotic water permeability was reported in these studies. However,

other phloretin concentration-dependent inhibitory effects were ignored. Phloretin inhibited

the Na^+-independent glucose transporter (glucose uniporter, GLUT) at 50 μM (Kasahara and

Kasahara, 1996), the urea transporter at 100-350 μM (Ishibashi et al., 1994), the Na^+-

dependent dicarboxylate transporter, SDCT1, at 500 μM (Chen et al., 1998), and myo-

inositol release at 200 μM (Reeves and Cammarata, 1996). The concentration of phloretin

used in our experiment was 40 μM, which was much lower than the concentrations needed to

inhibit other channels as previous studies indicated. Therefore, our result should mainly

reflect the inhibition of AQP9, although effects on other transporters cannot be ruled out.

Alpha-cyano-4-hydroxycinnamic acid (CIN or CHC) is a monocarboxylate transporter

(MCT) inhibitor. Fig. 8 shows that CIN inhibited hypotonic-induced swelling, which

suggests the involvement of MCT in RGC-5 cell volume regulation. However, Winkler et al.

(2004) reported that RGC-5 cells produce lactate slowly (0.28 mM/10^6 cells in 4 hours) and

thus changes in this product may not be involved in acute volume regulation. Although

Wang et al. (2006) used CIN and phloretin to inhibit D-lactate uptake, CIN was not known as

an aquaporin inhibitor, but it remained possible that CIN worked as an AQP9 inhibitor.

AQP9 is also known to transport lactate, and that solutes and water appear to share a

common pathway in AQP9 (Tsukaguch et al., 1998). When CIN was used as an MCT

inhibitor, the effective concentrations were 200 μM and 250 μM (Wang et al., 2006; Ruiz-

Sanchez and O'Donnell, 2006). Our study used 60 μM, which was lower than the known

effective concentrations. It was unclear if 60 μM was effective to inhibit AQP9. Further studies are needed to answer this question.

When identifying AQP9 in RGCs, both primary and secondary (differentiated and undifferentiated) cultured cells were used in addition to the whole retina. The *in vitro* PCR and Western blotting data were mainly based on undifferentiated RGC-5 cells, a transformed rat retinal ganglion cell line. The benefits of using a stable cell line were the ease of maintaining cell growth and the production of large quantities of cells. However, it was always questioned whether this transformed cell line was functioning like primary cells. RGC-5 cells have been proven to express many neuronal cell markers including Thy-1, a glycoprotein mainly expressed in retinal ganglion cells (Barnstable and Drager, 1984; Krishnamoorthy et al., 2001) and Brn-3C, a POU domain transcription factor expressed exclusively in retinal ganglion cells (Xiang et al., 1995; Krishnamoorthy et al., 2001). Moreover, RGC-5 cells were negative for other retinal cell markers including GFAP (Müller cells and astrocytes), HPC-1 (amacring cells), and 8A1 (horizontal cells). In addition, several RGC receptors were expressed in RGC-5 cells such as N-methyl-D-aspartate (NMDA) receptors, GABA-B receptors and neuortrophin receptors (Krishnamoorthy et al., 2001). However, the sensitivity of receptors in RGC-5 cells may have been altered. RGC-5 cells respond to 5 mM glutamate, whereas primary RGCs respond to 5-500 μM glutamate (Aoun et al., 2003; Otori et al., 1998; Pang et al., 1999; Govindaiah et al., 2002; Otori et al., 2003). Thus, the usage of differentiated RGC-5 cells became important.

Some characteristics of RGC-5 cells, including morphology, changed after being cultured for four days in human non-pigmented ciliary epithelial (HNPE) conditioned medium. These new characteristics appeared following differentiation of RGC-5 cells.

However, the factors (proteins) inducing differentiation have not yet been identified. These differentiated RGC-5 cells had longer axons and more neurite outgrowth, which had morphological characteristics similar to primary RGCs (Barres et al., 1998). Moreover, these RGC-5 cells had enhanced Thy-1 expression (compared with undifferentiated RGC-5 cells), responded to glutamate in concentrations of 50 μM, 250 μM, and 500 μM, and expressed Brn-3B, a POU-IV class RGC transcription factor involved in RGC differentiation (Liu et al., 2000). Both differentiated and undifferentiated RGC-5 cells showed AQP9 mRNA expression (Fig. 9) and protein expression (Fig. 10).

The presence of AQP9 was also examined in primary RGCs and the retina by immunostaining. Primary RGCs more closely resemble the native intact RGCs, but the preparation is extremely time consuming, laborious, and has a low yield. The number of cells obtained was usually barely enough for immunocytochemistry studies. Fig. 11 shows the co-localization of Thy-1 and AQP9 in primary culture. Fig. 12 shows the co-localization of Thy-1 and AQP9 in the RGC layer of the retina.

Mitochondria are the power plants of the cell involving metabolic and bioenergetic activities, such as respiration and ATP production. Most studies on mitochondrial function and dysfunction have been focused on the bioenergetic aspects. However, recently, water channels, AQP8 and AQP9, were found in the inner mitochondrial membrane (IMM) (Calamita et al., 2005; Amiry-Moghaddam et al., 2005). What role the water channel transport pathways play in mitochondria is not known, but they could participate in mitochondrial volume homeostasis.

Mitochondrial volume homeostasis is crucial because any dysfunction in this pathway may affect regulated oxidative capacity, mechanical signaling and, ultimately, apoptosis

(Safiuline et al., 2006; Desagher and Martinou, 2000; Lee and Thevenod, 2006; Garlid and Paucek, 2003). The finding of the expression of water channels in the IMM may provide insight into new molecular mechanisms and pathways involving AQP9 and AQP8, including providing pathways for other solutes besides water (Calamita et al., 2007). We have shown the co-localization of AQP9 with cytochrome c, a mitochondrial marker, and co-localization of AQP9 with adenine nucleotide translocator (ANT), an IMM marker, suggesting that AQP9 in RGCs may be important in mitochondrial function in these cells.

Mitochondrial pathological swelling involves the import of ions and water into the matrix leading to the unfolding of the cristae of the IMM, the disruption of the outer membrane (OMM), and the spill of intermembrane contents into the cytosol (Bernardi, 1996). Proapoptotic factors (e.g. cytochrome c and apoptosis-inducing factor) are then released (Liu et al., 1996; Susin et al., 1999). Thus, knowing the role of aquaporins in IMM may help prevent cell death. Lee and Thevenod (2006) suggested that mitochondrial aquaporins may mediate water transport in physiological and pathophysiological conditions. Calamita et al. (2006) reported the finding of high permeability for both mitochondria and their membrane subcompartments, but they suggested that AQP8, the Hg^{2+}-sensitive aquaporin, does not play a role in mitochondrial volume homeostasis. Calamita's report, agreed to by Yang and coworkers' (2006), provided evidence against functionally significant aquaporin expression in mitochondria using AQP8 knockout mice. However, there was no work on AQP9. More research is needed to determine the functional significance of aquaporins in IMM.

Project 2

A possible relationship between aquaporins and glaucoma has been appreciated only recently. Zhang et al. (2002) and Verkman (2003) suggested that the inhibition of AQP1 or AQP4 may reduce the intraocular pressure (IOP) in glaucoma patients. This was based on observations that mice lacking AQP1 alone or AQP1/AQP4 together had a significant reduction of aqueous fluid production and a lowered IOP. However, elevated IOP may not be observed in all glaucoma patients, although retinal ganglion cell damage is the same end result in all patients. AQP4 is strongly expressed in astrocytes, which are supportive cells to retinal ganglion cells (RGCs); AQP9 is expressed in RGCs and may have important physiological roles. This project used animal models to explore the possible relationship between aquaporins and glaucoma in addition to its possible role in neuron supportive cells.

An upregulation of the intermediate filament protein, glial fibrillary acidic protein (GFAP), is a cellular marker for retinal injury; the immunoreactivity of GFAP is often used as a gliosis index (Hernandez, 2000). Figs. 18 and 24 show an increase in GFAP protein levels using retina samples from two retina injury models - intravitreous ET-1 injection and the Morrison model of glaucoma. In addition to the Western blotting results, increased GFAP labeling was also observed at the rat optic nerve head (ONH) exposed to elevated IOP (as shown in Figs. 28 and 29, Morrison model). Our data agree with reports from Johnson et al. (2000) and Prasanna et al. (2005). Several reports showed an upregulation of GFAP upon elevation of IOP. Tanihara et al. (1997) showed the upregulation of GFAP mRNA, whereas Yu et al. (2006) showed the upregulation of GFAP protein without increased GFAP mRNA. Lau et al. (2006) used the model of intravitreous ET-1 and also reported increased GFAP

expression. More importantly, increased GFAP staining was observed in astrocytes at the ONH of primary open angle glaucoma (POAG) patients (Hernandez, 2000).

In addition to the increased GFAP expression in ONH, the expression of AQP4 and AQP9 were also increased in the Morrison model as shown in Figs. 29 and 30. This suggests that the IOP elevation may cause increased expression of AQP4, AQP9, and GFAP and may be related to glial activation at the ONH. Indeed, Xue et al. (2006) reported that elevated IOP induced Müller glial cell activation manifested by increased GFAP expression and suggested the metabolic change of cells in response to the degenerative changes of their neighboring ganglion cells. Thus, the changes of water channel expression may be compensatory to the damage caused by elevated IOP. The lack of selective aquaporin inhibitors may prevent an evaluation of whether AQP4 /AQP9 inhibition is harmful in glaucomatous conditions, although Manley et al. (2000) showed AQP4 knock-out mice had a better survival rate after ischemic stroke.

A number of studies showed that aquaporin expression levels vary upon insults. For example, Arima et al. (2003) showed that hyperosmotic stress can induce expression of AQP4 and AQP9. Yamamoto et al. (2001) reported that the expression of AQP4 and AQP9 decreased under hypoxic conditions. As shown in Figs. 22 and 23, elevated IOP increased both AQP9 mRNA and protein expression from the retinal extract of the ET-1 injected model. However, it was unclear what cell types the expression was derived. Both astrocytes and RGCs, even RPEs, express AQP9. Laser capture microdissection (LCM) is a method for obtaining single type cells from specific microscopic regions of tissue sections. Under the microscope, tissues are heterogeneous, complicated structures with hundreds of different cell types. The retina has ten layers, and each layer contains heterogeneous elements. For

example, the retinal ganglion cell layer is mainly composed of RGCs and amacrine cells. Therefore, microdissection is essential for molecular analysis to study details. The microdissected cDNA libraries are designed to approximate the true pattern of gene expression of the cell subpopulations in their actual tissue milieu. LCM may provide new details for AQP9 expression.

The up-regulation of AQP9 upon elevation of IOP may be related to lactate transport. It has been proposed that glucose is converted into lactate and then released into the extracellular space (ECM) by Müller cells and astrocytes and thus can serve as fuel for neurons (Pellerin, 2005). Schurr et al. (2001) reported the blockade of lactate transport exacerbated neuronal damage in a rat model of ischemia. Cater et al. (2001) reported the possible protective role of lactate to neurons during glucose deprivation. Indeed, when glucose and lactate compete, glucose is the primary brain metabolic fuel. However, it has been shown that the lactate-producing cells in the brain were not neurons, but probably astrocytes, with neurons using the generated lactate (Serres et al., 2004). Although lactate can be transported by the monocarboxylate transporters (MCTs), lactate can also be transported by AQP9. Unlike other water channels (aquaporins or aquaglyceroporins), AQP9 is permeable to a wide variety of non-charged solutes due to the ability of having a solute-induced change (Viadiu et al., 2007). Additionally, Melena et al. (2003) showed that lactate transport blockade had no effect on retinal ischemia. Thus, the up-regulation of AQP9 may help transport lactate and may be beneficial.

The retinal pigment epithelium (RPE) is packed tightly with hexagonal-shaped cells in one layer. These pigmented cells have tight junctions and melanin deposits. It is the layer of the retina facing the choroid, which plays an important barrier function for the retina. Fig. 26

shows the detection of AQP9 in the RPE layer. AQP9 may play a role in eliminating lactate accumulated in RPE by transferring lactate to the blood (Adler and Southwick, 1992).

As discussed before, down-regulation of AQP4 in the brain may have positive or negative results. AQP4 deletion improves the outcome of cytotoxic edema but worsens vasogenic (noncellular) edema. Fig. 28 shows the patterns of AQP4 and GFAP and suggests an up-regulated expression of AQP4 in astrocytes from the retina of eyes of elevated IOP. Da and Verkman (2004) reported that AQP4 deletion in mice is neuroprotective in a transient ischemia model of retinal injury. It is known that elevated IOP causes ischemia / hypoxia. Thus, the elevated IOP induced up-regulation of AQP4 expression in astrocytes may be harmful. Fig. 31 shows the up-regulation of AQP4 in Müller cells. This may be harmful, too. Müller glial cells mediate water transport within the inner retina and are responsible for neuronal cell swelling during ischemia. The water-absorbing function of Müller cells is coupled to its K^+ clearance function (Nagglhus et al., 1999). The co-expression of AQP4 and K^+ channels suggests that osmotic gradients between the retina and the blood and vitreous can be compensated by K^+ and water influxes and effluxes from Müller cells. As a result, water movement inhibition in the post-ischemic phase may prevent cytotoxic Müller cell swelling but impair the fluid clearance of vasogenic (non-cellular) edema (Bringmann et al., 2005).

Müller cells are the neuron-supporting microglial cells that span the retina between the external and internal limiting membranes. Müller cells control the metabolic activity of neurons including glucose uptake and neurotransmitter recycling in addition to CO_2 and K^+ buffering. Compared with neurons, Müller cells are more resistant to ischemia or hypoglycemia and may survive most retinal injuries (Bringmann et al., 2006). Glutamine

synthetase (GS) is a Müller cell-specific enzyme involved in neurotransmitter recycling and is considered a cellular marker for retinal injury (Chen and Weber, 2002). Fig. 31 indicates the up-regulation of GS in Muller cells upon elevation of IOP. Our data is in agreement with Woldemussie et al. (2004) and Carter-Dawson et al. (2004) who showed increased GS immunoreactivity in rats and monkeys upon elevation of IOP, respectively. In fact, GS expression levels in the retina depend on the type of injury. For example, rat retina damaged by light decreased the expression of GS in Müller cells (Grosche et al., 1995), whereas Reichenbach et al. (1995) reported enhanced expression during hepatic retinopathy. In addition, Chen and Weber (2002) observed no changes in GS expression in Müller cells after optic nerve crush. Most importantly, Tezel et al. (2005) identified GS as an oxidized protein following elevation of IOP in rats.

Although Müller cells normally do not express GFAP, they start to express GFAP upon elevation of IOP (Xue et al., 2006a). Figs. 18 and 24 show an up-regulation of GFAP in retinal extracts upon ET-1 injection and elevation of IOP. This agrees with Xue et al. (2006b) and Chang et al. (2007) who showed up-regulation of GFAP in injured retina.

In parallel with the finding of McKinnon et al. (2002), the elevation of IOP was accompanied by increases in caspase-3 expression. This is no surprise because increases in IOP cause ischemia, which induces apoptosis. Our data showed a decline in Thy-1 expression levels, which agrees with reports by Schlamp et al. (2001) and Nash and Osbourne (1999). This is expected, because the RGC layer was remarkably thinned in our animal models.

Finally, there appears to be a distinction between two models of retinal injury employed in the current study. While ET-1 intravitreal injection and the Morrison model

produced similar increased expression in GFAP and caspase-3, ET-1 injection decreased

AQP4 and AQP9 mRNA levels and AQP4 protein levels. To the contrary, the Morrison

model had increased AQP9 mRNA and protein levels while producing variable effects on

AQP4. This difference probably relates to the severity of the insult. ET-1 has been shown to

produce a more rapid reduction in the retinal ganglion cell number and thus perhaps a loss of

AQP9 from these neurons, whereas elevation of IOP produces a more gradual loss of RGCs.

Project 3

The ultimate cause of vision loss in glaucoma is thought to be the apoptosis of retinal

ganglion cells (Quigley et al., 1995). The RGC-5 cell line is a permanently transformed cell

culture system, which may provide a convenient avenue to study the mechanisms of

apoptotic cell death because RGC-5 cells proliferate and double in ~ 24 hours. Additionally,

TUNEL assay showed that serum deprivation produced apoptosis of RGC-5 cells; this

suggests that RGC-5 cells are dependent on trophic support for survival, which is one of the

characteristics of neurons. This complies with the hypothesis in glaucoma that the blockage

of retrograde axonal transport of neurotrophins may induce RGC apoptosis (Krishnamoorthy

et al., 2001). Using serum deprivation as an *in vitro* apoptotic model has been reported for

several cell lines (Wadia et al., 1998; Elizbeth et al., 2004). Other than growth factor

withdrawal, hypoxia and ischemia are also commonly used for apoptotic studies. Several

studies used hyopoxia /ischemia conditions to mimic brain damage, such as brain edema.

AQP4, often referred to as the brain water channel, is mainly expressed in astrocytes. Both

hypoxia and ischemia induce up-regulation of AQP4 (Kaur et al., 2006; Taniguchi et al.,

2000) and AQP9, another water channel in astrocytes (Badaut et al., 2001). Interestingly,

Fujita et al. (2003) reported down-regulation of AQP4 and AQP9 under hypoxia conditions and up-regulation of AQP4 when combined with mild hypothermia. They suggested that the restoration of AQP4 expression may be important in the reduction of brain edema, because mild hypothermia is helpful for brain injury (Marion et al., 1997). This conclusion agreed with Badaut's data and ours that AQP9 expression in RGC-5 cells was up-regulated under hypoxic conditions.

In our studies, RGC-5 cells, were tested under hypoxia and serum-free (SF) conditions as an apoptosis model. Apoptosis can be monitored using a number of different techniques. Unfortunately, using light microcopy with dye(s) to distingue the morphological changes is laborious. The TUNEL (TdT-mediated dUTP nick end labeling) method detects 3'-OH ends of DNA strand breaks by fluorescence intensity but may not be specific for apoptosis (Grasl-Kraupp et al., 1995). The method of DNA laddering detects the internucleosomal DNA fragmentation by electrophoresis. This method is simple and easy and does not require experienced personnel nor expensive instrumentation. We selected this method to detect apoptosis and demonstrated DNA fragmentation of RGC-5 cells after hypoxia treatment. We also tried to use water channel inhibitors to determine their effects on hypoxia-induced apoptosis. However, DNA laddering was only demonstrated in the positive control, serum with 24-hour hypoxia. Although this result was surprising, it was understandable. Lee and coworkers (2006) reported the disappearance of DNA fragmentation when much higher doses of a water channel inhibitor were needed ($HgCl_2$, 10 M). Such false negative results were due to the formation of higher molecular weight fragments (50-300 kbp) that are undetected using conventional electrophoresis (Cohn et al., 1992; Oberhammer et al., 1993). Thus, the technique of flow cytometry (FCM) using a fluorescent dye was utilized. A flow

cytometer can easily detect and quantify nonviable cells (Darzynkiewicz et al., 1992). The fluorescence dye, propidium iodide, was used because the subpopulation in the cell cycle profile can be well defined (Telford et al., 1991). When using FCM to study apoptosis, an aquaporin inhibitor, $HgCl_2$, was used to examine whether aquaporin inhibition is beneficial.

Mercury is a heavy metal and toxic to the nervous and the immune systems (Silva et al., 2005). Unlike inorganic mercury, e.g. $HgCl_2$, organic mercury and elemental mercury vapor are capable of penetrating the intact blood-brain barrier and thus have a higher toxicity (Goyer, 1996b; Aschner and Aschner, 1990). In addition, the toxicity of $HgCl_2$ specifically targets the renal system instead of the nervous system (Bartolome et al., 1985; Daston et al., 1986).

The toxicity of $HgCl_2$ depends on dose and the types of cells used. Silva et al. (2005) reported that 0.5 μM is toxic to primary culture cells of spleen, thymus, and lymph node, primarily due to inhibition of cell proliferation. In the report from Parran et al. (2000), undifferentiated and differentiated pheochromocytoma (PC12) cells have a different sensitivity to $HgCl_2$. The EC_{50} values for undifferentiated and differentiated PC12 cells are 8.2 μM and 4.0 μM, respectively. However, undifferentiated PC12 cells increased both the neurite outgrowth and the number of branch points at concentrations of 0.1-3 μM, whereas both neurite outgrowth and the number of branch points for differentiated PC12 cells were inhibited at 0.03 μM. Hemdan et al. (2007) used isolated human peripheral blood mononuclear cells and reported reduced cell vitality at 55 nM. Stoiber et al. (2004) used IMR-32 human neuroblastoma cells and reported that 30 μM was toxic. Yang et al. (2006) reported an IC_{50} value of 10 μM on mice erythrocytes for AQP1 inhibition. Jablonski et al. (2006) pretreated hepatocytes and hepatic tumor cells with $HgCl_2$ (100 μM) for 15 min to

inhibit aquaporins. Although our experiments used 50 μM $HgCl_2$, it was not as toxic because transformed cells may have lower sensitivities (Krishnamoorthy et al., 2001; Parran et al., 2000). RGC-5 cell profiles under normoxia and hypoxia conditions showed that the number of sub-G_1 cells in the hypoxia group was greater than the normoxia group, which suggested more cells went through apoptosis under hypoxia. Moreover, the number of sub-G_1 cells after serum-free (SF), $HgCl_2$-treatment was lower than SF without $HgCl_2$. This suggests that the AQP9 inhibition may be protective.

Indeed, several groups suggested that AQP inhibition may be protective. Calamita et al. (2006) showed that immortalized mouse hepatocytes have no mitochondrial AQP8, whereas primary liver cells contain AQP8 in their mitochondria. Lee and Thevenod (2006) proposed that the inhibition of AQP8 activation may block caspase-dependent apoptosis. Also, Jablonski et al. (2006) showed that AQP8 and AQP9 had decreased expression of mRNA and protein in tumor cells compared to normal liver cells. Those cancer cells had diminished responsiveness to osmotic challenge and apoptotic stimulation. Interestingly, the expression of AQP8 and AQP9 increased after being cultured *in vitro* for 24 hours compared with freshly isolated samples. Tumor cells with elevated aquaporin expression had increased responsiveness to apoptotic stimuli. However, our results were only preliminary, because RGC-5 cells may be less sensitive to the toxicity of $HgCl_2$ than primary RGCs. AQP9-specific inhibitors with less toxicity are needed.

Project 4

AQP4 or MIWC (mercurial-insensitive water channel) is stongly expressed in astrocyte plasma membranes but absent from neurons (Nicchia et al., 2003; Ma et al., 1997). AQP4

may be the main channel for water transport in astrocytes, because the osmotic water permeability (P_f) is reduced by 7.1-fold in astrocytes in AQP4-knockout mice compared with those from wild-type mice (Solenov et al., 2004). This was confirmed by Nicchia et al. (2003) using RNAi (RNA interference). AQP4 expression appears highest in osmoregulatory areas of the brain (higher expression in glial membrane facing blood-brain and brain-CSF, cerebrospinal fluid, interfaces) suggesting the involvement of water movement between blood and brain, and between brain and CSF compartments (Nielsen et al., 1997; Oshio et al., 2004).

Brain edema is defined as a net increase in water content of the brain parenchyma. Because the skull is rigid, brain edema induces an increase in intracranial pressure (ICP), which may cause brain ischemia and death. Brain edema is classified in two typies as cytotoxic, cell swelling, and as vasogenic, fluid accumulation in the extracellular space (ECS) of brain parenchyma that occurs through the blood-brain barrier (BBB). AQP4 is suggested to be critically involved in brain edema under various injurious conditions (Papadopoulos et al., 2002; Venero et al., 2004). However, pathways involved in the regulation of AQP4 are not fully understood.

A number of ion and water channels may be regulated by undergoing ubiquitination, such as the epithelial sodium channel (Wang et al., 2006), voltage-gate potassium channel Kv1.5 (Kate et al., 2005), and aquaporin-1 (Leitch et al., 2001). Cells can direct proteins to different targets by tagging them with ubiquitin (Ub). This ubiquitous protein is a well-known signal whereby misfolded and damaged proteins are recognized by the 26S proteasome and are targeted for degradation. This ubiquitin-proteasome pathway allows cells to remove unwanted proteins and also regulate the turnover of proteins. This ubiquitin-

proteasome system (UPS) is the major non-lysosomal degradation route for proteins and is critical in regulating short-lived cellular proteins (Hochstrasser, 1995). Because AQP4 is critical in water movement, it may be a target for the ubiquitin-proteasomal degradation pathway.

AQP4 exists in multiple isoforms (32, 37, 87, and 100 kDa). In the presence of proteasomal inhibitors, there was an increase in the 32 kDa AQP4 isoform, whereas purified ubiquitinated AQP4 protein isoforms were identified at 87 and 100 kDa (Fig. 38). This suggested that the cytosolic or higher molecular weight AQP4s are ubiquitinated and are potential targets for degradation by the proteasomal system. This may provide an explanation for the weak cytosolic localization of AQP4 (Zelenina et al., 2002). In addition, Fig. 39 shows an up-regulated protein expression of AQP4 in astrocytes after treatment of Mg132, a proteasome inhibitor. However, the use of proteasomal inhibitors is likely to be detrimental in cytotoxic edema injuries (e.g., water intoxication and permanent focal cerebral ischemia) as edema production is AQP4-dependent; therefore, its accumulation would likely be damaging (Manley et al., 2000). By contrast, proteasomal inhibitors are likely to be protective in vasogenic brain edema (e.g., intraparenchymal fluid infusion, focal freeze injury, and brain tumor) (Papadopoulos et al., 2004), as edema production is AQP4-independent, but its drainage is AQP4-dependent; therefore, AQP4 accumulation may be therapeutic.

Mayne et al. (2001) used a proteasomal inhibitor to suppress the inflammatory responses to reduce brain edema and improve functional outcome. Also, in cerebral ischemia, using proteasomal inhibition reduced inflammatory responses and neuronal degeneration along with decreased infarct volume, leading to neuroprotection (Henninger et

al., 2006; Williams, et al., 2003; Phillips et al., 2000). Sinn et al. (2007) used a proteasome inhibitor to reduce hemorrhage volume and brain edema. Thus, it is likely that the regulation of AQP4 levels by a proteasome inhibitor may be useful under some conditions. However, our data is far from suggesting that the therapeutic effects of proteasome inhibitors should be utilized. The first potential problem encountered for *in vivo* use will be the blood-brain barrier (BBB), because the BBB has to be disrupted before the proteasome inhibitor can reach its target. Nevertheless, this approach may provide insight into novel therapeutic options for disorders of the CNS associated with altered brain water balance.

Project 5

The retinal pigment epithelium (RPE) is essential for visual function. The RPE interacts with outer segments of photoreceptors and are separated from the choroid by Bruch's membrane. The outer segments of photoreceptors is renewed regularly, and the debris are eliminated by the RPE through phagocytosis. The RPE also captures and recycles used retinal molecules released from the outer segments. The constant shedding and phagocytosis have to be delicately balanced or the excitability of photoreceptors may be compromised (Finnemann, 2003). The RPE also controls the nutrient supply from the blood vessels of the choroid. This involves the control of the amount of fluid and the composition of the fluid. These RPE functions may cause a constant change of cell volume and external environment. Thus, water channels may play crucial roles.

Aquaporin-1, a water-only channel, is expressed in RPE (Stamer et al., 2003). Efficient movement of solutes and water define healthy RPE, and aquaporin-9, which is expressed in RPE (our observation), transports solutes and water. So the role of AQP9 in RPE may be

important. Our data showed that the expression of AQP9 varied with the time of hypotonic and hypoxic stress (Figs. 42 and 43). This suggests that AQP9 is involved in the cell response to insults. This observation is supported by others in which the involvement of AQP9 in hypotonic-induced swelling was demonstrated (Tsukaguchi et al., 1999; Dibas et al., 2007). Indeed, the 30-minute hypotonic shock induced about a 2-fold increase of AQP9 mRNA expression, whereas 4.5-hour hypotonic shock caused a significant decrease in expression compared with its expression in an isotonic solution. Therefore, AQP9 could be essential for cell survival under stress.

CONCLUSIONS

AQP9 is an aquaglyceroporin, permeable to water, glycerol, lactate, and a number of other solutes. AQP9 is expressed in retinal ganglion cells (RGCs, neurons in the retina) and astrocytes (neuron supportive cells). Recently, the transport of lactate between astrocytes and neurons is in debate, but the possible involvement of AQP9 has never been discussed. Besides, AQP9 may play a role in glaucoma. The aims of this research were to confirm the presence of AQP9 in RGCs and determine the roles of AQP9 under insults *in vivo*, and *in vitro* along with a number of proteins.

This research was carried out in five projects. The first one used differentiated and undifferentiated RGC-5 cells with techniques of RT-PCR (mRNA expression), Western blotting (protein expression), and immunocytostaining (protein distribution). AQP9 expression was confirmed in RGC-5 cells and was localized to the inner mitocondrial membrane. The second project used animal models of glaucoma – optic nerve damage by endothelin-1 injection and elevated intraocular pressure. The expression of AQP4, AQP9, Thy-1, caspase-3, XIAP, GFAP, and GS were examined by real-time RT-PCR, Western blotting, and immunohistostaining. Expression of these proteins responded to optic nerve damage differently. Some of theses responses were damaging and some were protective. The third project used a water channel inhibitor on RGC-5 cells under hypoxia, which suggested that the inhibition of apoptotic volume decrease was protective. The fourth project used U373MG, astrocytoma, with proteasomal inhibitors. It showed that AQP4 may be targeted by ubiquitin and that the inhibition of ubiquitin may be protective in vasogenic brain edema. The fifth project used ARPE19, transformed retinal pigment epithelial cells, under hypotonic

and hypoxic stress. Real-time RT-PCR showed AQP9 mRNA expression was time-dependent.

In summary, this research showed the importance of AQP9 to cell function and viability under different insults *in vivo* and *in vitro*, in addition to the expression of other proteins. The inhibition of water channels can be protective or harmful depending on the initial insult.

APPENDIX

Abbreviation	Full name	Definition
AH	aqueous humor	The aqueous humor is a thick watery substance that is located in the eye.
AQPs	aquaporins	Aquaporins are a class of integral membrane proteins or more commonly referred to as a class of major intrinsic proteins (MIP) that form pores in the membrane of biological cells.
AUC	area-under curve	In the field of pharmacokinetics, the area under the curve is the area under the curve in a plot of concentration of drug in plasma against time.
AVD	apoptotic volume decrease	The term describes the cell volume decrease during apoptosis
BBB	blood-brain barrier	The blood-brain barrier is composed of endothelial cells packed tightly in brain capillaries that more greatly restrict passage of substances from the bloodstream than do endothelial cells in capillaries elsewhere in the body. Processes from astrocytes surround the endothelial cells of the BBB providing biochemical support to those cells.
BCA	bicinchoninic acid protein assay	The bicinchoninic acid assay or BCA assay is a biochemical assay for determining the total level of protein in a solution, similar to Lowry protein assay, Bradford protein assay or biuret reagent. The total protein concentration is exhibited by a color change of the sample solution from green to purple in proportion to protein concentration, which can then be measured using colorimetric techniques.
BDNF	brain-derived neurotrophic factor	Brain-derived neurotrophic factor is exactly as it states; a neurotrophic factor found originally in the brain, but also found in the periphery. More specifically, it is a protein which has activity on certain neurons of the central nervous system and the peripheral nervous system; it helps to support the survival of existing neurons, and encourage the growth and differentiation of new neurons and synapses. In the brain, it is active in the hippocampus, cortex, and basal forebrain-areas vital to learning, memory, and higher thinking.
BSA	bovine serum albumin	Bovine serum albumin is a serum albumin protein that can be used as a diluent or a blocking agent in numerous applications including ELISAs (Enzyme-Linked Immunosorbent Assay), blots and immunohistochemistry. It is also used as a nutrient in cell and microbial culture. In restriction digests, BSA is used to stabilize some enzymes during digestion of DNA and to prevent adhesion of the enzyme to reaction tubes and other vessels. This protein does not affect other enzymes that do not need it for stabilization. BSA is used because of its stability, its lack of effect in many biochemical reactions, and its low cost since it is readily available in large quantities as it is purified from bovine blood, a byproduct of the beef industry.
CBCECs	cultured bovine corneal endothelial cells	
cDNA	complementary DNA	Complementary DNA is DNA synthesized from a mature mRNA template. cDNA is often used to clone eukaryotic genes in prokaryotes.
CHIP28	channel-like integral protein of 28 kDa	
CIN or CHC	alpha-cyano-4-hydroxycinnamic acid	
CNTF	ciliary neurotrophic factor	Ciliary neurotrophic factor is a nerve growth factor.

CSF	cerebrospinal fluid	Cerebrospinal fluid, Liquor cerebrospinalis, is a clear bodily fluid that occupies the subarachnoid space in the brain (the space between the skull and the cerebral cortex-more specifically, between the arachnoid and pia layers of the meninges). It is a very pure saline solution with microglia and acts as a "cushion" or buffer for the cortex.
DAPI	4',6-diamidino-2-phenylindole	DAPI or 4', 6-diamidino-2-phenylindole is a fluorescent stain that binds strongly to DNA. It is used extensively in fluorescence microscopy. Since DAPI will pass through an intact cell membrane, it may be used to stain live and fixed cells.
DMEM	dulbecco's modified eagle's medium	A variation of this EMEM, called DMEM, (Dulbecco/Vogt Modified Eagle's Minimal Essential Medium), which contains approximately four times as much of the vitamins and amino acids present in the original formula and two to four times more glucose.
DMSO	dimethyl sulfoxide	Dimethyl sulfoxide (DMSO) is the chemical compound with the formula $(CH_3)_2SO$. This colorless liquid is an important polar aprotic solvent that dissolves both polar and nonpolar compounds and is miscible in a wide range of organic solvents as well as water.
ECM	extracellular matrix	Extracellular matrix is any material part of a tissue that is not part of any cell. Extracellular matrix is the defining feature of connective tissue.
ELM	external limiting membrane	In the outer nuclear layer they form a network around the rod- and cone-fibrils, and unite to form the external limiting membrane at the bases of the rods and cones.
ET-1	endothelin-1	Endothelin is a 21-amino acid vasoconstricting peptide that plays a key part in vascular homeostasis. It is one of the strongest vasoconstrictors currently studied. There are three isoforms with varying regions of expression and two key receptor types, ETA and ETB.
FBS	fetal bovine serum	Fetal bovine serum (or fetal bovine serum) is serum taken from the fetuses of cows. Fetal Bovine Serum is the most widely used serum in the culturing of cells. In some papers the expression foetal calf serum is used.
FCM	flow cytometric analysis	Flow cytometry is a method for quantitating components or structural features of cells primarily by optical means. Although it makes measurements on one cell at a time, it can process thousands of cells in a few seconds. Since different cell types can be distinquished by quantitating structural features, flow cytometry can be used to count cells of different types in a mixture.
Fura-2/AM	Fura-2-acetoxymethyl ester	A ratiometric calcium indicator (measured by changes in fluorescence). Measurement of Ca^{2+}-induced fluorescence at both 340nm and 380nm allows for 340/380 ratios. This helps in cancellation of artefacts produced by changes in dye concentrations.
GCL	ganglion cell layer	The ganglion cell layer consists of a single layer of large ganglion cells, except in the macula lutea, where there are several strata.
GFAP	glial fibrillary acidic protein	Glial fibrillary acidic protein is an intermediate filament (IF) protein that is found in glial cells and astrocytes. GFAP is a type III IF protein that maps, in humans, to 17q21. It is closely related to its non-epithelial family members, vimentin, desmin, and peripherin, which are all involved in the structure and function of the cell's cytoskeleton. GFAP helps to maintain astrocyte mechanical strength, as well as the shape of cells.
GS	glutamine synthetase	Glutamine synthetase is an enzyme that plays an essential role in the metabolism of nitrogen by catalyzing the condensation of glutamate and ammonia to form glutamine.

HNPE	human non-pigmented ciliary epithelial cells	
hONAs	human optic nerve head astrocytes	
ICP	intracranial pressure	Intracranial pressure is the pressure exerted by the cranium on the brain tissue, cerebrospinal fluid, and the brain's circulating blood volume. ICP is a dynamic phenomenon constantly fluctuating in response to activities such as exercise, coughing, straining, arterial pulsation, and respiratory cycle. ICP is measured in millimeters of mercury (mmHg) and, at rest, is normally less than 10-15 mmHg. Changes in ICP are attributed to volume changes in one or more of the constituents contained in the cranium.
IH	immunohistochemistry	Immunohistochemistry or IHC refers to the process of localizing proteins in cells of a tissue section exploiting the principle of antibodies binding specifically to antigens in biological tissues. IH is also widely used in basic research to understand the distribution and localization of biomarkers in different parts of a tissue.
ILM	internal limiting membrane	
IMM	inner mitochondrial membrane	The inner mitochondrial membrane contains proteins with four types of functions: 1. Those that carry out the oxidation reactions of the respiratory chain. 2. ATP synthase, which makes ATP in the matrix. 3. Specific transport proteins that regulate the passage of metabolites into and out of the matrix. 4. Protein import machinery. Unlike the outer membrane, the inner membrane does not contain porins, and is highly impermeable; almost all ions and molecules require special membrane transporters to enter or exit the matrix. In addition, there is a membrane potential across the inner membrane. The inner mitochondrial membrane is compartmentalized into numerous cristae, which expand the surface area of the inner mitochondrial membrane, enhancing its ability to generate ATP.
IOP	intraocular pressure	Intraocular pressure is the fluid pressure inside the eye. It may become elevated due to anatomical problems, inflammation of the eye, genetic factors, as a side-effect from medication, or during exercise.
IPL	inner nuclear layer	The inner nuclear layer or layer of inner granules is made up of a number of closely packed cells, of which there are three varieties, viz.: bipolar cells, horizontal cells, and amacrine cells.
LCM	laser capture microdissection	Laser Capture Microdissection is a method for isolating pure cells of interest from specific microscopic regions of tissue sections.
MCT	monocarboxylate transporter	Proton-linked monocarboxylate transporter. Catalyzes the rapid transport across the plasma membrane of many monocarboxylates such as lactate, pyruvate, branched-chain oxo acids derived from leucine, valine and isoleucine, and the ketone bodies acetoacetate, beta-hydroxybutyrate and acetate.
MIP	major intrinsic protein	The major intrinsic protein of the ocular lens fiber membrane is an abundant protein that appears during differentiation of the ocular lens. MIPs act as channels in membranes to facilitate passive transport across the membrane. Some MIPs allow small polar molecules like glycerol or urea to pass through the membrane. However, the majority of MIPs are thought to be aquaporins (AQPs), i.e., they are specific for water transport.

MIWC	mercurial-insensitive water channel	Water channels, which are not inhibited by mercurial compounds.
NCAM	neural cell adhersion molecule	Neural Cell Adhesion Molecule is a homophilic binding glycoprotein expressed on the surface of neurons, glia and skeletal muscle. NCAM has been implicated as having a role in cell-cell adhesion, neurite outgrowth, synaptic plasticity, and learning and memory.
NDI	nephrogenic diabetes insipidus	A disease characterized by excretion of large amounts of severely diluted urine, which cannot be reduced when fluid intake is reduced. It denotes inability of the kidney to concentrate urine.
NPA regions	asparagine-proline-alanine regions	It is a region within the water channel.
NPE	nopigmented ciliary epithelium	
OFL	optic nerve fiber layer	
OMDVR	outer medullary decending vasa recta	
OMM	outer mitochondrial membrane	The outer mitochondrial membrane, which encloses the entire organelle. It contains numerous integral proteins called porins, which contain a relatively large internal channel (about 2-3 nm) that is permeable to all molecules of 5000 daltons or less. Larger molecules can only traverse the outer membrane by active transport through mitochondrial membrane transport proteins.
ONH	optic nerve head	The optic disc or optic nerve head is the location where ganglion cell axons exit the eye to form the optic nerve. There are no light sensitive rods or cones to respond to a light stimulus at this point thus it is also known as "the blind spot"; the break in the visual field created by the optic disc is also called "the blind spot" or "physiological blind spot". The optic nerve head in a normal human eye carries from 1 to 1.2 million neurons from the eye towards the brain.
ONL	outer nuclear layer	The outer nuclear layer (or layer of outer granules or external nuclear layer), like the inner nuclear layer, contains several strata of oval nuclear bodies; they are of two kinds, viz.: rod and cone granules, so named on account of their being respectively connected with the rods and cones of the next layer.
OPL	outer plexiform layer	The outer plexiform layer (external plexiform layer) is a layer of neuronal synapses in the retina of the eye. It consists of a dense network of synapses between dendrites of horizontal cells from the inner nuclear layer, and photoreceptor cell inner segments from the outer nuclear layer. It is much thinner than the inner plexiform layer, where horizontal cells synapse with retinal ganglion cells.
OS/IS	rods and cones / out and inner segments	
PBS	phosphate buffered saline	A buffer solution commonly used in biochemistry. It is a salty solution containing sodium chloride, sodium phosphate and potassium phosphate. The buffer helps to maintain a constant pH. The concentration usually matches the human body (isotonic).
PI	propidium iodide	Propidium iodide is a fluorescent biomolecule that can be used to stain DNA. PI also binds to RNA, necessitating treatment with nucleases to distinguish between RNA and DNA staining. It can be used to differentiate necrotic, apoptotic and normal cells.

POAG	primary open angle glaucoma	Primary open-angle glaucoma is described as optic nerve damage from multiple possible causes that is chronic and progresses over time, with a loss of optic nerve fibers that is characteristic of the disease.
PRE	retinal pigment epithelium	The retinal pigment epithelium is the pigmented cell layer just outside the neurosensory retina that nourishes retinal visual cells, and is firmly attached to the underlying choroid and overlying retinal visual cells. The RPE is composed of a single layer of hexagonal cells that are densely packed with pigment granules.
Q-PCR	quantitative polymerase chain reaction	Quantitative polymerase chain reaction is a modification of the polymerase chain reaction used to rapidly measure the quantity of DNA, complementary DNA or ribonucleic acid present in a sample. Like other forms of polymerase chain reaction, the process is used to amplify DNA samples, via the temperature-mediated enzyme DNA polymerase.
RGCs	retinal ganglion cells	A ganglion cell (sometimes called a gangliocyte) is a type of neuron located in the retina of the eye that receives visual information from photoreceptors via various intermediate cells such as bipolar cells, amacrine cells, and horizontal cells. Retinal ganglion cells' axons are myelinated. The myelinated parts are outside the eye. These axons form the optic nerve and connect mainly to the lateral geniculate nucleus in the brain.
RNAi	RNA interference	RNA interference (also called "RNA-mediated interference", abbreviated RNAi) is a mechanism for RNA-guided regulation of gene expression in which double-stranded ribonucleic acid inhibits the expression of genes with complementary nucleotide sequences. Conserved in most eukaryotic organisms, the RNAi pathway is thought to have evolved as a form of innate immunity against viruses and also plays a major role in regulating development and genome maintenance.
RVI/RVD	regulatory volume increase / regulatory volume decrease	
SDS-PAGE	sodium dodecyl sulfate-polyacrylamide gel electrophoresis	SDS-PAGE, officially sodium dodecyl sulfate polyacrylamide gel electrophoresis, is a technique used in biochemistry, genetics and molecular biology to separate proteins according to their electrophoretic mobility (a function of length of polypeptide chain or molecular weight as well as higher order protein folding, posttranslational modifications and other factors).
SF	serum-free	
TDLH	thin desending limb of Henle	The thin descending limb of Henle in kidney has been proposed to have an important role in the formation of concentrated urine by the countercurrent multiplication mechanism. Countercurrent multiplication relies on active solute transport out of the lumen in the thick ascending limb of Henle, rapid osmotic equilibration along the lumen of TDLH, and efficient uptake of water by the renal microvasculature.
TF	trophic factor	One kind of growth factor.
TM	trabecular meshwork	The trabecular meshwork is an area of tissue in the eye located around the base of the cornea, near the ciliary body, and is responsible for draining the aqueous humor from the eye via the anterior chamber (the chamber on the front of the eye covered by the cornea).
TNF	tumor necrosis factor	Tumor necrosis factors (or the TNF-family) refer to a group of cytokines family which can cause apoptosis.

| UPS | ubiquitin-proteasome system | A cellular quality control system that tags misfolded proteins for refolding or degradation. The ubiquitin-proteasome system controls many cellular processes either by proteolytic or non-proteolytic means. |
| XIAP | X-linked inhibitor of apoptosis protein | Negative regulation of apoptosis. A process which directly inhibits any of the steps required for cell death by apoptosis. |

REFERENCES

Adle-Biassette, H., Olivier, P., Verney, C., Fontaine, R. H., Evrard, P., Heńin, D., Massias, L., Gressens, P., Baud, O. (2007) Cortical Consequences of In Vivo Blockade of Monocarboxylate Transport During Brain Development in Mice. *Pediatric Research* **61**: 54-60.

Adler, A. J., Southwick, R. E. (1992) Distribution of glucose and lactate in the interphotoreceptor matrix. *Ophthalmol. Res.* **24**: 243-252.

Adorante, J. S. (1995) Regulatory volume decrease in frog retinal pigment epithelium. *Am J Physiol.* **268**: 89-100.

Agre, P. (1997) Molecular physiology of water transport: aquaporin nomenclature workshop. *Biol. Cell* **89**: 255-257.

Agre, P. (2004) Aquaporin water channels (Nobel Lecture). *Angew. Chem. Int. Ed. Engl.* **43**: 4278-4290.

Agre, P., King, L., Yasui, M., Guggino, W., Ottersen, O., Fujiyoshi, Y., Engel, A., Nielsen, S. (2002) Aquaporin water channels - from atomic structure to clinical medicine. *J. Physiol.* **542**: 3-16.

Agre, P., Preston, G. M., Smith, B. L., Jung, J. S., Raina, S., Moon, C., Guggino, W. B, Nielsen, S. (1993) Aquaporin CHIP: the archetypal molecular water channel. *Am. J. Physiol.* **265**: F463-476.

Agre, P., Saboori, A. M., Asimos, A., Smith, B. L. (1987) Purification and partial characterization of the Mr 30,000 integral membrane protein associated with the erythrocyte Rh (D) antigen. *J. Biol. Chem.* **262**: 17497-17503.

Aharon, R., Bar-Shavit, Z. (2006) Involvement of Aquaporin 9 in Osteoclast Differentiation. *J. Biol. Chem.* **281**: 19305-19309.

Ainscow, E. K., Mirshamsi, S., Tang, T., Ashford, M. L., Rutter, G. A. (2002) Dynamic imaging of free cytosolic ATP concentration during fuel sensing by rat hypothalamic neurones: evidence for ATP-independent control of ATP-sensitive (K^+) channels. *J. Physiol.* **544**: 429-445.

Altamirano, J., Brodwick, M. S., Alvarez-Leefmans, F. J. (1998) Regulatory volume decrease and intracellular Ca^{2+} in murine neuroblastoma cells studied with fluorescent probes. *J. Gen. Physiol.* **112**: 145-160.

Alvarez-Leefmans, F. J., Gamiño, S. M., Reuss, L. (1992) Cell volume changes upon sodium pump inhibition in Helix aspersa neurones. *J. Physiol.* **458**: 603-619.

Amiry-Moghaddam, M., Lindland, H., Zelenin, S., Roberg, B. A., Gundersen, B. B., Petersen, P., Rinvik, E., Torgner, I. A., Ottersen, O. P. (2005) Brain mitochondria contain aquaporin water channels: evidence for the expression of a short AQP9 isoform in the inner mitochondrial membrane. *FASEB J.* **19**: 1459-1467.

Amiry-Moghaddam, M., Ottersen, O. P. (2003) The molecular basis of water transport in the brain. *Nat. Rev. Neurosci.* **4**, 991-1001.

Applied Biosystems, Inc. (2006) *SYBR® Green PCR and RT-PCR Reagents Protocol.* Available at http://docs.appliedbiosystems.com/pebiodocs/04304965.pdf, Foster City, CA.

Arima, H., Yamamoto, N., Sobue, K., Umenishi, F., Tada, T., Katsuya, H., Asai, K. (2003) Hyperosmolar mannitol stimulates expression of aquaporin 4 and 9 through a p38 mitogen activated protein kinase-dependent pathway in rat astrocytes. *J. Biol. Chem.* **278**: 44525-44534.

Aschner, M., Aschner, J. L. (1990) Mercury neurotoxicity: mechanisms of blood-brain barrier transport. *Neurosci. Biobehav. Rev.* **14**: 169-176.

Badaut, J., Hirt, L., Granziera, C., Bogousslavsky, J., Magistretti, P. J., Regli, L. (2001) Astrocyte-specific expression of aquaporin-9 in mouse brain is increased after transient focal cerebral ischemia. *J. Cereb. Blood Flow Metab.* **21**: 477-482.

Badaut, J., Petit, J. M., Brunet, J. F., Magistretti, P. J., Charriaut-Marlangue, C., Regli, L. (2004) Distribution of aquaporin 9 in the adult rat brain: preferential expression in catecholaminergic neurons and in glial cells. *Neuroscience* **128**: 27-38.

Bai, C., Fukuda, N., Song, Y., Ma, T., Matthay, M. A, Verkman, A. S. (1999) Lung fluid transport in aquaporin-1 and aquaporin-4 knockout mice. *J. Clin. Invest.* **103**: 555-561.

Bartolome, J., Grignolo, A., Bartolome, M., Trepanier, P., Lerea, L., Weigel, S., Whitmore, W., Michalopoulos, G., Kavlock, R., Slotkin, T. (1985) Postnatal methyl mercury exposure: effects on ontogeny of renal and hepatic ornithine decarboxylase responses to trophic stimuli. *Toxicol. Appl. Pharmacol.* **80**: 147-154.

Bernardi, P. (1996) The permeability transition pore. Control points of a cyclosporin A-sensitive mitochondrial channel involved in cell death. *Biochim. Biophys. Acta* **1275**: 5-9.

Berry, V., Francis, P., Kaushal, S., Moore, A., Bhattacharya, S. (2000) Missense mutations in MIP underlie autosomal dominant 'polymorphic' and lamellar cataracts linked to 12q. *Nature Genetics* **25**, 15-17.

Bloch, O., Papadopoulos, M. C., Manley, G. T., Verkman, A. S. (2005). Aquaporin-4 gene deletion in mice increases focal edema associated with brain abscess. *J. Neurochem.* **95**: 254-262.

Borgnia, M., Nielsen, S., Engel, A., Agre, P. (1999) Cellular and molecular biology of the aquaporin water channels. *Annu. Rev. Biochem.* **68**: 425-458.

Borok, Z., Verkman, A. S. (2002) Lung edema clearance: 20 years of progress: invited review: role of aquaporin water channels in luid transport in lung and airways. *J. Appl. Physiol.* **93**: 2199-2206.

Bortner, C. D., Gomez-Angelats, M., Cidlowski, J. A. (2001) Plasma membrane depolarization without repolarization is an early molecular event in anti- Fas induced apoptosis. *J. Biol. Chem.* **276**: 4304–4314.

Bortner, C. D., Hughes, F. M., Cidlowski, J. A. (1997) A primary role for K+ and Na+ efflux in the activation of apoptosis. *J. Biol. Chem.* **272**: 32436-32442.

Bradley, J. M., Anderssohn, A. M., Colvis, C. M. (2000) Mediation of laser trabeculoplasty-induced matrix metalloproteinase expression by IL-1beta and TNF-alpha. *Invest. Ophthalmol. Vis. Sci.* **41**: 422-430.

Bringmann, A., Pannicke, T., Grosche, J., Francke, M., Wiedemann, P., Skatchkov, S. N., Osborne, N. N., Reichenbach, A. (2006) Muller cells in the healthy and diseased retina. *Prog. Retin. Eye Res.* **25**: 397-424.

Bringmann, A., Uckermann, O., Pannicke, T., Iandiev, I., Reichenbach, A., Wiedemann, P. (2005) Neuronal versus glial cell swelling in the ischaemic retina. *Acta Ophthalmol. Scand.* **83**: 528-538.

Brubaker, R. F. (2001) Mechanism of action of bimatoprost (Lumigum). *Surv. Ophthalmol.* **45**: 5347-5351.

Calamita, G., Ferri, D., Gena, P., Liquori, G. E., Cavalier, A., Thomas, D., Svelto, M. (2005) The inner mitochondrial membrane has aquaporin-8 water channels and is highly permeable to water. *J. Biol. Chem.* **280**: 17149-17153.

Calamita, G., Gena, P., Meleleo, D., Ferri, D., Svelto, M. (2006) Water permeability of rat liver mitochondria: A biophysical study. *Biochim. Biophys. Acta* **1758**: 1018-1024.

Calamita, G., Moreno, M., Ferri, D., Silvestri, E., Roberti, P., Schiavo, L., Gena, P., Svelto, M., Goglia, F. (2007) Triiodothyronine modulates the expression of aquaporin-8 in rat liver mitochondria. *J. Endocrinol.* **192**: 111-120.

Carbrey, J. M., Gorelick-Feldman D. A., Kozono D, Praetorius J, Nielsen S, Agre P. (2003) Aquaglyceroporin AQP9: solute permeation and metabolic control of expression in liver. *Proc. Natl. Acad. Sci. U. S. A.* **100**: 2945-2950.

Carter-Dawson, L., Shen, F., Harwerth, R. S., Smith, E. L., Crawford, M. L., Chuang, A. (2004) Glutamine immunoreactivity in Muller cells of monkey eyes with experimental glaucoma. *Exp. Eye Res.* **66**: 537-545.

Castle, N. A. (2005) Aquaporins as targets for drug discovery. *Drug Discov. Today* **10**: 485-493.

Cater, H. L., Benham, C. D., Sundstrom, L. E. (2001) Neuroprotective role of monocarboxylate transport during glucose deprivation in slice cultures of rat hippocampus. *J. Physiol.* **531**: 459-466.

Chang, M. L., Wu, C. H., Jiang-Shieh, Y. F., Shieh, J. Y., Wen, C. Y. (2007) Reactive changes of retinal astrocytes and Muller glial cells in kainate-induced neuroexcitotoxicity. *J Anat.* **210**: 54-65.

Chen, H., Weber, A. J. (2002) Expression of glial fibrillary acidic protein and glutamine synthetase by Muller cells after optic nerve damage and intravitreal application of brain-derived neurotrophic factor. *Glia* **38**: 115-125.

Chen, X. -Z., Shayakul, C., Berger, U. V., Tian, W., Hediger, M. A. (1998). Characterization of a rat Na^+-dicarboxylate cotransporter. *J. Biol. Chem.* **273**: 20972- 20981.

Cheung, K. H., Leung, C. T., Leung, G. P. H., Wong, P. Y. D. (2003) Synergistic Effects of Cystic Fibrosis Transmembrane Conductance Regulator and Aquaporin-9 in the Rat Epididymis. *BOR* **68**: 1505-1510.

Cho, Y.S., Svelto, M., Calamita, G. (2003) Possible functional implications of aquaporin water channels in reproductive physiology and medically assisted procreation. *Cell. Mol. Biol.* **49**: 515-519.

Chou, C. L., Ma, T., Yang, B., Knepper, M. A., Verkman, A. S. (1998) Fourfold reduction of water permeability in inner medullary collecting duct of aquaporin-4 knockout mice. *Am. J. Physiol.* **274**: C549-C554.

Civan, M. M., Peterson-Yantorno K., Coca-Prados M., Yantorno, R. E. (1992) Regulatory volume decrease by cultured nonpigmented ciliary epithelial cells. *Exp. Eye Res.* **54**: 181-191.

Clark, A. F. (1999) Current trends in Antiglaucoma Therapy. *Emerging Drugs* **4**: 333-353.

Cohen, G. M., Sun, X. M., Snowden, R. T., Dinsdale, D., Skilleter, D. N. (1992) Key morphological features of apoptosis may occur in the absence of internucleosomal DNA fragmentation. *Biochem. J.* **286**: 331-334.

Csillag, A. (2005) *Atlas of the sensory organs: functional and clinical anatomy.* Totowa, N.J., Humana Press.

Da, T., Verkman, A. S. (2004) Aquaporin-4 gene disruption in mice protects against impaired retinal function and cell death after ischemia. *Invest. Ophthalmol. Vis. Sci.* **45**: 4477-4483.

Dalloz, C., Sarig, R., Fort, P., Yaffe, D., Bordais, A., Pannicke, T., Grosche, J., Mornet, D., Reichenbach, A., Sahel, J., Nudel, U., Rendon, A. (2003) Targeted inactivation of dystrophin gene product Dp71: phenotypic impact in mouse retina. *Hum. Mol. Genet.* **12**: 1543-1554.

Dan, J. A., Honavar, S. G., Belyea, D. A., Mandal, A. K., Garudadri, C., Levy, B., Ramakrishnan, R., Krishnadas, R., Lieberman, M. F., Stamper, R. L., Yaron, A. (2002) Enzymatic sclerostomy: pilot human study. *Arch. Ophthalmol.* **120**: 548-553.

Daston, G. P., Rehnberg, B. F., Hall, L. L., Kavlock, R. J. (1986) Toxicity of mercuric chloride to the developing rat kidney. III. Distribution and elimination of mercury during postnatal maturation, *Toxicol. Appl. Pharmacol.* **85**: 39-48.

Delporte, C., Steinfeld, S. (2006) Distribution and roles of aquaporins in salivary glands. *Biochim. Biophys. Acta* **1758**: 1061-1070.

Denker, B. M., Smith, B. L., Kuhajda, F. P., Agre, P. (1988) Identification, purification, and partial characterization of a novel Mr. 28,000 integral membrane protein from erythrocytes and renal tubules. *J. Biol. Chem.* **263**: 15634-15642.

Desagher, S., Martinou, J. C. (2000) Mitochondria as the central control point of apoptosis. *Trends Cell Biol.* **10**: 369-377.

Dibas, A., Prasanna, G., Yorio, T. (2005) Characterization of endothelin system in Bovine optic nerve and retina. *J. Ocu. Pharm. Therap.* **21**: 288-297.

Dibas, A., Yang, M. H., Bobich, J., Yorio, T. (2007) Stress-induced changes in neuronal Aquaporin-9 (AQP9) in a retinal ganglion cell-line. *Pharmacol. Res.* doi:10.1016/j.phrs.2007.01.021.

Ecelbarger, C. A., Terris, J., Frindt, G., Echevarria, M., Marples, D., Nielsen, S., Knepper, M. A. (1995) Aquaporin-3 water channel localization and regulation in rat kidney. *Am. J. Physiol.* **269**: F663-672.

Echevarria, M., Verkman A. S. (1992) Optical measurement of osmotic water transport in cultured cells. Role of glucose transporters. *J. Gen. Physiol.* **99**: 573-589.

Edmunds, B., Thompson, J. R., Salmon, J. F., Wormald, R. P. (2002) The National Survey of Trabeculectomy. III. Early and late complications. *Eye* **16**: 297-303.

Einarson, T. R., Kulin, N. A., Tingey, D., Iskedjian, M. (2000) Meta-analysis of the effect of latanoprost and brimonidine on intraocular pressure in the treatment of glaucoma. *Clin. Ther.* **22**: 1502-1515.

Elkjaer, M. L., Nejsum, L. N., Gresz, V., Kwon, T. H., Jensen, U. B., Frokiaer, J., Nielsen, S. (2001) Immunolocalization of aquaporin-8 in rat kidney, gastrointestinal tract, testis, and airways. *Am. J. Physiol. Renal. Physiol.* **281**: F1047-1057.

Elkjaer, M. L., Vajda, Z., Nejsum, L. N., Kwon, T. H., Jensen, U. B., Amiry-Moghaddam, M., Frokiaer, J., Nielsen, S. (2000) Immunolocalization of AQP9 in liver, epididymis, testis, spleen, and brain. *Biochem. Biophys. Res. Commun.* **276**: 1118-1128.

Endo, M., Jain, R. K., Witwer, B., Brown, D. (1999) Water channel (Aquaporin 1) expression and distribution in mammary carcinomas and glioblastomas. *Microvas. Res.* **58**: 89-98.

Ferrer, E. (2006) Trabecular meshwork as a new target for the treatment of glaucoma. *Drug News Perspect.* **19**: 151-158.

Finnemann, S. C. (2003) Role of alphavbeta5 integrin in regulating phagocytosis by the retinal pigment epithelium. *Adv. Exp. Med. Biol.* **533**: 337-342.

Fischbarg, J. (2003) On the mechanism of fluid transport across corneal endothelium and epithelia in general. *J. Exp. Zoolog. A Comp. Exp. Biol.* **300**: 30-40.

Fischbarg, J., Diecke, F. P. (2005) A mathematical model of electrolyte and fluid transport across corneal endothelium. *J. Membr. Biol.* **203**: 41-56.

Francis, P., Chung, J. J., Yasui, M., Berry, V., Moore, A., Wyatt, M. K., Wistow, G., Bhattacharya, S. S., Agre, P. (2000) Functional impairment of lens aquaporin in two families with dominantly inherited cataracts. *Hum. Mol. Genet.* **9**: 2329-2334.

Frigeri, A., Nicchia, G. P., Nico, B., Quondamatteo, F., Herken, R., Roncali, L., Svelto, M. (2001) Aquaporin-4 deficiency in skeletal muscle and brain of dystrophic mdx mice. *FASEB J.* **15**: 90-98.

Frigeri, A., Nicchia, G. P., Verbavatz, J. M., Valenti, G., Svelto, M. (1998) Expression of aquaporin-4 in fast-twitch fibers of mammalian skeletal muscle. *J. Clin. Invest.* **102**: 695-703.

Fu, D., Libson, A., Miercke, L. J., Weitzman, C., Nollert, P., Krucinski, J., Stroud, R. M. (2000) Structure of a glycerol-conducting channel and the basis for its selectivity. *Science* **290**: 481-486.

Fujita, Y., Yamamoto, N., Sobue, K., Inagaki, M., Ito, H., Arima, H., Morishima, T., Takeuchi, A., Tsuda, T., Katsuya, H., Asai, K. (2003) Effect of mild hypothermia on the expression of aquaporin family in cultured rat astrocytes under hypoxic condition. *Neurosci. Res.* **47**: 437-444.

Gabelt, B. T., Kaufman, P. L. (1989) Prostaglandin F2 alpha increases uveoscleral outflow in the cynomolgus monkey. *Exp. Eye Res.* **49**: 389-402.

Garlid, K. D., Paucek, P. (2003) Mitochondrial potassium transport: the K(+) cycle. *Biochim. Biophys. Acta* **1606**: 23-41.

Gordon, M. O., Beiser, J. A., Brandt, J. D. (2002) The Ocular Hypertension Treatment Study: baseline factors that predict the onset of primary open-angle glaucoma. *Arch. Ophthalmol.* **120**: 714-720.

Gorelick, D. A., Praetorius, J., Tsunenari, T., Nielsen, S., Agre, P. (2006) Aquaporin-11: a channel protein lacking apparent transport function expressed in brain. *BMC Biochem.* **7**: 1-14.

Goyer, R. A. (1996) Toxic effects of metals. Mercury. In: Klaassen CD (ed) Casarett and Doull's toxicology. The basic science of poisons. McGraw-Hill, New York, 709–712.

Grasl-Kraupp, B., Ruttkay-Nedecky, B., Koudelka, H., Bukowska, K., Bursch, W., Schulte-Hermann, R. (1995) In situ detection of fragmented DNA (TUNEL assay) fails to discriminate among apoptosis, necrosis, and autolytic cell death: a cautionary note. *Hepatology* **21**: 1465-1468.

Greenfield, D. S., Bagga, H., Knighton, R. W. (2003) Macular thickness changes in glaucomatous optic neuropathy detected using optical coherence tomography. *Arch. Ophthalmol.* **121**: 41-46.

Grill, H. J., Kaplan, J. M. (2002) The neuroanatomical axis for control of energy balance. *Front. Neuroendocrinol.* **23**: 2-40.

Grosche, J., Härtig, W., Reichenbach, A. (1995) Expression of glial fibrillary acidic protein (GFAP), glutamine synthetase (GS), and Bcl-2 protooncogene protein by Muller (glial) cells in retinal light damage of rats. *Neurosci. Lett.* **185**: 119-122.

Grynkiewicz, G., Poenie, M., Tsien, R. Y. (1985) A new generation of Ca2+-indicators with greatly improved fluorescence properties. *J. Biol. Chem.* **260**: 3440-3450.

Hama, Y., Katsuki, H., Tochikawa, Y., Suminaka, C., Kume, T., Akaike, A. (2006) Contribution of endogenous glycine site NMDA agonists to excitotoxic retinal damage in vivo. *Neurosci. Res.* **56**: 279-285.

Hamann, S. (2002). Molecular mechanisms of water transport in the eye. *Int. Rev. Cytol.* **215**: 395-431.

Hamann, S., Zeuthen, T., La Cour, M., Nagelhus, E. A., Ottersen, O. P., Agre, P., Nielsen, S. (1998) Aquaporins in complex tissues: distribution of aquaporins 1-5 in human and rat eye. *Am. J. Physiol.* **274**: C1332–1345.

Hara-Chikuma, M., Ma, T., Verkman, A. S. (2002) Selectively reduced glycerol in skin of aquaporin-3-deficient mice may account for impaired skin hydration, elasticity, and barrier recovery. *J Biol Chem* **277**: 46616-46621.

Hara-Chikuma, M., Sohara, E., Rai, T., Ikawa, M., Okabe, M., Sasaki, S., Uchida, S., Verkman, A. S. (2005) Progressive adipocyte hypertrophy in aquaporin-7 deficient mice: adipocyte glycerol permeability as a novel regulator of fat accumulation. *J. Biol. Chem.* **280**: 15493-15496.

Harries, W. E., Akhavan, D., Miercke, L. J., Khademi, S., Stroud, R. M. (2004) The channel architecture of aquaporin 0 at a 2.2-A resolution. *Proc. Natl. Acad. Sci. U. S. A.* **101**: 14045-14050.

Hatakeyama, S., Yoshida, Y., Tani, T., Koyama, Y., Nihei, K., Ohshiro, K., Kamiie, J. I., Yaoita, E., Suda, T., Hatakeyama, K., Yamamoto, T. (2001) Cloning of a new aquaporin (AQP10). abundantly expressed in duodenum and jejunum. *Biochem. Biophys. Res. Commun.* **287**: 814-819.

Hemdan, N. Y., Lehmann, I., Wichmann, G., Lehmann, J., Emmrich, F., Sack, U. (2007) Immunomodulation by mercuric chloride in vitro: application of different cell activation pathways. *Clin. Exp. Immunol.* doi:10.1111/j.1365-2249.2007.03338.x.

Henninger, N., Sicard, K. M., Bouley, J., Fisher, M., Stagliano, N. E. (2006) The proteasome inhibitor VELCADE reduces infarction in rat models of focal cerebral ischemia. *Neurosci. Lett.* **398**: 300-305.

Hernandez, M. R. (2000) The optic nerve head in glaucoma: role of astrocytes in tissue remodeling. *Prog. Retina Eye Res.* **19**: 297-321.

Hernandez, M. R., Igoe, F., Neufeld, A. H. (1988) Cell culture of the human lamina cribrosa. *Invest. Ophthalmol. Vis. Sci.* **29**: 78-89.

Hochstrasser, M. (1995) Ubiquitin, proteasomes, and the regulation of intracellular protein degradation. *Curr. Opin. Cell Biol.* **7**: 215-223.

Hortelano, S., Zeini, M., Castrillo, A., Alvarez, A. M., Bosca, L. (2002) Induction of apoptosis by nitric oxide in macrophages is independent of apoptotic volume decrease. *Cell Death Differ.* **9**: 643-650.

Hughes, F. M., Bortner, C. D., Purdy, G. P., Cidlowski, J. A. Intracellular K+ suppresses the activation of apoptosis in lymphocytes. *J. Biol. Chem.* **272**: 30567-30576.

Hurley, P. T., Ferguson, C. J., Kwon, T. H., Andersen, M. L., Norman, A. G., Steward, M. C., Nielsen, S., Case, R. M. (2001) Expression and immunolocalization of aquaporin water channels in rat exocrine pancreas. *Am. J. Physiol.* **280**: G701-709.

Iandiev, I., Pannicke, T., Reichel, M. B., Wiedemann, P., Reichenbach, A., Bringmann, A. (2005) Expression of aquaporin-1 immunoreactivity by photoreceptor cells in the mouse retina. *Neurosci.Lett.* **388**: 96-99.

Ishibashi, K., Kuwahara, M., Gu, Y., Kageyama, Y., Tohsaka, A., Suzuki, F., Marumo, F., Sasaki, S. (1997) Cloning and functional expression of a new water channel abundantly expressed in the testis permeable to water, glycerol, and urea. *J. Biol. Chem.* **272**: 20782-20786.

Ishibashi, K., Sasaki, S., Fushimi, K., Uchida, S., Kuwahara, M., Sato, H., Furukawa, T., Nakajima, K., Yamaguchi, Y., Gojobori, T., Marumo, F. (1994) Molecular cloning and

expression of a member of the aquaporin family with permeability to glycerol and urea in addition to water expressed at the basolateral membrane of kidney collecting duct cells. *Proc. Natl. Acad. Sci. U.S.A.* **91**: 6269-6273.

Itoh, T., Rai, T., Kuwahara, M., Ko, S. B., Uchida, S., Sasaki, S., Ishibashi, K. (2005) Identification of a novel aquaporin, AQP12, expressed in pancreatic acinar cells. *Biochem. Biophys. Res. Commun.* **330**: 832-838.

Jablonski, E. M., Adrian, M. M., Sokolov, E., Koniaris, L. G., Hughes, F. M, Fausto, N., Pierce, R. H., McKillop, I. H. (2006) Decreased aquaporin expression leads to increased resistance to apoptosis in hepatocellular carcinoma. *Cancer Lett.* doi:10.1016/j.canlet.2006.09.013.

Jablonski, E., Webb, A., McConnell, N., Riley, M., Hughes, F. Jr. (2004) Plasma membrane aquaporin activity can affect the rate of apoptosis but is inhibited after apoptic volume decrease. *Am. J. Physiol. Cell Physiol.* **286**: C975-985.

Jakab, M., Schmidt, S., Grundbichler, M., Paulmichl, M., Hermann, A., Weiger, T., Ritter, M. (2006) Hypotonicity and ethanol modulate BK channel activity and chloride currents in GH4/Cl pituitary tumour cells. *Acta Physiol.* **187**: 51-59.

Johnson, E. C., LaVail, M. M., Cepurna, W. O., Jia, L., Ackhavong, K., Morrison, J. C. (1999) Housing in low level, constant light stabilizes circadian intraocular pressure (IOP) oscillations in Brown Norway rats, simplifying a glaucomatous neuropathy model [ARVO abstract]. *Invest. Ophthalmol. Vis. Sci.* **40**: abstract no. 3547.

Johnson, E. C., Morrison, J. C., Farrell, S., Deppmeier, L., Moore, C. G., McGinty, M. R. (1996) The effect of chronically elevated intraocular pressure on the rat optic nerve head extracellular matrix. *Exp. Eye Res.* **62**: 663-674.

Jung, J. S., Bhat, R. V., Preston, G. M., Guggino, W. B., Baraban, J. M., Agre, P. (1994) Molecular characterization of an aquaporin cDNA from brain: candidate osmoreceptor and regulator of water balance. *Proc. Natl. Acad. Sci. U. S. A.* **91**: 13052-13056.

Kaasik, A., Safiulina, D., Zharkovsky, A., Veksler, V. (2007) Regulation of mitochondrial matrix volume. *Am. J. Physiol. Cell Physiol.* **292**: C157-163.

Kasahara, T., Kasahara, M. (1996) Expression of the rat GLUT1 glucose transporter in the yeast. Saccharomyces cerevisiae. *Biochem. J.* **315**: 177-182.

Kato, M., Ogura, K., Miake, J., Sasaki, N., Taniguchi, S., Igawa, O., Yoshida, A., Hoshikawa, Y., Murata, M., Nanba, E., Kurata, Y., Kawata, Y., Ninomiya, H., Morisaki, T., Kitakaze, M., Hisatome, I. (2005) Evidence for proteasomal degradation of Kv1.5 channel protein. *Biochem. Biophys. Res. Commun.* **337**: 343-348.

Kaur, C., Sivakumar, V., Zhang, Y., Ling, E. A. (2006) Hypoxia-induced astrocytic reaction and increased vascular permeability in the rat cerebellum. *Glia* **54**: 826-839.

Ke, C., Poon, W. S., Ng, H. K., Pang, J. C., Chan, Y. (2001) Heterogeneous responses of aquaporin-4 in oedema formation in a replicated severe traumatic brain injury model in rats. *Neurosci. Lett.* **301**: 21-24.

Kim, I. B., Lee, E. J., Oh, S. J., Park, C. B., Pow, D. V., Chun, M. H. (2002) Light and electron microscopic analysis of aquaporin 1- like-immunoreactive amacrine cells in the rat retina. *J.Comp. Neurol.* **452**: 178-191.

Kim, I. B., Oh, S. J., Nielsen, S., Chun, M. H. (1998) Immunocytochemical localization of aquaporin 1 in the rat retina. *Neurosci. Lett.* **244**: 52-54.

Kondo, H., Shimomura, I., Kishida, K., Kuriyama, H., Makino, Y., Nishizawa, H., Matsuda, M., Maeda, N., Nagaretani, H., Kihara, S., Kurachi, Y., Nakamura, T., Funahashi, T., Matsuzawa, Y. (2002) Human aquaporin adipose (AQPap) gene. Genomic structure, promoter analysis and functional mutation. *Eur. J. Biochem.* **269**: 1814-1826.

Koyama, Y., Yamamoto, T., Kondo, D., Funaki, H., Yaoita, E., Kawasaki, K., Sato, N., Hatakeyama, K., Kihara, I. (1997) Molecular cloning of a new aquaporin from rat pancreas and liver. *J. Biol. Chem.* **272**: 30329-30333.

Kroemer, G. (2003) Mitochondrial control of apoptosis: an introduction. *Biochem. Biophys. Res. Commun.* **304**: 433-435.

Kuang, K., Yiming, M., Wen, Q., Li, Y., Ma, L., Iserovich, P., Verkman, A. S., Fischbarg, J. (2004) Fluid transport across cultured layers of corneal endothelium from aquaporin-1 null mice. *Exp. Eye Res.* **78**: 791-798.

Kuang, K., Yiming, M., Zhu, Z., Iserovich, P., Diecke, F. P., Fischbarg, J. (2006) Lack of threshold for anisotonic cell volume regulation. *J. Mem. Biol.* **211**: 27-33.

Kuriyama, H., Kawamoto, S., Ishida, N., Ohno, I., Mita, S., Matsuzawa, Y., Matsubara, K., Okubo, K. (1997) Molecular cloning and expression of a novel human aquaporin from adipose tissue with glycerol permeability. *Biochem. Biophys. Res. Commun.* **241**: 53-58.

Kuriyama, H., Shimomura, I., Kishida, K., Kondo, H., Furuyama, N., Nishizawa, H, Maeda, N., Matsuda, M., Nagaretani, H., Kihara, S., Nakamura, T., Tochino, Y., Funahashi, T., Matsuzawa, Y. (2002) Coordinated regulation of fat-specific and liver-specific glycerol channels, aquaporin adipose and aquaporin 9. *Diabetes* **51**: 2915-2921.

Lambert, W., Agarwal, R., Howe, W., Clark, A. F., Wordinger, R. J. (2001) Neurotrophin and neurotrophin receptor expression by cells of the human lamina cribrosa. *Invest. Ophthalmol. Vis. Sci.* **42**: 2315-2323.

Lau, J., Dang, M., Hockmann, K., Ball, A. K. (2006) Effects of acute delivery of endothelin-1 on retinal ganglion cell loss in the rat. *Exp. Eye Res.* **82**: 132-145.

Lee, J. H., Youm, J. H., Kwon, K. S. (2006) Mercuric chloride induces apoptosis in MDCK cells. *J. Prev. Med. Pub. Health* **39**: 199-204.

Lee, W. K., Thevenod, F. (2006) A role for mitochondrial aquaporins in cellular life-and-death decisions? *Am. J. Physiol. Cell Physiol.* **291**: C195-202.

Leitch, V., Agre, P., King, L. S. (2001). Altered ubiquitination and stability of aquaporin-1 in hypertonic stress. *Proc. Natl. Acad. Sci. USA.* **98**: 2894-2898.

Levin, M. H., Verkman, A. S. (2004) Aquaporin-Dependent Water Permeation at the Mouse Ocular Surface: In Vivo Microfluorimetric Measurements in Cornea and Conjunctiva. *Invest. Ophthalmol. Vis. Sci.* **45**: 4423-4432.

Levin, M. H., Verkman, A. S. (2006) Aquaporin-3-dependent cell migration and proliferation during corneal re-epithelialization. *Invest. Ophthalmol. Vis. Sci.* **47**: 4365-4372.

Li, J., Patil, R. V., Verkman, A. S. (2002) Mildly abnormal retinal function in transgenic mice without Muller cell aquaporin-4 water channels. *Invest. Ophthalmol. Vis. Sci.* **43**: 573-579.

Li. J., Verkman. A. S. (2001) Impaired hearing in mice lacking aquaporin-4 water channels. *J. Biol. Chem.* **276**: 31233-31237.

Lipton, S. A. (2003) Possible role for memantine in protecting retinal ganglion cells from glaucomatous damage. *Surv. Ophthalmol.* **48**: S38-46.

Liu, B., Neufeld, A. H. (2001) Nitric oxide synthase-2 in human optic nerve head astrocytes induced by elevated pressure in vitro. *Arch. Ophthalmol.* **119**: 240-245.

Liu, X., Kim, C. N., Yang, J., Jemmerson R., Wang, X. (1996) Induction of apoptotic program in cell-free extracts: requirement for dATP and cytochrome c. *Cell* **86**: 147-157.

Liu, Z., Shen, J., Carbery, J. M., Mukhopadhyay, R., Agre, P., Rosen, B. (2002) Arsenite transport by mammalian aquaglyceroporins AQP7 and AQP9. *Proc. Natl. Acad. Sci. U. S. A.* **99**: 6053-6058.

Loitto, V. M., Forslund, T., Sundqvist, T., Magnusson, K. E., Gustafsson, M. (2002) Neutrophil leukocyte motility requires directed water influx. *J. Leukoc. Biol.* **71**: 212-222.

Ma, T., Fukuda, N., Song, Y., Matthay, M. A., Verkman, A. S. (2000) Lung fluid transport in aquaporin-5 knockout mice. *J. Clin. Invest.* **105**: 93-100.

Ma, T., Hara, M., Sougrat, R., Verbavatz, J. M., Verkman, A. S. (2002) Impaired stratum corneum hydration in mice lacking epidermal water channel aquaporin-3. *J. Biol. Chem.* **277**: 17147-17153.

Ma, T., Song, Y., Gillespie, A., Carlson, E. J., Epstein, C. J., Verkman, A. S. (1999) Defective secretion of saliva in transgenic mice lacking aquaporin-5 water channels. *J. Biol. Chem.* **274**: 20071-20074.

Ma, T., Yang, B., Gillespie, A., Carlson, E. J., Epstein, C. J., Verkman, A. S. (1997) Generation and phenotype of a ransgenic knockout mouse lacking the mercurial-insensitive water channel aquaporin-4. *J. Clin. Invest.* **100**: 957-962.

Maeno, E., Ishizaki, Y., Kanaseki, T., Hazama, A., Okada, Y. (2000) Normotonic cell shrinkage because of disordered volume regulation is an early prerequisite to apoptosis. *Proc. Natl. Acad. Sci. U. S. A.* **97**: 9487-9492.

Magistretti, P. J., Pellerin, L. (1999) Cellular mechanisms of brain energy metabolism and their relevance to functional brain imaging. *Philos. Trans. R. Soc. Lond. B Biol. Sci.* **354**: 1155-1163.

Manley, G. T., Fujimura, M., Ma, T., Noshita, N., Filiz, F., Bollen, A. W., Chan, P., Verkman, A. S. (2000) Aquaporin-4 deletion in mice reduces brain edema after acute water intoxication and ischemic stroke. *Nat. Med.* **6**: 159-163.

Marion, D. W., Penrod, L. E., Kelsey, S. F., Obrist, W. D., Kochanek, P. M., Palmer, A. M., Wisniewski, S. R., DeKosky, S. T. (1997) Treatment of traumatic brain injury with moderate hypothermia. *N. Engl. J. Med.* **336**: 540-546.

Markert, J. M., Fuller, C. M., Gillespie, G. Y., Bubien, J. K., McLean, L. A., Hong, R. L., Lee, K., Gullans, S. R., Mapstone, T. B., Benos, D. J. (2001) Differential gene expression profiling in human brain tumors. *Physiol. Genomics* **5**: 21-33.

Mayne, M., Ni, W., Yan, H. J., Xue, M., Johnston, J. B., Del Bigio, M. R., Peeling, J., Power, C. (2001) Antisense oligodeoxynucleotides inhibition of tumor necrosis factor-alpha expression is neuroprotective after intracerebral hemorrhage. *Stroke* **32**: 240-248.

McKinnon, S. J., Lehman, D. M., Kerrigan-Baumrind, L. A., Merges, C. A., Pease, M. E., Kerrigan, D. F., Ransom, N. L., Tahzib, N. G., Reitsamer, H. A., Levkovitch-Verbin, H., Quigley, H. A., Zack, D. J. (2002) Caspase activation and amyloid precursor protein cleavage in rat ocular hypertension. *Invest. Ophthalmol. Vis. Sci.* **43**: 1077-1087.

Melena, J., Safa, R., Graham, M., Casson, R. J., Osborne, N. N. (2003) The monocarboxylate transport inhibitor, alpha-cyano-4-hydroxycinnamate, has no effect on retinal ischemia. *Brain Res.* **989**: 128-134.

Mitchell, P., Smith, W., Attebo, K., Healey, P. R. (1996) Prevalence of open-angle glaucoma in Australia: the Blue Mountains eye study. *Ophthalmology* **103**: 1661-1669.

Morrison, J. C., Moore, C. G., Deppmeier, L. M., Gold, B. G., Meshul, C. K., Johnson, E. C. (1997) A rat model of chronic pressure-induced optic nerve damage. *Exp. Eye Res.* **64**: 85-96.

Muallem, S., Zhang, B. X., Loessberg, P. A., Star, R. A. (1992) Simultaneous recording of cell volume changes and intracellular pH or Ca^{2+} concentration in single osteosarcoma cells UMR-106-01. *J. Biol. Chem.* **267**: 17658-17664.

Murata, K., Mitsuoka, K., Hirai, T., Walz, T., Agre, P., Heymann, J. B., Engel, A., Fujiyoshi, Y. (2000) Structural determinants of water permeation through aquaporin-1. *Nature* **407**: 599-605.

Nagelhus, E. A., Horio, Y., Inanobe, A., Fujita, A., Haug, F. M., Nielsen, S., Kurachi, Y., Ottersen, O. P. (1999) Immunogold evidence suggests that coupling of K+ siphoning and water transport in rat retinal Muller cells is mediated by a coenrichment of Kir4.1 and AQP4 in specific membrane domains. *Glia* **26**: 47-54.

Nagelhus, E. A., Veruki, M. L., Torp, R., Haug, F. M., Laake, J. H., Nielsen, S., Agre, P., Ottersen, O. P. (1998) Aquaporin-4 water channel protein in the rat retina and optic nerve: polarized expression in Muller cells and fibrous astrocytes. *J. Neurosci.* **18**: 2506-2519.

Nash, M. S., Osborne, N. N. (1999) Assessment of Thy-1 mRNA levels as an index of retinal ganglion cell damage. *Invest. Ophthalmol. Vis. Sci.* **40**: 1293-1298.

Nejsum, L. N., Kwon, T. H., Jensen, U. B., Fumagalli, O., Frokiaer, J., Krane, C. M., Menon, A. G., King, L. S., Agre, P. C., Nielsen, S. (2002) Functional requirement of aquaporin-5 in plasma membranes of sweat glands. *Proc. Natl. Acad. Sci. U. S. A.* **99**: 511-516.

Nguyen, M. K., Nielsen, S., Kurtz, I. (2003) Molecular pathogenesis of nephrogenic diabetes insipidus. *Clin. Exp. Nephrol.* **7**, 9-17.

Nguyen, N. H., Brathe, A., Hassel, B. (2003) Neuronal uptake and metabolism of glycerol and the neuronal expression of mitochondrial glycerol-3-phosphate dehydrogenase. *J. Neurochem.* **85**: 831-842.

Nicchia, G. P., Frigeri, A., Liuzzi, G. M., Santacroce, M. P., Nico, B., Procino, G., Quondamatteo, F., Herken, R., Roncali, L., Svelto, M. (2000) Aquaporin-4-containing astrocytes sustain a temperature- and mercury-insensitive swelling in vitro. *Glia* **31**: 29-38.

Nicchia, G. P., Frigeri, A., Liuzzi, G. M., Svelto, M. (2003) Inhibition of aquaporin-4 expression in astrocytes by RNAi determines alteration in cell morphology, growth, and water transport and induces changes in ischemia-related genes. *FASEB J.* **17**, 1508-1510.

Nielsen, S., King, L. S., Christensen, B. M., Agre, P. (1997a) Aquaporins in complex tissues. II. Subcellular distribution in respiratory and glandular tissues of rat. *Am. J. Physiol.* **273**: C1549-1561.

Nielsen, S., Nagelhus, E. A., Amiry-Moghaddam, M., Bourque, C., Agre, P., Ottersen, O. P. (1997) Specialized membrane domains for water transport in glial cells: high-resolution immunogold cytochemistry of aquaporin-4 in rat brain. *J. Neurosci.* **17**: 171-180.

Oberhammer, F., Wilson, J. W., Dive, C., Morris, I. D., Hickman, J. A., Wakeling, A. E., Walker, P. R., Sikorska, M. (1993) Apoptotic death in epithelial cells: cleavage of DNA to 300 and/or 50 kb fragments prior to or in the absence of internucleosomal fragmentation. *EMBO J.* **12**: 3679-3684.

Oen, H., Cheng, P., Turner, H. C., Alvarez, L. J., Candia, O. A. (2006) Identification and localization of aquaporin 5 in the mammalian conjunctival epithelium. *Exp. Eye Res.* **83**: 995-998.

Osborne, N. N., Lascaratos, G., Bron, A. J., Chidlow, G., Wood, J. P. M. (2006) A hypothesis to suggest that light is a risk factor in glaucoma and the mitochondrial optic neuropathies. *Br. J. Ophthalmol.* **90**: 237-241.

Oshio, K., Binder, D .K., Yang, B., Schecter, S., Verkman, A. S., Manley, G. T. (2004) Expression of aquaporin water channels in mouse spinal cord. *J. Neurosci.* **127**: 685-693.

Oshio, K., Shields, S., Basbaum, A., Verkman, A. S., Manley, G. T. (2001) Reduced pain sensation and impaired nociception in mice lacking the aquaporin-1 membrane water channel. *J. Am. Soc. Nephrol.* **12**: 20A-21A.

Papadopoulos, M. C., Krishna, S., Verkman, A. S. (2002) Aquaporin water channels and brain edema. *Mt. Sinai, J. Med.* **69**: 343-348.

Papadopoulos, M. C., Manley, G. T., Krishna, S., Verkman, A. S. (2004) Aquaporin-4 facilitates reabsorption of excess fluid in vasogenic brain edema. *FASEB J.* **18**: 1291-1293.

Papadopoulos, M. C., Verkman, A. S. (2005) Aquaporin-4 gene disruption in mice reduces brain swelling and mortality in pneumococcal meningitis. *J. Biol. Chem.* **280**: 13906-13912.

Parker, J. C. (1993) In defense of cell volume? *Am. J. Physiol.* **265**: C1191-C1200.

Parran. D. K., Mundy, W. R., Barone, S. (2001) Effects of methylmercury and mercuric chloride on differentiation and cell viability in PC12 cells. *Toxicol. Sci.* **59**: 278-290.

Peng, J., Zhang, H., Li, T., Li, Z., Wu, Y. (2006) Effect of dexamethasone and aquaporin-1 antisense oligonucleotides on the aquaporin-1 expression in cultured human trabecular meshwork cells. *J. Huazhong Univ. Sci. Technolog Med. Sci.* **26**: 137-140.

Phillips, J. B., Williams, A. J., Adams, J., Elliott, P. J., Tortella, F. C. (2000) Proteasome inhibitor PS519 reduces infarction and attenuates leukocyte infiltration in a rat model of focal cerebral ischemia. *Stroke* **31**: 1686-1693.

Prasanna, G., Hulet, C., Desai, D., Krishnamoorthy, R. R., Narayan, S., Anne-Marie Brun, A., Suburo, A. M., Yorio, T. (2005) Effect of elevated intraocular pressure on endothelin-1 in a rat model of glaucoma. *Pharmacol. Res.* **51**: 41-50.

Preston, G. M., Jung, J. S., Guggino, W. B., Agre, P. (1993) The mercury-sensitive residue at cysteine 189 in the CHIP28 water channel. *J. Biol. Chem.* **268**: 17-20.

Preston, G. M., Smith, B. L., Zeidel, M. L., Moulds, J. J., Agre, P. (1994) Mutations in aquaporin-1 in phenotypically normal humans without functional CHIP water channels. *Science* **265**: 1585-1587.

Preston, G. M., Carroll, T. P., Guggino, W. B., Agre, P. (1992) Appearance of water channels in Xenopus oocytes expressing red cell CHIP28 protein. *Science* **256**: 385-387.

Promeneur, D., Kwon, T. H., Yasui, M., Kim, G. H., Frokiaer, J., Knrpper, M. A., Agre, P., Nielsen, S. (2000) Regulation of AQP6 mRNA and protein expression in rats in response to altered acidbase or water balance. *Am. J. Physiol.* **279**: F1014-1026.

Quigley, H. A. (1996) Number of people with glaucoma worldwide. *Br. J. Ophthalmol.* **80**: 389-393.

Quigley, H. A., Broman, A. T. (2006) The number of people with glaucoma worldwide in 2010 and 2020. *Br. J. Ophthalmol.* **90**: 262-267.

Quigley, H. A., Nickells, R. W., Kerrigan, L. A., Pease, M. E., Thibault, D. J., Zack, D. J. (1995) Retinal ganglion cell death in experimental glaucoma and after axotomy occurs by apoptosis, *Invest. Ophthalmol. Vis. Sci.* **36**: 774-786.

Rash, J. E., Yasumura, T., Hudson, C. S., Agre, P., Nielsen, S. (1998) Direct immunogold labeling of aquaporin-4 in square arrays of astrocyte and ependymocyte plasma membranes in rat brain and spinal cord. *Proc. Natl. Acad. Sci. U. S. A.* **95**: 11981-11986.

Reeves, R. E., Cammarata, P. R. (1996) Osmoregulatory alterations in myo-inositol uptake by bovine lens epithelial cells. Part 5: Mechanism of the myo-inositol e.ux pathway. *Invest. Ophthalmol. Vis. Sci.* **37**: 619-629.

Ritter, S., Llewellyn-Smith, I., Dinh, T. T. (1998) Subgroups of hindbrain catecholamine neurons are selectively activated by 2-deoxy-d-glucose induced metabolic challenge. *Brain Res.* **805**: 41-54.

Rodieck, R. W. (1998) *The first steps in Seeing.* Sunderland, MA. Sinauer Associates, Inc.

Rojec, A. M., Skowronski, M. T., Füchtbauer, E. -M., Frøkiaer, J., Nielsen, S. (2005) Generation of aquaporin-9 (AQP9) gene knock-out mice reveal normal phenotype in unstressed conditions and allow identification of specific organ/cell expression sites in mice. *FASEB J.* **19**: A637.

Ruiz, A., Rok, D. (1996) Characterization of the 3¢ UTR sequence encoded by the AQP-1 gene in human retinal pigment epithelium. *Biochim. Biophys. Acta.* **1282**: 174-178.

Ruiz-Sanchez, E., O'Donnell, M. J. (2006) Characterization of salicylate uptake across the basolateral membrane of the Malpighian tubules of Drosophila melanogaster. *J. Insect Physiol.* **52**: 920-928.

Russell V. A., Oades, R. D., Tannock, R., Killeen, P. R., Auerbach, J. G., Johansen, E. B., Sagvolden, T. (2006) Response variability in Attention-Deficit/Hyperactivity Disorder: a neuronal and glial energetics hypothesis. *Behav. Brain Funct.* **2**:30-54.

Saadoun, S., Papadopoulos, M. C., Davies, D. C., Krishna, S., Bell, B. A. (2002) Aquaporin-4 expression is increased in oedematous human brain tumours. *J. Neurol. Neurosurg. Psychiatry* **72**: 262-265.

Saadoun, S., Papadopoulos, M. C., Hara-Chikuma, M., Verkman, A. S. (2005) Impairment of angiogenesis and cell migration by targeted aquaporin-1 gene disruption. *Nature* **434**: 786-792.

Safiulina, D., Veksler, V., Zharkovsky, A., Kaasik, A. (2006) Loss of mitochondrial membrane potential is associated with increase in mitochondrial volume: physiological role in neurones. *J. Cell. Physiol.* **206**: 347-353.

Schlamp, C. L., Johnson, E. C., Li, Y., Morrison, J. C., Nickells, R. W. (2001) Changes in Thy1 gene expression associated with damaged retinal ganglion cells. *Mol. Vis.* **7**: 192-201.

Schreiber, R., Nitschke, R., Greger, R., Kunzelmann, K. (1999) The cystic fibrosis transmembrane conductance regulator activates aquaporin 3 in airway epithelial cells. *J. Biol. Chem.* **274**: 11811-11816.

Schrier, R. W., Fassett, R. G., Ohara, M., Martin, P. Y. (1998) Vasopressin release, water channels, and vasopressin antagonism in cardiac failure, cirrhosis, and regnancy. *Proc. Assoc. Am. Physicians* **110**: 407-411.

Schurr, A., Payne, R. S., Miller, J. J., Tseng, M. T., Rigor, B. M. (2001) Blockade of lactate transport exacerbates delayed neuronal damage in a rat model of cerebral ischemia. *Brain Res.* **895**: 268-272.

Schwartz, B., Rieser, J. C., Fishbein, S. L. (1977) Fluorescein angiographic defects of the optic disc in glaucoma. *Arch. Ophthalmol.* **95**: 1961-1974.

Schwartz, M. (2003) Neurodegeneration and neuroprotection in glaucoma: development of a therapeutic neuroprotective vaccine-the Friedenwald lecture. *Invest. Ophthalmol. Vis. Sci.* **44**: 1407-1711.

Serres, S., Bezancon, E., Franconi, J. M., Merle, M. (2004) Ex vivo analysis of lactate and glucose metabolism in the rat brain under different states of depressed activity. *J Biol Chem.***279**: 47881-47889.

Serve, G., Endres, W., Grafe, P. (1988) Continuous electrophysiological measurements of changes in cell volume of motoneurones in the isolated frog spinal cord. *Pflügers Arch.* **411**: 410–415.

Seshadri, T. R. (1951) Biochemistry of natural pigments. *Ann. Rev. Biochem.* **20**: 487-512.

Silva, I. A., Graber, J., Nyland, J. F., Silbergeld, E. K. (2005) In vitro HgCl2 exposure of immune cells at different stages of maturation: effects on phenotype and function. *Environ. Res.* **98**: 341-348.

Sinn, D. I., Lee, S. T., Chu, K., Jung, K. H., Kim, E. H., Kim, J. M., Park, D. K., Song, E. C., Kim, B. S., Yoon, S. S., Kim, M., Roh, J. K. (2007) Proteasomal inhibition in intracerebral hemorrhage: Neuroprotective and anti-inflammatory effects of bortezomib. *Neurosci. Res.* doi:10.1016/j.neures.2007.01.006.

Solenov, E., Watanabe, H., Manley, G. T., Verkman, A. S. (2004) Sevenfold-reduced osmotic water permeability in primary astrocyte cultures from AQP-4-deficient mice, measured by a fluorescence quenching method. *Am. J. Physio.l Cell Physiol.* **286**: C426-432.

Song, Y., Ma, T., Matthay, M.A, Verkman, A.S. (2000) Role of aquaporin-4 in airspace-to-capillary water permeability in intact mouse lung measured by a novel gravimetric method. *J. Gen. Physiol.* **115**: 17–27.

Song, Y., Verkman, A. S. (2001) Aquaporin-5-dependent fluid secretion in airway submucosal glands. *J. Biol. Chem.* **276**, 41288–41292.

Srinivas, S. P., Bonanno, J. A. (1997) Measurement of changes in cell volume based on fluorescence quenching. *Am. J. Physiol.* **272**: C1405-C1414.

Stamer, W. D., Bok, D., Hu, J., Jaffe, G. J., McKay, B. S. (2003) Aquaporin-1 channels in the human retinal pigment epithelium: role in transepithelial water movement. *Invest.Ophthalmol.Vis. Sci.* **44**: 2803-2808.

Stoiber, T., Degen, G. H., Bolt, H. M., Unger, E. (2004) Interaction of mercury (II) with the microtubule cytoskeleton in IMR-32 neuroblastoma cells. *Toxicol. Lett.* **151**: 99-104.

Stokely, M. E., Brady, S. T., Yorio, T. (2002) Effects of endothelin-1 on components of anterograde axonal transport in optic nerve. *Invest. Ophthalmol. Vis. Sci.* **43**: 3223-3230.

Strange, K. (2004) Cellular volume homeostasis. *Adv. Physiol. Educ.* **28**: 155-159.

Sui, H., Han, B. G., Lee, J. K., Walian, P. and Jap, B. K. (2001) Structural basis of water-specific transport through the AQP1 water channel. *Nature* **414**: 872-878.

Susin, S. A., Lorenzo, H. K., Zamzami, N, Marzo, I., Snow, B. E., Brothers, G. M., Mangion, J., Jacotot, E., Costantini, P., Loeffler, M., Larochette, N., Goodlett, D. R., Aebersold, R., Siderovski, D. P., Penninger, J. M., Kroemer, G. (1999) Molecular characterization of mitochondrial apoptosisinducing factor. *Nature* **397**: 441-446.

Tanghe, A., Kayingo, G., Prior, B. A., Thevelein, J. M., Van Dijck, P. (2005) Heterologous aquaporin (AQY2-1) expression strongly enhances freeze tolerance of Schizosaccharomyces pombe. *J. Mol. Microbiol. Biotechnol.* **9**: 52-56.

Tanghe, A., Van Dijck, P., Thevelein, J. M. (2006) Why do microorganisms have aquaporins? *TRENDS Microbiol.* **14**: 78-85.

Taniguchi, M., Yamashita, T., Kumura, E., Tamatani, M., Kobayashi, A., Yokawa, T., Maruno, M., Kato, A., Ohnishi, T., Kohmura, E., Tohyama, M., Yoshimine, T. (2000)

Induction of aquaporin-4 water channel mRNA after focal cerebral ischemia in rat. *Brain Res. Mol. Brain Res.***78**: 131-137.

Tanihara, M., Hangai, S., Sawaguchi, H., Abe, M., Kageyama, F., Nakazawa F, Shirasawa E, Honda Y. (1997) Up-regulation of glial fibrillary acidic protein in the retina of primate eyes with experimental glaucoma. *Arch. Ophthalmol.* **115**: 752-756.

Telford, W. G., King, L. E., Fraker, P. J. (1991) Evaluation of glucocorticoid-induced DNA fragmentation in mouse thymocytes by flow cytometry. *Cell Prolif.* **24**: 447-459.

Tezel, G., Yang, X., Cai, J. (2005) Proteomic identification of oxidatively modified retinal proteins in a chronic pressure-induced rat model of glaucoma. *Invest. Ophthalmol. Vis. Sci.* **46**: 3177-3187.

Thiagarajah, J. R. Verkman, A. S. (2002) Aquaporin deletion in mice reduces corneal water permeability and delays restoration of transparency after swelling. *J. Biol. Chem.* **277**: 19139-19144.

Tielsch, J. M., Katz, J., Singh, K. (1991) A population-based evaluation of glaucoma screening: the Baltimore eye survey. *Am. J. Epidemiol.* **134**: 1102-1110.

Tsukaguchi, H., Shayakul, C., Berger, U. V., Mackenzie, B., Devidas, S., Guggino, W. B., Vanhoek, A. N., Hediger, M. A. (1998) Molecular characterization of a broad selectivity neutral solute channel. *J. Biol. Chem.* **273**: 24737-24743.

Tsukaguchi, H., Weremowicz, A., Morton, C. C., Hediger, M. A. (1999) Functional and molecular characterization of the human solute channel aquaporin-9. *Am. J. Physiol.* **277**: F685-F696.

Varadaraj, K., Kumari, S., Shiel, A., Mathias, T. (2005) Regulation of aquaporin water permeability in the lens. *Invest. Ophthalmol. Vis. Sci.***46**: 1393-1402.

Varela, H. J., Hernandez, M. R. (1997) Astrocyte responses in human optic nerve head with primary open-angle glaucoma. *J. Glaucoma.* **5**: 303-313.

Venero, J. L., Machado, A., Cano, J. (2004) Importance of aquaporins in the physiopathology of brain edema. *Curr. Pharm. Des.***10**: 2153-2161.

Verbavatz, J. M., Brown, D., Sabolic, I., Valenti, G., Ausiello, D. A., Van Hoek, A. N., Ma, T., Verkman, A. S. (1993) Tetrameric assembly of CHIP28 water channels in liposomes and cell membranes: a freeze-fracture study. *J. Cell Biol.* **123**: 605-618.

Verkman, A. S. (2003) Role of aquaporin water channels in eye function. *Exp. Eye Res.* **76**: 137-143.

Verkman, A. S. (2005) More than just water channels: unexpected cellular roles of aquaporins. *J. Cell Sci.* **118**: 3225-3232.

Verkman, A. S. (2005) Novel roles of aquaporins revealed by phenotype analysis of knockout mice. *Rev Physiol. Biochem. Pharmacol.* **155**: 31-55.

Verkman, A. S. (2006) Aquaporins in endothelia. *Kidney Int.* **69**: 1120-1123.

Viadiu, H., Gonen, T., Walz, T. (2007) Projection map of aquaporin-9 at 7 a resolution. *J. Mol. Biol.* **367**: 80-88.

Vizuete, M. L., Venero, J. L., Vargas, C., Ilundain, A. A., Echevarria, M., Machado, A., Cano, J. (1999) Differential upregulation of AQP4 mRNA expression in reactive astrocytes after brain injury: potential role in brain edema. *Neurobiol. Dis.* **6**: 245-258.

Vu, C. C., Bortner, C. D., Cidlowski, J. A. (2001) Differential involvement of initiator caspases in apoptotic volume decrease and potassium efflux during Fas- and UV-induced cell death. J. Biol. Chem. 276: 37602-37611.

Wadia, J. S., Chalmers-Redman, R. M. E., Ju, W. J. H., Carlile, G. W., Phillips, J. L., Fraser, A. D., Tatton, W. G. (1998) Mitochondrial membrane potential and nuclear changes in apoptosis caused by serum and nerve growth factor withdrawal: time course and modification by deprenyl. *J. Neurosci.* **18**: 932-947.

Wang, H., Traub, L. M., Weixel, K. M., Hawryluk, M. J., Shah, N., Edinger, R. S., Perry, C. J., Kester, L., Butterworth, M. B., Peters, K. W., Kleyman, T. R., Frizzell, R. A., Johnson, J. P. (2006) Clathrin-mediated endocytosis of the epithelial sodium channel: Role of epsin. *J. Biol. Chem.* **281**: 14129-14135.

Wang, Q., Lu, Y., Yuan, M., Darling, I. M., Repasky, E. A., Morris, M. E. (2006) Characterization of Monocarboxylate Transport in Human Kidney HK-2 Cells. *Mol. Pharm.* **3**: 675-685.

Wang, X. (2001) The expanding role of mitochondria in apoptosis. *Genes Dev.* **15**: 2922-2933.

Weinreb, R. N., Cioffi, G. A., Harris, A. (1997) Optic nerve blood flow. In: Shields B, ed. *100 Years of progress in glaucoma.* Philadelphia: Lippincott Raven Healthcare, 59-78.

Weinreb, R. N., Toris, C. B., Gabelt, B. T., Lindsey, J. D., Kaufman, P. L. (2002) Effects of prostaglandins on the aqueous humor outflow pathways. *Surv. Ophthalmol.* **47**: S53–64.

Weinreb, R. N., Tsai, C., Morsman, D. (1995) Laser trabeculoplasty. In: Krupin T, ed. *The Glaucomas*, 2nd edition. St. Louis: CV Mosby, 1575-1590.

Wellner, R. B., Redman, R. B., Swain, W. D., Baum, B. J. (2006) Further evidence for AQP8 expression in the myoepithelium of rat submandibular and parotid glands. *Pflugers Arch.* **451**: 642-645.

Williams, A. J., Hale, S. L., Moffett, J. R., Dave, J. R., Elliott, P. J., Adams, J., Tortella, F. C. (2003) Delayed treatment with MLN519 reduces infarction and associated neurologic deficit

caused by focal ischemic brain injury in rats via antiinflammatory mechanisms involving nuclear factor-kappaB activation, gliosis, and leukocyte infiltration. *J. Cereb. Blood Flow Metab.* **23**: 75-87.

Wilson, M. R., Mendis, U., Paliwal, A., Haynatzka, V. (2003) Long-term followup of primary glaucoma surgery with Ahmed glaucoma valve implant versus trabeculectomy. *Am. J. Ophthalmol.* **136**: 464-470.

Winkler, B. S., Starnes, C. A., Sauer, M. W., Firouzgan, Z., Chen, S. C. (2004) Cultured retinal neuronal cells and Muller cells both show net production of lactate. *Neurochem. Int.* **45**: 311-320.

Woldemussie, E., Wijono, M., Ruiz, G. (2004) Muller cell response to laser-induced increase in intraocular pressure in rats. *Glia* **47**: 109-119.

Wolfs, R. C., Klaver, C. C., Ramrattan, R. S., van Duijn, C. M., Hofman, A, de Jong, P. T. (1998) Genetic risk of primary open-angle glaucoma. Population-based familial aggregation study. *Arch. Ophthalmol.* **116**: 1640-1645.

Xiong, X., Miao, J., Xi, Z., Zhang, H., Han, B., Hu, Y. (2005) Regulatory effect of dexamethasone on aquaporin-1 expression in cultured bovine trabecular meshwork cells. *J. Huazhong Univ. Sci. Technolog. Med. Sci.* **25**: 735-737.

Xue, L. P., Lu, J., Cao, Q., Hu, S., Ding, P., Ling, E. A. (2006) Muller glial cells express nestin coupled with glial fibrillary acidic protein in experimentally induced glaucoma in the rat retina. *Neuroscience* **139**: 723-732.

Xue, L. P., Lu, J., Cao, Q., Kaur, C., Ling, E. A. (2006) Nestin expression in Muller glial cells in postnatal rat retina and its upregulation following optic nerve transection. *Neuroscience* **143**: 117-127.

Yamamoto, N., Kazuhiro, Y., Kiyofumi, A., Kazuya, S., Toyohiro, T., Yoshihito F., Hirotada, K., Masataka, F., Noritaka, A., Mitsuhito, M., Kazuo, Y., Yutaka, M., Taiji. K. (2001) Alterations in the expression of the AQP family in cultured rat astrocytes during hypoxia and reoxygenation. *Brain Res. Mol. Brain Res.* **90**: 26-38.

Yamamoto, N., Sobue, K., Miyachi, T., Inagaki, M., Miura, Y., Katsuya, H., Asai, K. (2001) Differential regulation of aquaporin expression in astrocytes by protein kinase C. *Brain Res. Mol. Brain Res.* **95**: 110-116.

Yan, X., Tezel, G., Wax, M.B., Edward, D.P. (2000) Matrix metalloproteinases and tumor necrosis factor alpha in glaucomatous optic nerve head. *Arch. Ophthalmol.* **118**: 666-673.

Yang, B., Kim, J. K., Verkman, A. S. (2006) Comparative efficacy of HgCl2 with candidate aquaporin-1 inhibitors DMSO, gold, TEA+ and acetazolamide. *FEBS Letters* **580**: 6679-6684.

Yang, B., Song, Y., Zhao, D., Verkman, A. S. (2005) Phenotype analysis of aquaporin-8 null mice. *Am. J. Physiol. Cell Physiol.* **288**: C1161-C1170.

Yang, B., Verkman, A. S. (1997) Water and glycerol permeability of aquaporins 1-5 and MIP determined quantitatively by expression of epitope-tagged constructs. *J. Biol. Chem.* **272**: 20782-20786.

Yang, B., Zhao, D., Verkman, A. S. (2006) Evidence against functionally significant aquaporin expression in mitochondria, *J. Biol. Chem.* **281**: 16202-16206.

Yasui, M., Hazama, A., Kwon, T. H., Nielsen, S., Guggino, W. B., Agre, P. (1999) Rapid gating and anion permeability of an intracellular aquaporin. *Nature* **402**: 184-187.

Yorio, T., Dibas, A. (2004) New therapies for glaucoma: are they all up to the task? *Expert. Opin. Ther. Patents* **14**: 1743-1762.

Yu, S., Tanabe, T., Yoshimura, N. (2006) A rat model of glaucoma induced by episcleral vein ligation. *Exp. Eye Res.* **83**: 758-770.

Zangwill, L. M., Bowd, C., Berry, C. C. (2001) Discriminating between normal and glaucomatous eyes using the Heidelberg Retina Tomograph, GDx Nerve Fiber Analyzer, and Optical Coherence Tomograph. *Arch. Ophthalmol.* **119**: 985-993.

Zangwill, L. M., Bowd, C., Weinreb, R. N. (2000) Evaluating the optic disc and retinal nerve fiber layer in glaucoma II: optical image analysis. *Sem. Ophthalmol.* **15**: 206-220.

Zelenina, M., Zelenin, S., Aperia, A. (2005) Water channels (aquaporins) and their role for postnatal adaptation. *Pediatr. Res.* **57**: 47R-53R.

Zelenina, M., Zelenin, S., Bondar, A. A., Brismar, H., and Aperia, A. (2002) Water permeability of aquaporin-4 is decreased by protein kinase C and dopamine. *Am. J. Physiol. Renal Physiol.* **283**: F309-F318.

Zeuthen, T., Klaerke, D.A. (1999) Transport of water and glycerol in aquaporin 3 is gated by H+. *J. Biol. Chem.* **274**: 21631-21636.

Zhang, D., Vetrivel, L., Verkman, A. S. (2002) Aquaporin Deletion in Mice Reduces Intraocular Pressure and Aqueous Fluid Production. *J. Gen. Physiol.* **119**: 561-569.

Zhang, X., Krishnamoorthy, R. R., Prasanna, G., Narayan, S., Clark, A., Yorio, T. (2003) Dexamethasone regulates endothelin-1 and endothelin receptors in human non-pigmented ciliary epithelial (HNPE) cells. *Exp. Eye Res.* **76**: 261-272.
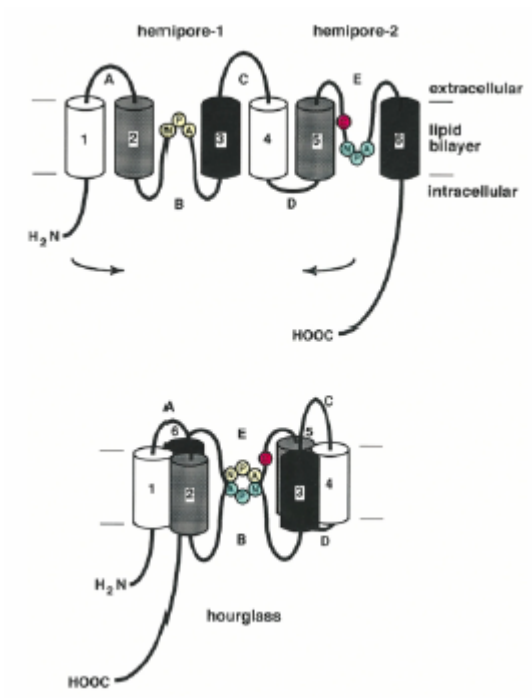
Fig. 1. The hourglass model for AQP1 topology. (Jung et al., 1994).
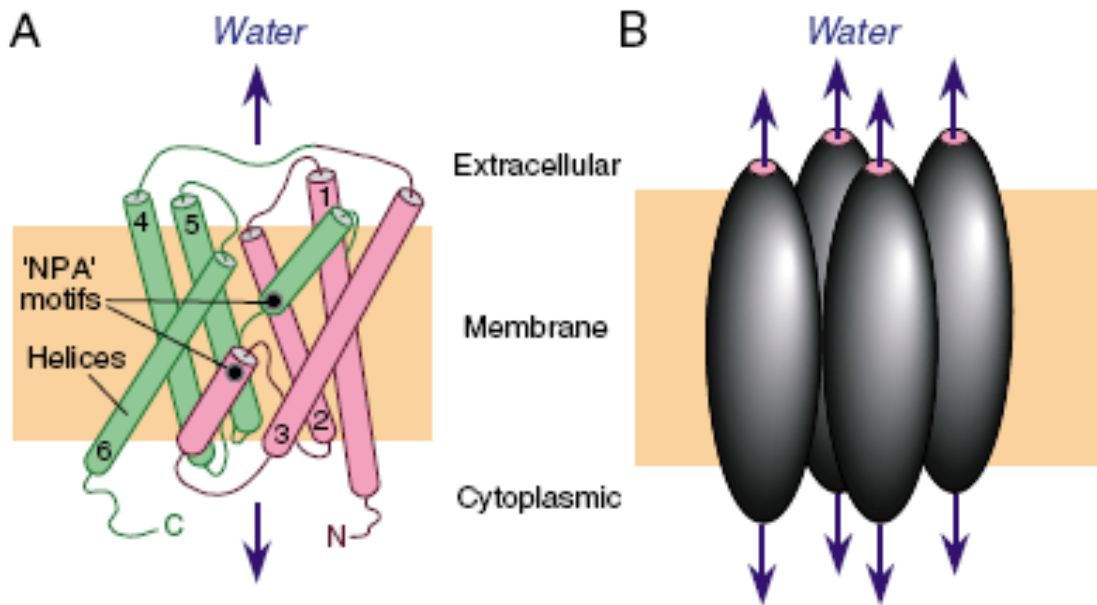
Fig. 2. Structure of AQP1 monomers and their tetrameric assembly in membranes.

(A) Structure of AQP1 monomer showing tilted transmembrane α-helical domains (numbered 1-6) surrounding a water pore. Conserved 'NPA' motifs are indicated. (B) Tetrameric assembly of AQP1 in a membrane in which individual monomers contain water pores (Verkman, 2005).
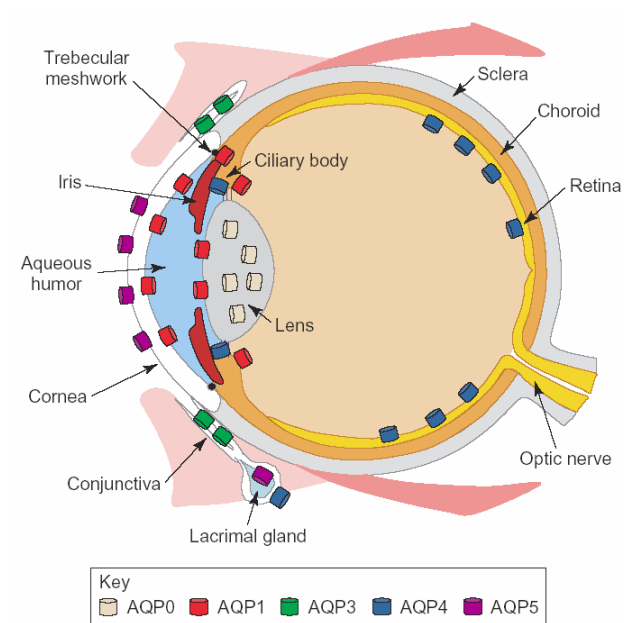
Fig. 3. Distribution of aquaporins in human eye. (Castle, 2005).
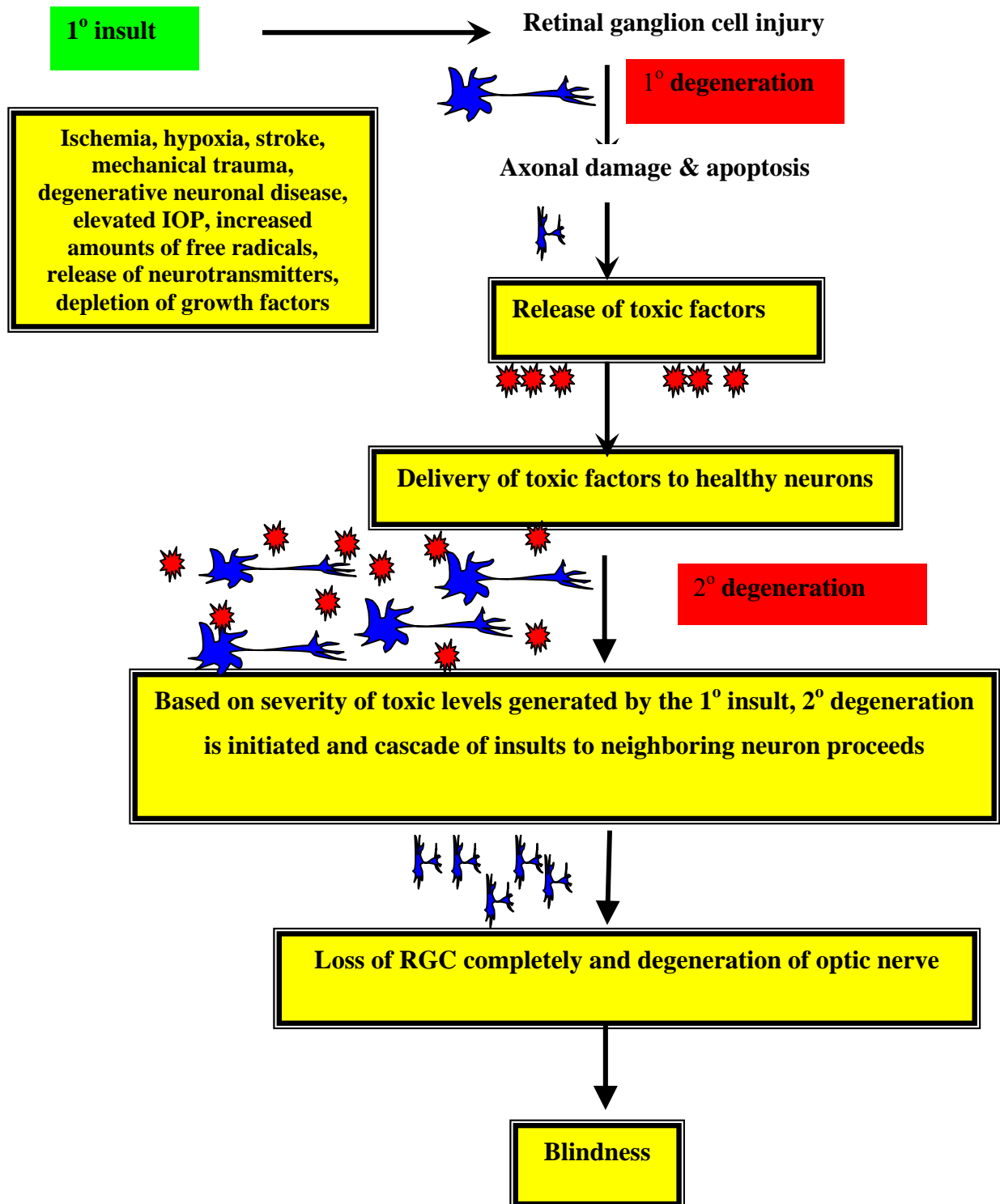
Fig. 4. Proposed model of RGC apoptosis in glaucoma. (Yorio T. et al., 2004).
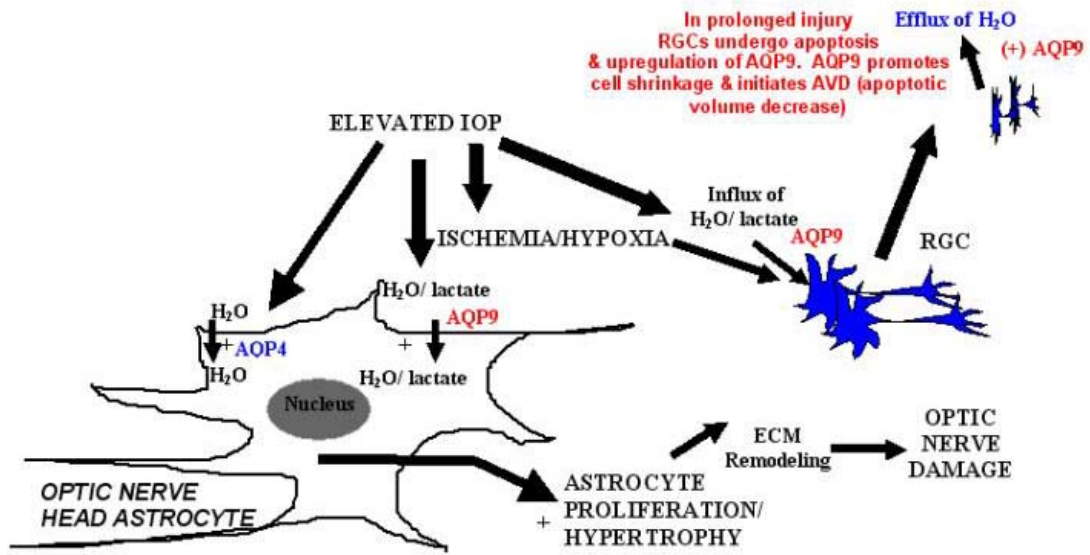
Fig. 5. Proposed role of AQP9 in RGC apoptosis in glaucoma.
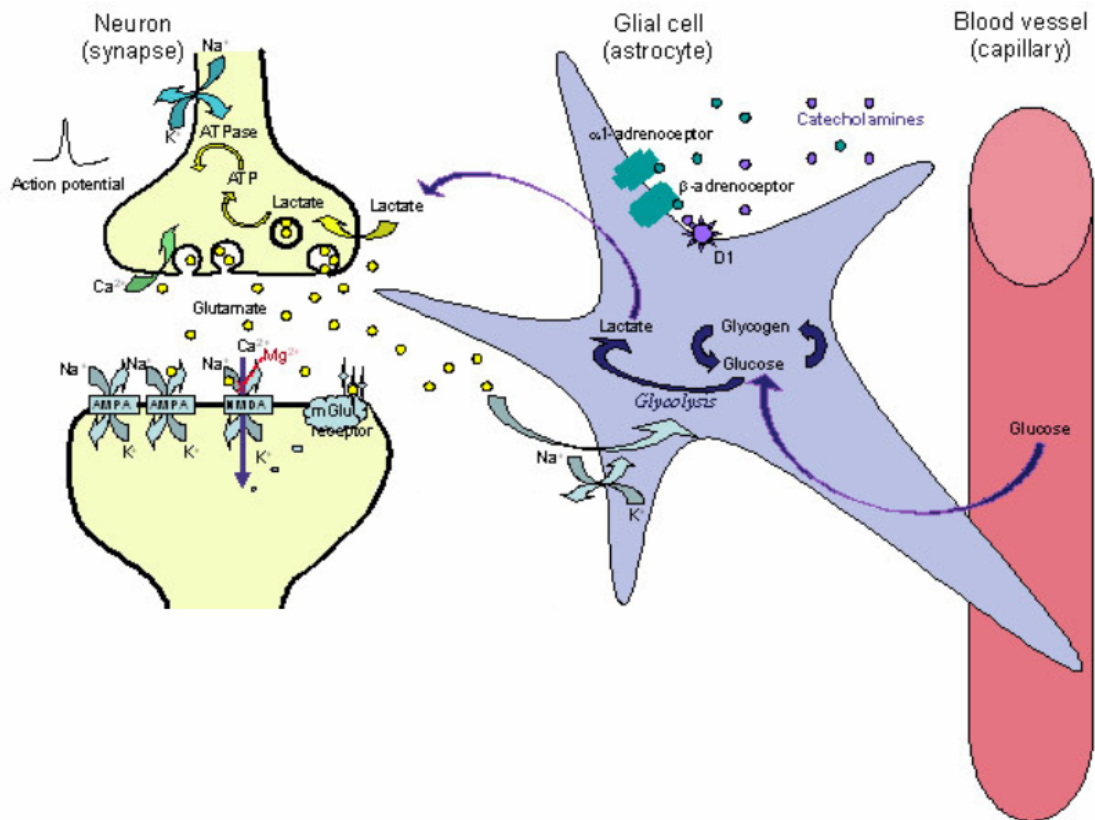
Fig. 6. A scheme illustrating a glutamatergic neuron (left) a glial cell (astrocyte) and a small blood vessel (right) and the major components contributing to hypotheses. (Russell V. A. et al., 2006)
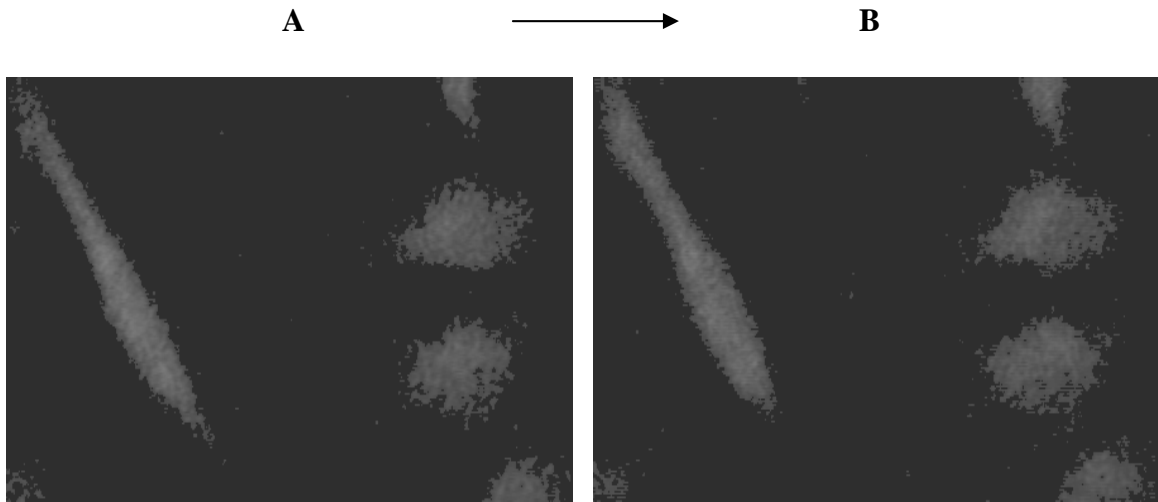
Fig. 7. Evidence for hypoosmolarity-induced changes in retinal ganglion cells

cellular volume.

RGC-5 cells were labeled with fura-2 (4 µM), and volume changes were followed by measuring fluorescence at the excitation wavelength of 360 nm. Cells were incubated in isotonic solution, then switched to a hypotonic solution, resulting in a decrease in the fluorescence intensity, indicating cellular swelling. A. Picture of cells in isotonic medium. B. Picture of the same cells after a hypotonic shock (picture was taken 3 min after shock).

A Effect of hypotonic shock (20%) on volume increase in RGC-5 cells

B Effect of phloretin (40 μM) on volume increase in RGC-5 cells upon hypotonic shock (20%)

Effect of CIN (60 μM) on volume increase in RGC-5 cells upon hypotonic shock
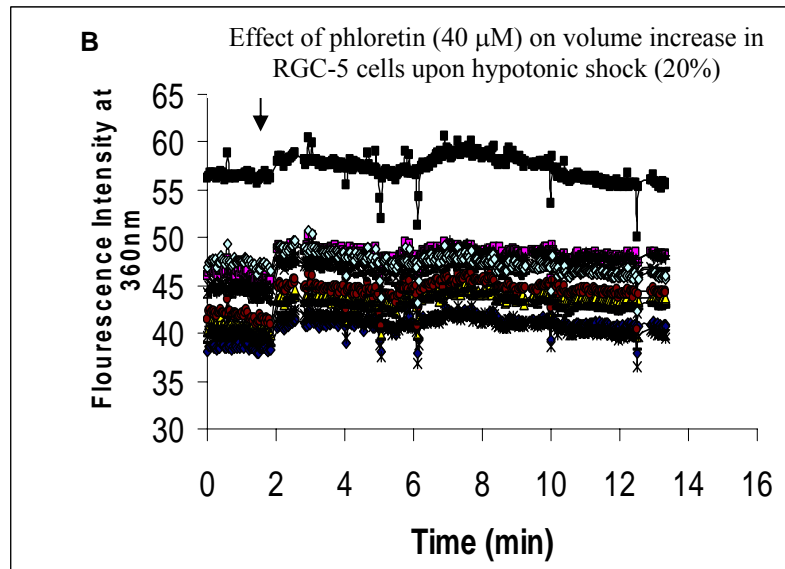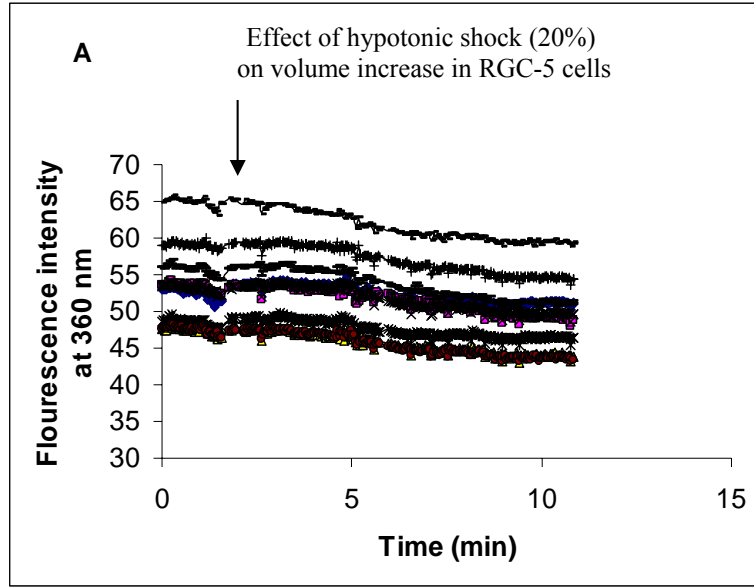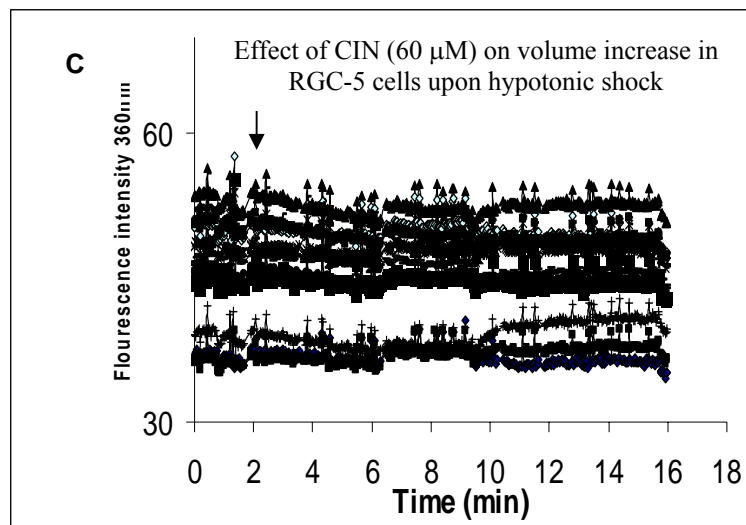
Fig. 8. Known inhibitors of aquaporin-9 prevented volume changes in retinal ganglion cells upon hypotonic stress.

Cells were incubated in isotonic solution, then switched to a hypotonic solution, resulting in a decrease in the fluorescence intensity, indicating cell swelling. Pretreatment of cells with either phloretin (40 μM, B) or CIN (60 μM, α-Cyano-4- hydroxycinnamic acid, C), known inhibitors of AQP9, for 2 minutes prior to hypotonic shock, prevented cellular swelling (no decrease in fluorescence intensity). The arrow indicates the start of hypotonic shock. Both inhibitors had no effect on basal fluorescence.

103

A

500bp→ ←AQP9

B

500bp→ ←AQP9
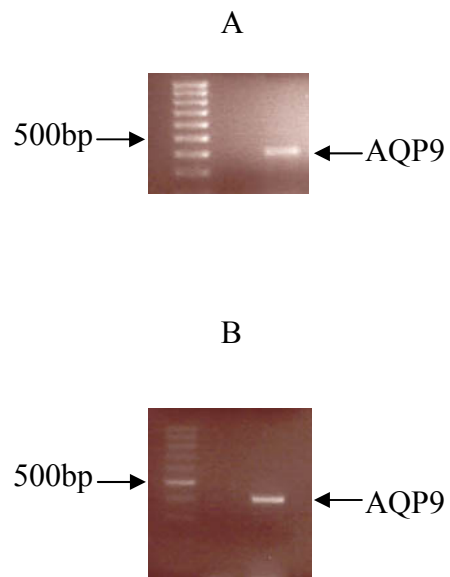
Fig. 9. PCR results of AQP9 from RGC-5 (A) and differentiated RGC-5 cells (B).

Both have a product size of 401 bp.

Fig. 10. Detection of AQP9 in RGC-5 cells and testing the effect of hypoxia on

AQP-9 expression.

After exposure to hypoxia for the indicated periods (from 1 to 4 h), the cells were processed for Western blotting. A: Western blotting against AQP-9. A doublet of 35 & 50 kDa was seen in RGC-5 cells that was absent in the presence of the competing peptide antigen (B). 1: con, 2: 1hr hypoxia, 3: 2h hypoxia, 4: hypoxia 3hr, and 5: 4hr hypoxia. Membrane in A was stripped and probed with anti β-tubulin antibodies for normalization (C).
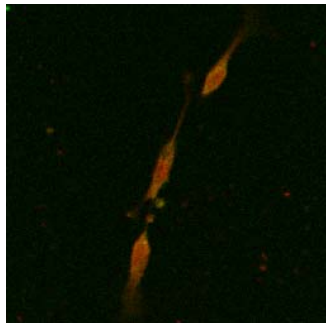
A. Primary RGC stained with anti-AQP9/Thy-1

B. Primary RGC stained without primary antibody

Fig. 11. Immunolocalization studies for Thy-1 and AQP9 in primary RGC cells.

Primary RGC cells were positive for Thy-1 and AQP9 (A). A single typical control without primary antibody is included (B). These results support the hypothesis that primary RGCs isolated from retinas express AQP9 similar to the transformed RGC-5 cells.

RGC layer

| A. DIC picture | B. Retina stained with anti-AQP9 (green) and Thy-1 (red) | C. Retina without primary antibody |

Fig. 12. Immunolocalization studies for Thy-1 and AQP9 in the retinal ganglion cell layer of Wistar rats.

DIC image (A), double AQP9/Thy-1 labeling (B), and the labeling in the absence of primary antibodies (C, negative control) are shown.
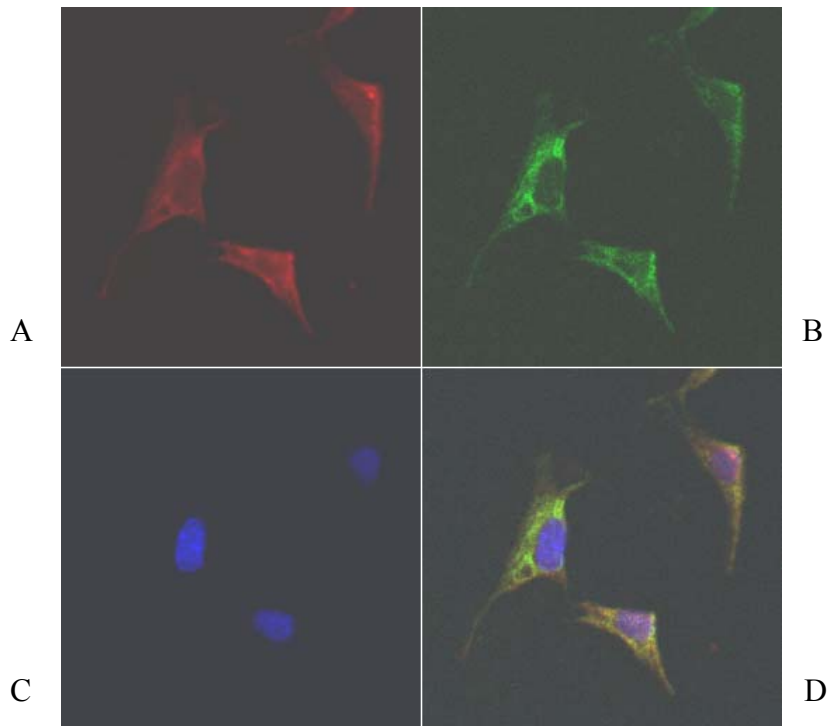
Fig. 13. Immunolocalization studies for cytochrome c and AQP9 in RGC-5 cells.

Panel A is stained with anti-AQP9 (red), panel B is stained with anti-cytochrome c (green), panel C is stained with DAPI for nuclei, and panel D is the overlay of anti-AQP9/cytochrome c and DAPI.
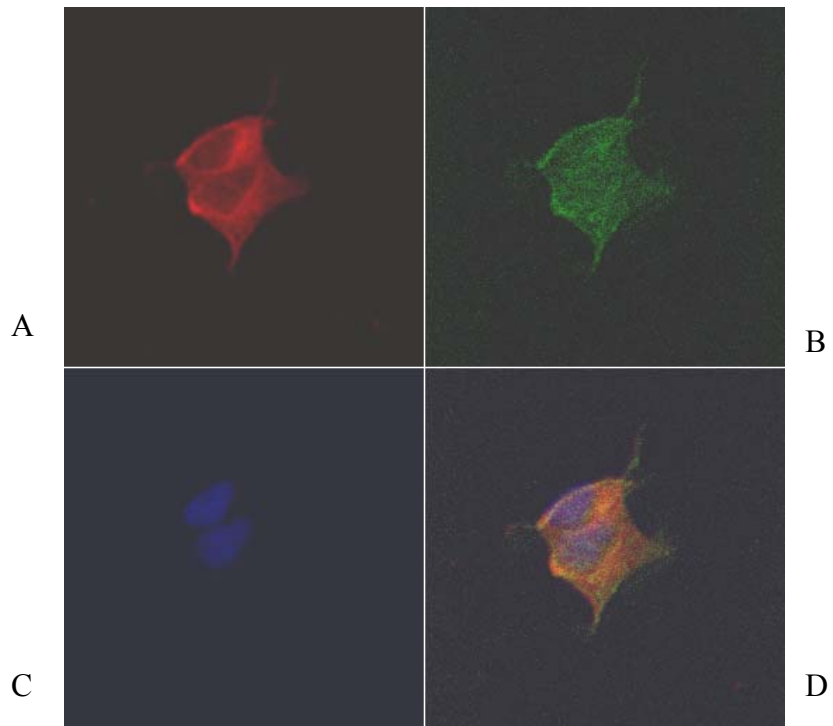
Fig. 14. Immunolocalization studies for adenine nucleotide translocator (ANT) and AQP9 in RGC-5 cells.

Panel A shows staining with anti-AQP9 (red), panel B shows staining with anti-ANT (green), panel C shows staining with DAPI for nuclei, and panel D shows the overlay of anti-AQP9/ANT and DAPI.
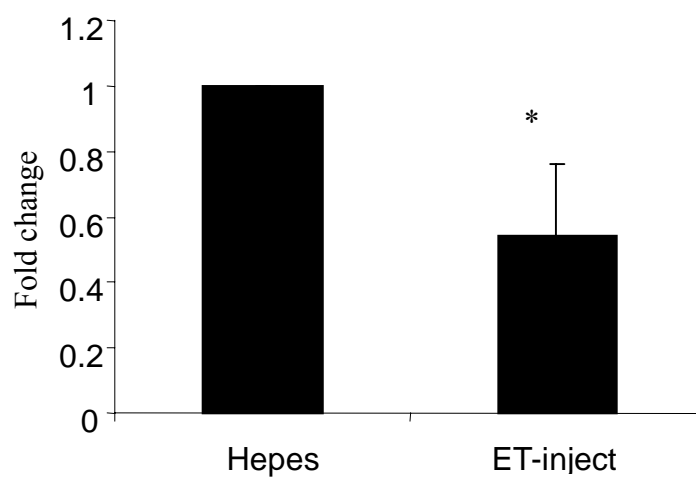
Fig. 15. A single intravitreous ET-1 injection produced significant reductions of

AQP4 mRNA in rat retinas.

As shown, ET-1 injection resulted in a decrease in AQP4 mRNA as determined by Q-RT-PCR. Five out of seven rats (71%) showed a significant reduction in mRNA [54 $\pm$ 22%, $P<0.001$ vs. control or HEPES-injected (vehicle)].
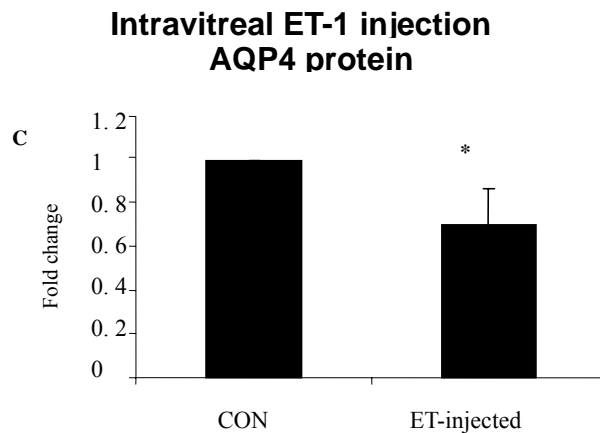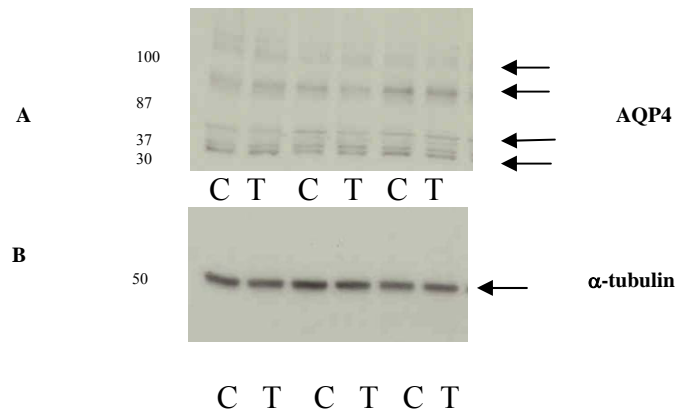
Fig. 16. A single intravitreous ET-1 injection reduced AQP4 protein levels in rat retinas.

As shown (A), ET-1 injection resulted in a decrease in AQP4 protein levels. Nine out of 11 rats (82%, Fig. 16a shows data for 3 rats) showed a decrease in AQP4 protein levels. C is the control sample; T is ET-1 treated eye. B is for normalizing using anti-α-tubulin, and C is densitometric quantification of A (P<0.05 vs. control).
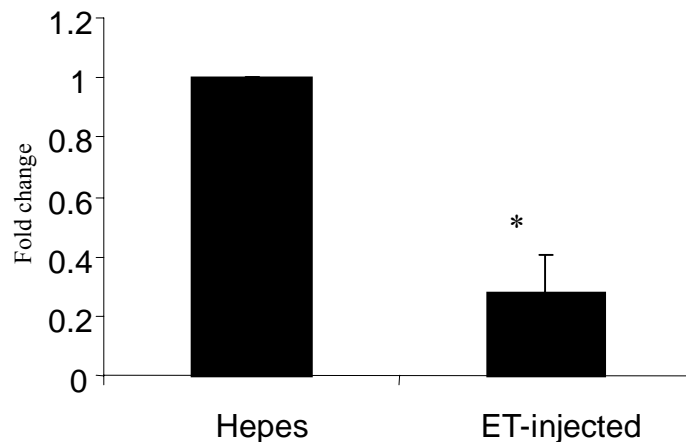
Fig. 17. A single intravitreous ET-1 injection produced significant reductions

AQP9 mRNA in rat retinas.

In six out of seven rats (86%), ET-injection produced a reduction in AQP9 [$28 \pm 12\%$, P<0.001 vs. control or HEPES-injected (vehicle)].

GFAP   50KDa   ⟶

C T C T C T

A

Caspase-3   31KDa   ⟶

C T C T C T

B

Thy-1   23KDa   ⟶

C T C T

C

XIAP   55KDa   ⟶

C T   C T   C T

D
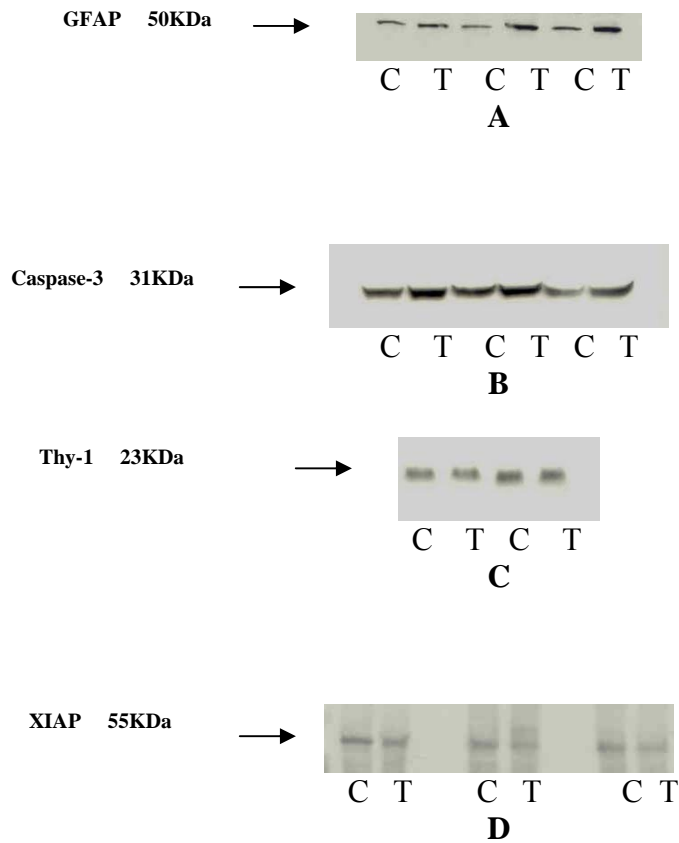
Fig. 18. A single intravitreous ET-1 injection (T) increased GFAP and caspase-3

protein levels while decreasing Thy-1 and XIAP protein levels in rat retinas.

ET-1 injection resulted in an increase in GFAP protein levels (A) and caspase-3 protein levels (B). By contrast, ET-1 injection resulted in a decrease in Thy-1 protein levels (C) and XIAP protein levels (D).

113

Intraocular Pressure Measurments -Rat #6 Cohort 3-29-06

Intraocular Pressure via Tonolab (mmHg)

Treated Eye
Control Eye

Days Following Injection
314 mmHg/days on 5-10-06

IOP Measurments for Rat #8-Cohort 3-30-06

Intraocular Pressure via Tonolab (mmHg)

Treated eye
Control eye

Days following Injection
342 mmHg/days on 5-10-06
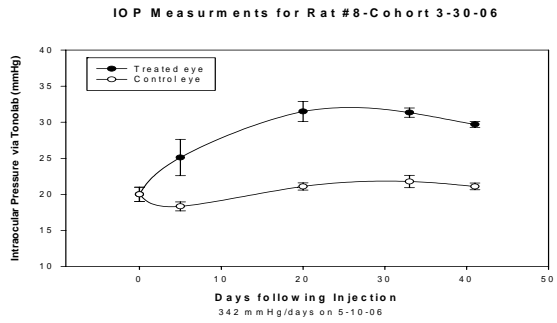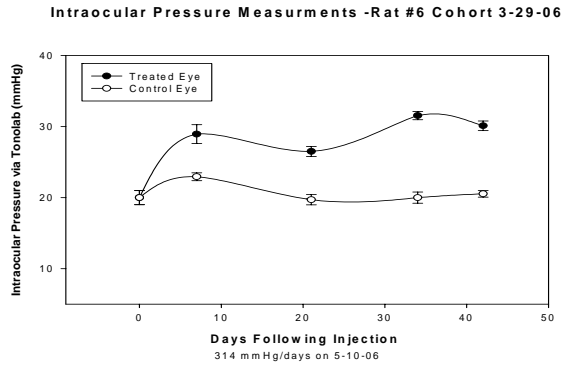
Fig. 19 Examples of the intraocular pressure measurement of rats (N=20).
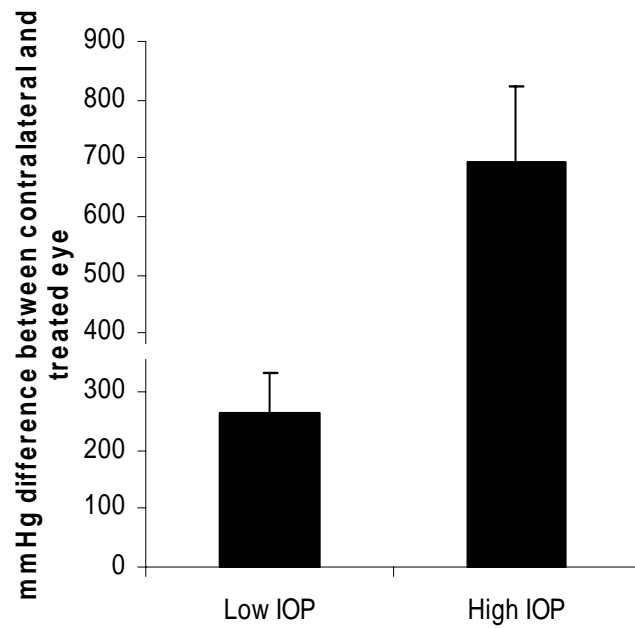
Fig. 20. IOP measurements in the Morrison rat model of glaucoma.

IOP was elevated in one eye of Brown Norway rats using hypertonic saline while the contralateral eye served as a control. Rats were maintained for up to 90 days post-surgery. Low IOP was the data from the contralateral eye and high IOP was the data from the treated eye (N=19, P<0.05 vs. control).

A

100
87

37

30

1C 1T 2C 2T 3C 3T

B

1C 1T 2C 2T 3C 3T
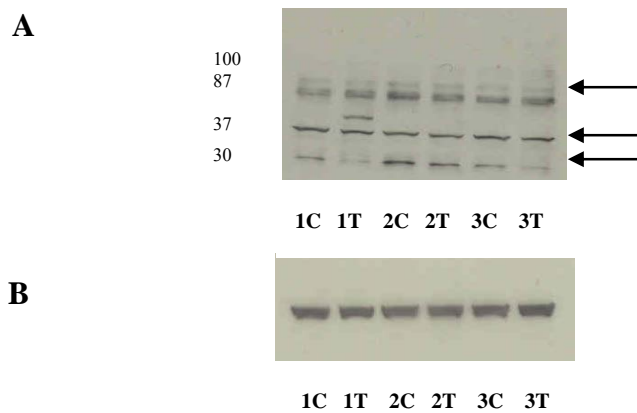
Fig. 21. Elevation of IOP affected AQP4 isoforms differently.

Plasma membrane fractions were isolated as described in Methods. Elevated IOP appears to lower the expression of the smaller AQP isoform (~30 kDa) while increasing the levels of the higher molecular weight AQP4 isoforms (~37, 87 and 100 kDa) (A). The higher molecular weight isoforms are ubiquitinated AQP4. C: control eye and T: elevated IOP eye. Membranes were stripped, and then re-probed with anti-α-tubulin for normalization (B).
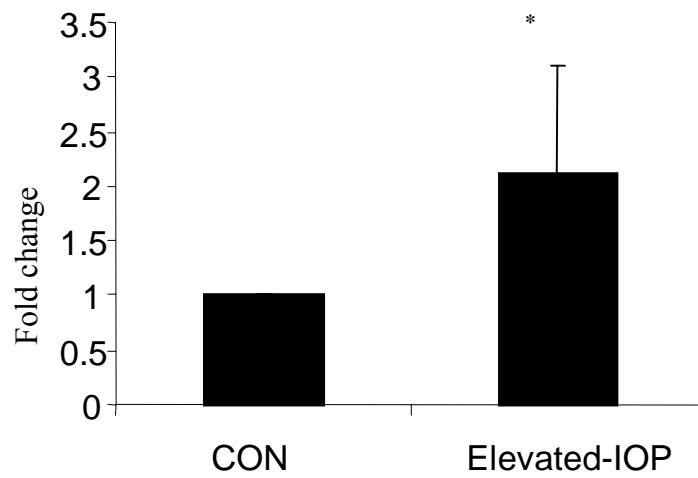
Fig. 22. Elevation of IOP-increased AQP9 mRNA in rat retinas.

As shown, in five out egiht rats (63%), IOP elevation increased in AQP9 mRNA (211 ±
100%, P<0.05 vs. control retina).
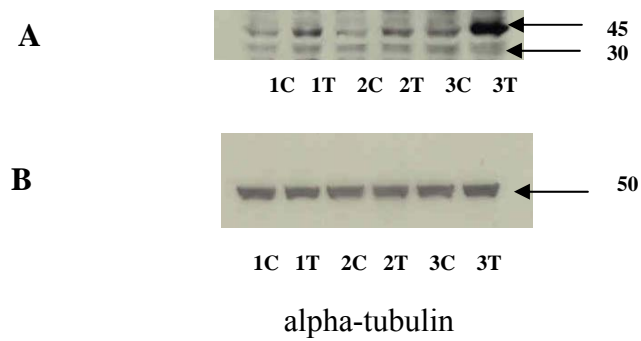
Fig. 23. Elevation of IOP-increased AQP9 protein levels in rat retinas.

Similar to increased AQP9 mRNA, elevated IOP increased AQP9 protein levels in six out of seven rats (86%)(377 $\pm$ 200%, P<0.05 vs. control retina, A). B shows normalization using α-tubulin antibodies. C: control eye and T: elevated IOP eye.

GFAP   50KDa ⟶   [gel image]   A

1C 1T 2C 2T

Thy-1   23KDa ⟶   [gel image]   B

1C 1T 2C 2T
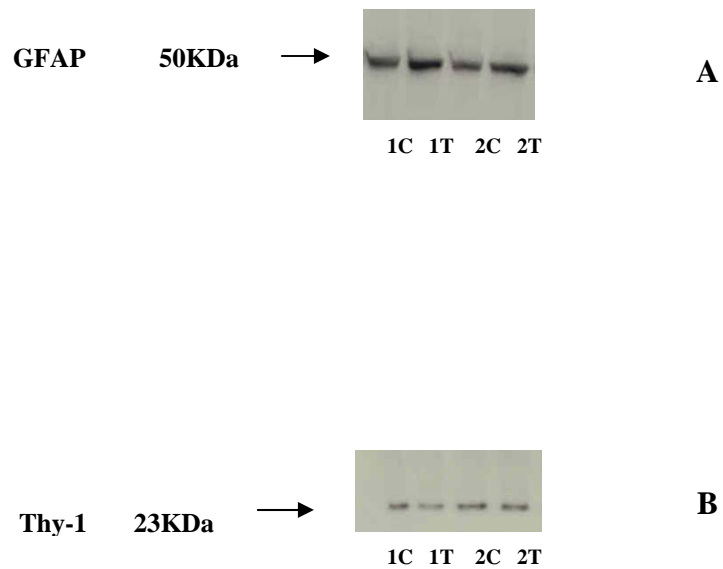
Fig. 24. Elevation of IOP-increased GFAP protein levels but decreased Thy-1

protein levels in rat retinas.

GFAP levels increased by ~ 33% upon elevation of IOP (A). C: control eye and T: elevated IOP eye. Elevation of IOP Thy-1, a retinal ganglion cell marker, decreased with elevation of IOP (B). C: control eye and T: elevated IOP eye.
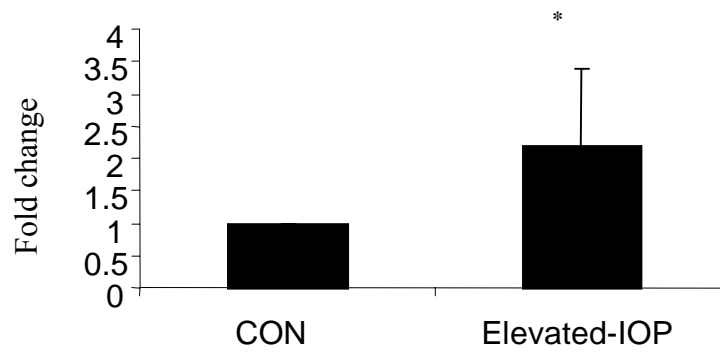
Fig. 25. Elevation of IOP-increased caspase-3 mRNA in rat retinas.

In five out eight rats tested, (63%), caspase-3 mRNA increased with elevation of IOP (220 ± 120%, P<0.05 vs. control retina).
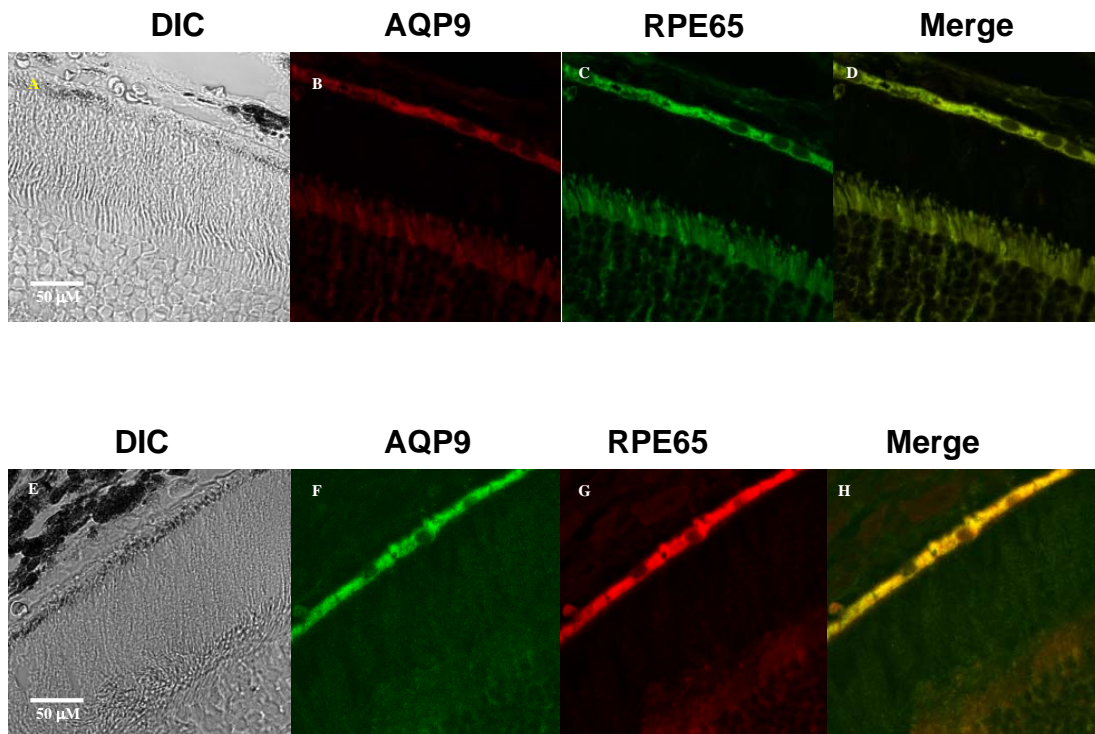
Fig. 26. Colocalization of AQP9 and RPE65 in rat retina.

Panels A and E are DIC images, panels B and F are AQP9 labeling using rabbit anti-AQP9 and goat anti-AQP9, respectively. Panels C and G are RPE65 labeling, and panels D and H represent merged images of AQP9 and RPE65 labeling (yellow). Scale bars: 50 μm.

DIC	AQP9	Thy-1	Merge
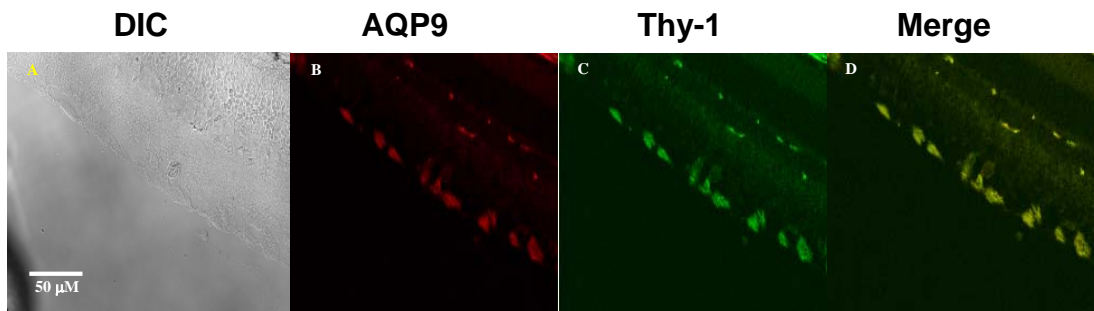
Fig. 27. Colocalization of AQP9 (red) and Thy-1 (green) in rat retina.

Panel A is a DIC image, panel B is AQP9 labeling using rabbit anti-AQP9, panel C is Thy-1 labeling, and panel D represents merged images of AQP9 and Thy-1 labeling. Scale bars: 50 μm.
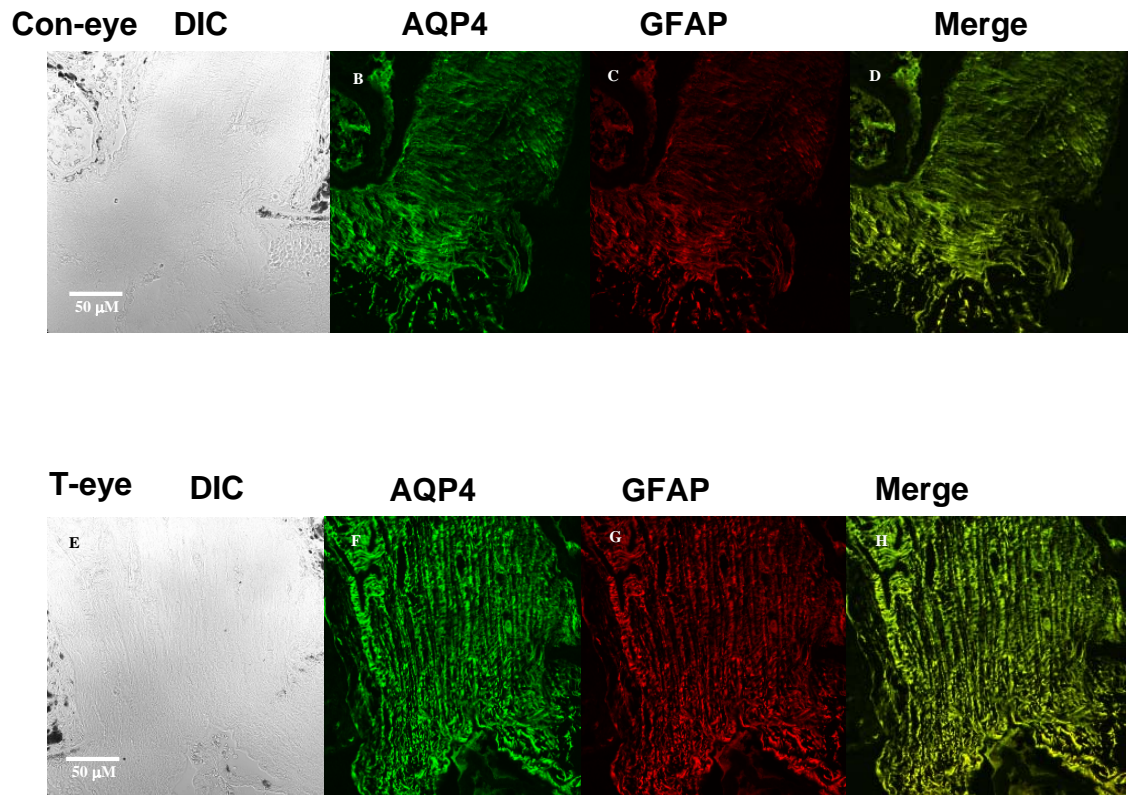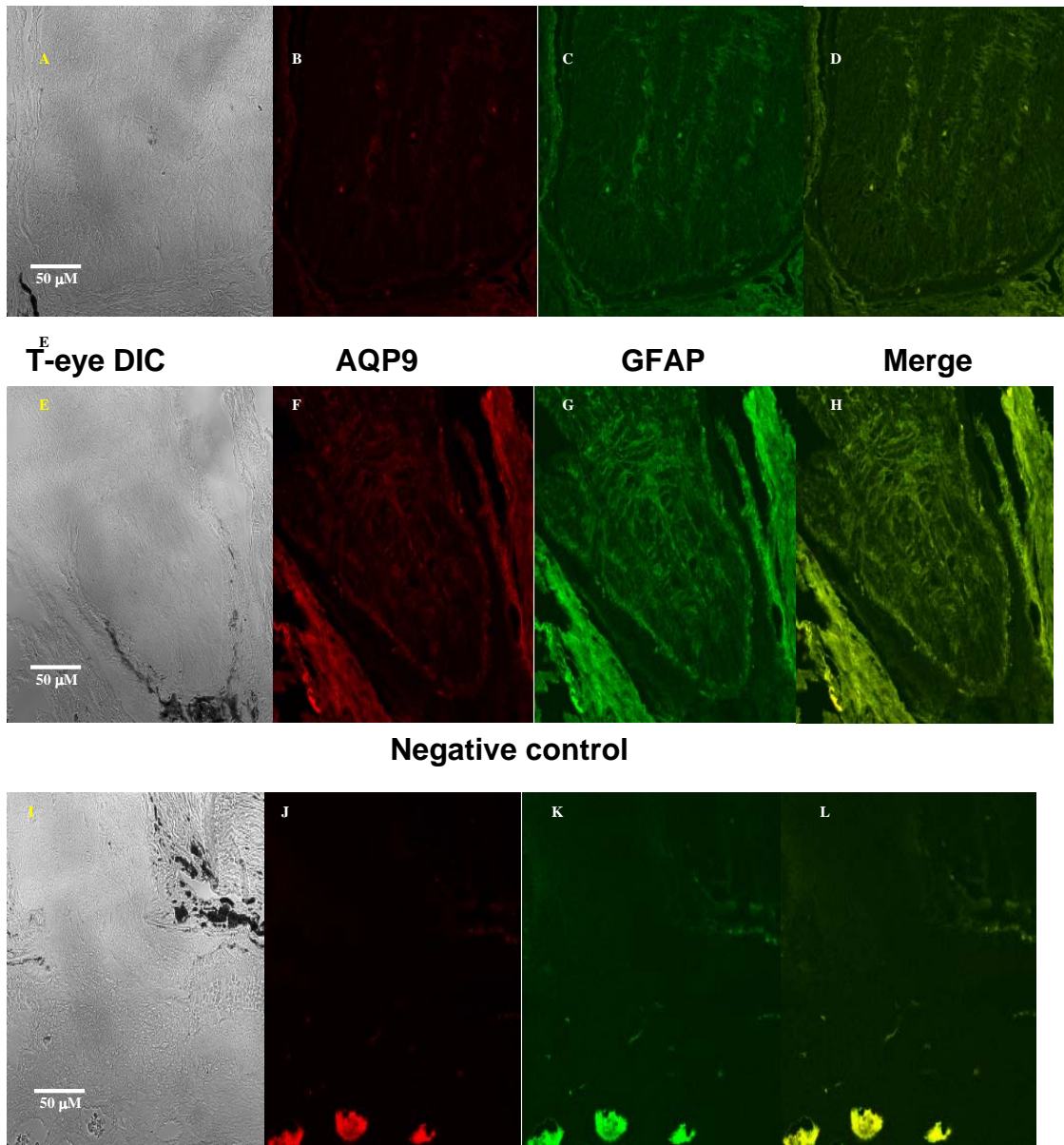
Fig. 28. Expression of immunoreactive AQP4 (green) and glial fibrillary acidic protein (GFAP, red) in the optic nerve of rats exposed to experimentally elevated IOP (T)(Morrison model of glaucoma; Panels E–H) and their contralateral controls (C)(Panels A–D).

A representative figure of the optic nerve is shown for one rat exposed to >500 mmHg days of IOP elevation. Panels A and E are DIC images, panels B and F represent AQP4 labeling, panels C and G represent GFAP labeling, and panels D and H represent merged images of AQP4 and GFAP labeling (yellow). Scale bars: 50 μm.

T-eye DIC   **AQP9**   **GFAP**   **Merge**

Negative control

Fig. 29. Expression of immunoreactive AQP9 (red) and glial fibrillary acidic protein (GFAP, green) in the optic nerve of rats exposed to experimentally elevated IOP. (T)(Morrison model of glaucoma; Panels E–H) and their contralateral controls (C)(Panels A–D).

A representative figure of the optic nerve is shown for one rat exposed to >500 mmHg days of IOP elevation. Panels A and E are DIC images, panels B and F are AQP9 labeling, panels C and G are GFAP labeling, and panels D and H are merged images of AQP9 and GFAP labeling (yellow). Panels I-L are negative control without primary antibodies. Scale bars: 50 μm.

| C-eye DIC | AQP9 | AQP4 | Merge |

| T-eye DIC | AQP9 | AQP4 | Merge |
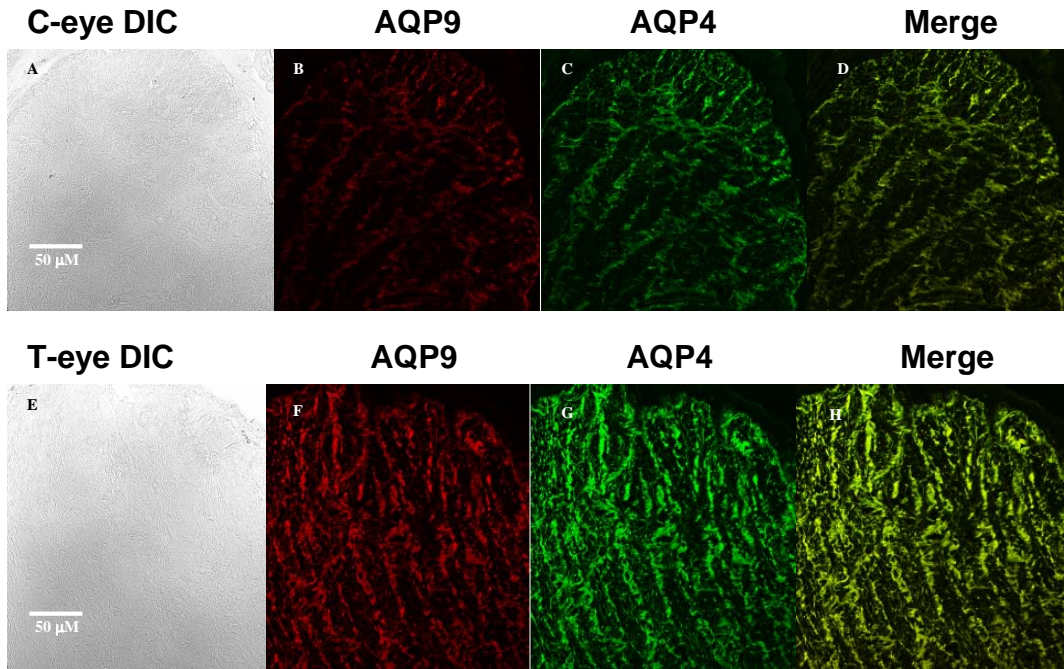
Fig. 30. Colocalization of immunoreactive AQP4 (green) and AQP9 (red) in the optic nerve of rats exposed to experimentally elevated IOP (T)(Morrison model of glaucoma; Panels E–H) and their contralateral controls (C)(Panels A–D).

A representative figure of the optic nerve is shown for one rat exposed to >500 mmHg days of IOP elevation. Panels A and E are DIC images, panels B and F are AQP9 labeling, panels C and G are AQP4 labeling, and panels D and H are merged images of AQP9 and AQP4 labeling (yellow). Scale bars: 50 μm.

C-eye DIC	AQP4	GS	Merge

T-eye DIC	AQP4	GS	Merge
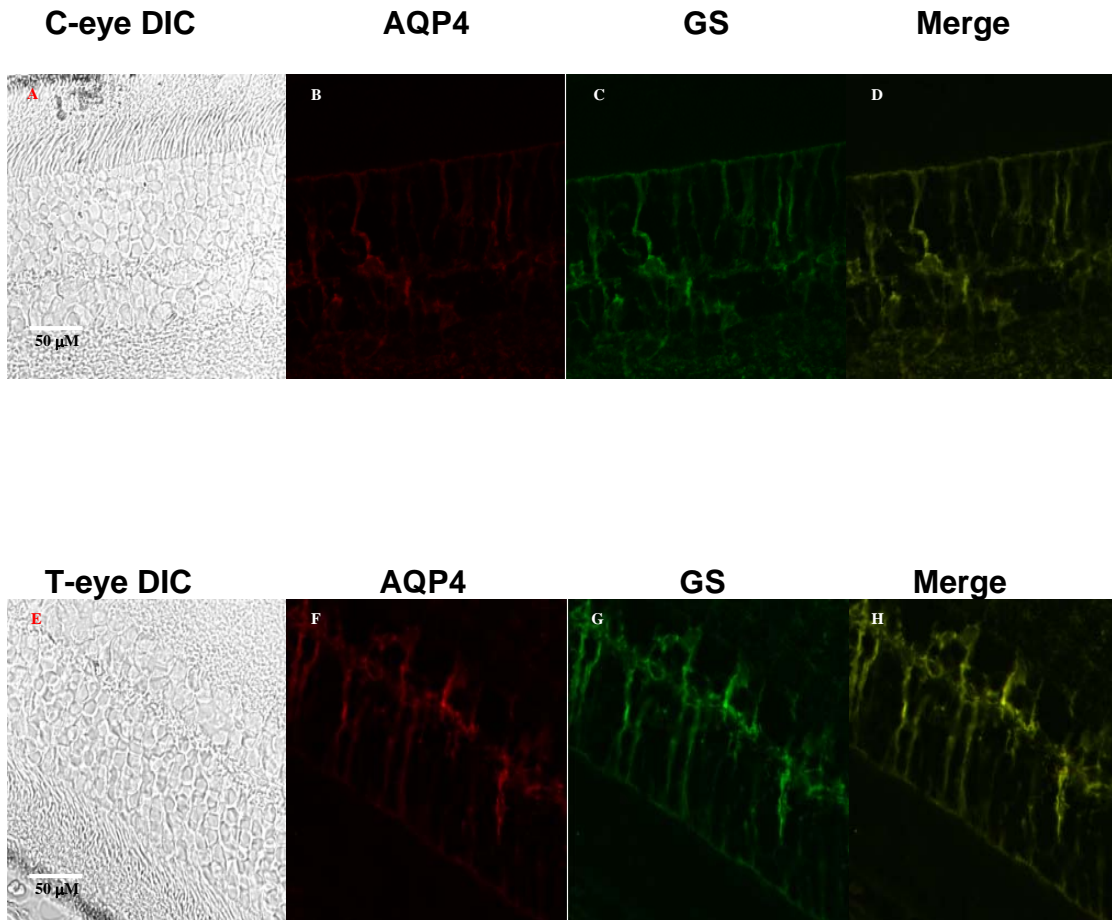
Fig. 31. Colocalization of immunoreactive AQP4 (red) and glutamine synthetase (a Müller cell marker, green) in retinas of rats exposed to experimentally elevated IOP (T)(Morrison model of glaucoma; Panels E–H) and their contralateral controls (C)(Panels A–D).

Panels A and E are DIC images, panels B and F are AQP4 labeling, panels C and G are glutamine synthetase labeling, and panels D and H are merged images of AQP4 and glutamine synthetase labeling (yellow). Scale bars: 50 μm.
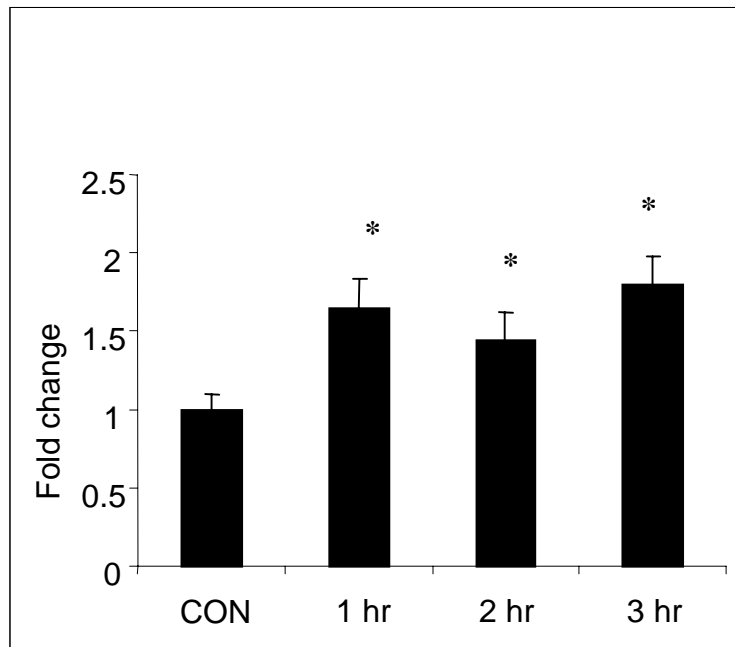
Fig. 32. Effect of hypoxia on AQP-9 mRNA in RGC-5 cells.

After exposure to hypoxia for the indicated periods (from 1 to 3 h), cells were processed for RT-PCR. β-actin was used as an internal control for these experimental conditions. Hypoxia increased AQP9 expression in rat retina by 70% (N=5, P<0.05 vs. control).
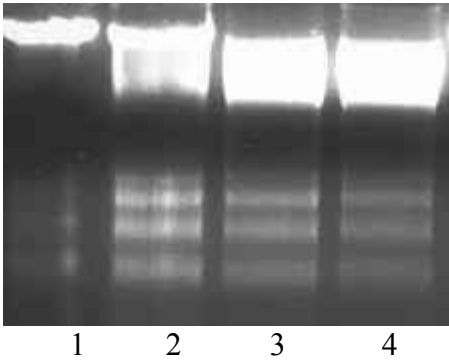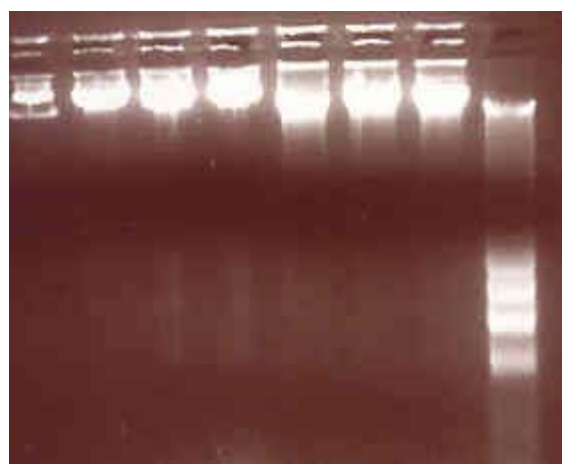
Fig. 33. DNA fragmentation after hypoxia treatment.

RGC-5 cells were incubated in serum-free medium during hypoxia treatment. 1: Control, SF for 24 hours. 2: hypoxia treatment for 12 hours. 3: hypoxia treatment for 16 hours. 4: hypoxia treatment for 24 hours. Each lane was loaded with 20 μg DNA.

Fig. 34. DNA fragmentation after hypoxia treatment with drugs.

RGC-5 cells were incubated in serum-free medium for 24 hours with or without hypoxia treatment. 1: Control, SF for 24 hours. 2: Vehicle (methanol, 0.1 % v/v) for 24 hours. 3: CIN (40 μM) for 24 hours. 4: Phloretin (60 μM) for 24 hours. 5: Vehicle (methanol, 0.1 % v/v) with hypoxia for 24 hours. 6: CIN (40 μM) with hypoxia for 24 hours. 7: Phloretin (60 μM) with hypoxia for 24 hours. 8: Serum with hypoxia treatment for 24 hours. Each lane was loaded with 10 μg DNA.
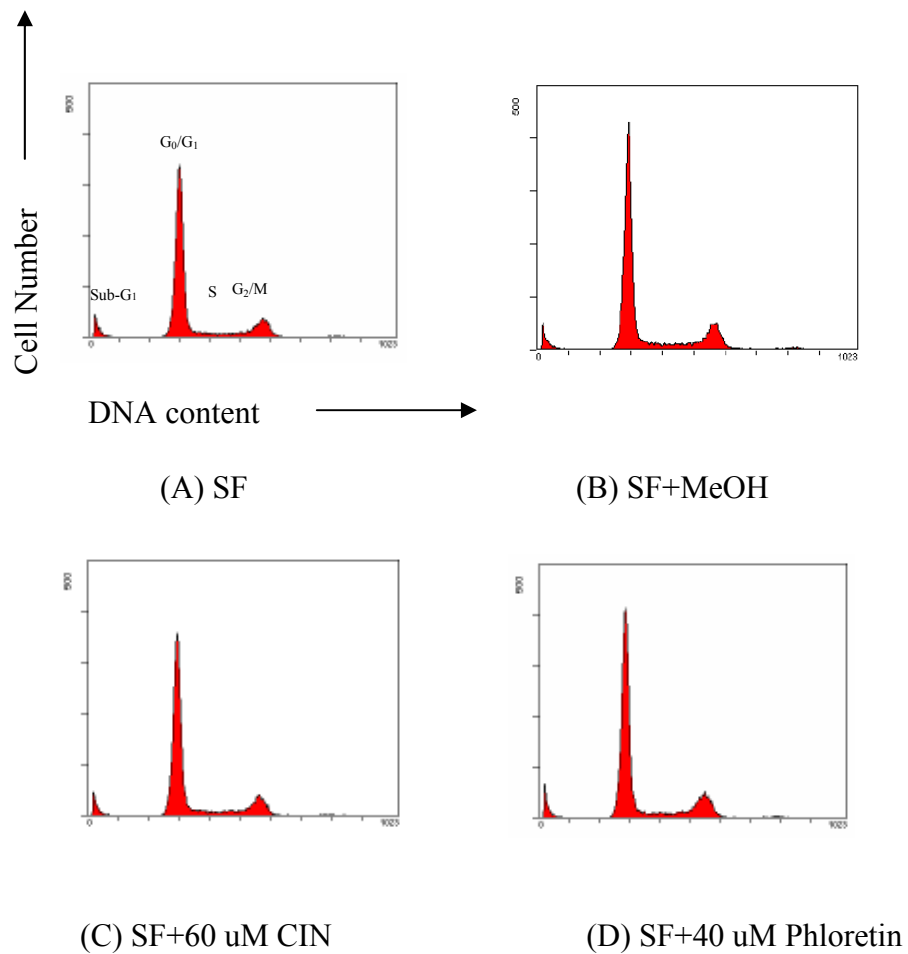
Fig. 35. RGC-5 cells under 24-hour serum-free conditions with different treatments.

Results from fluorescence-activated cell sorting (FACS) analysis. The life cycle of cells is divided into four stages – Gap (G_0, quiescence and G_1, main period of cell growth); Synthesis (S, DNA replication); G2, preparation for mitosis; Mitosis (M, mitosis and cell division). Growth factor withdrawal is known to cause apoptosis. Apoptotic cells have decreased cell sizes and lowered DNA contents. Serum-free (SF) in (A) is the control. Cells were treated with vehicle for 24 hours (B). Cells were treated with CIN for 24 hours (C). Cells were treated with Phloretin for 24 hours (D). There are no significant differences among these treatments.
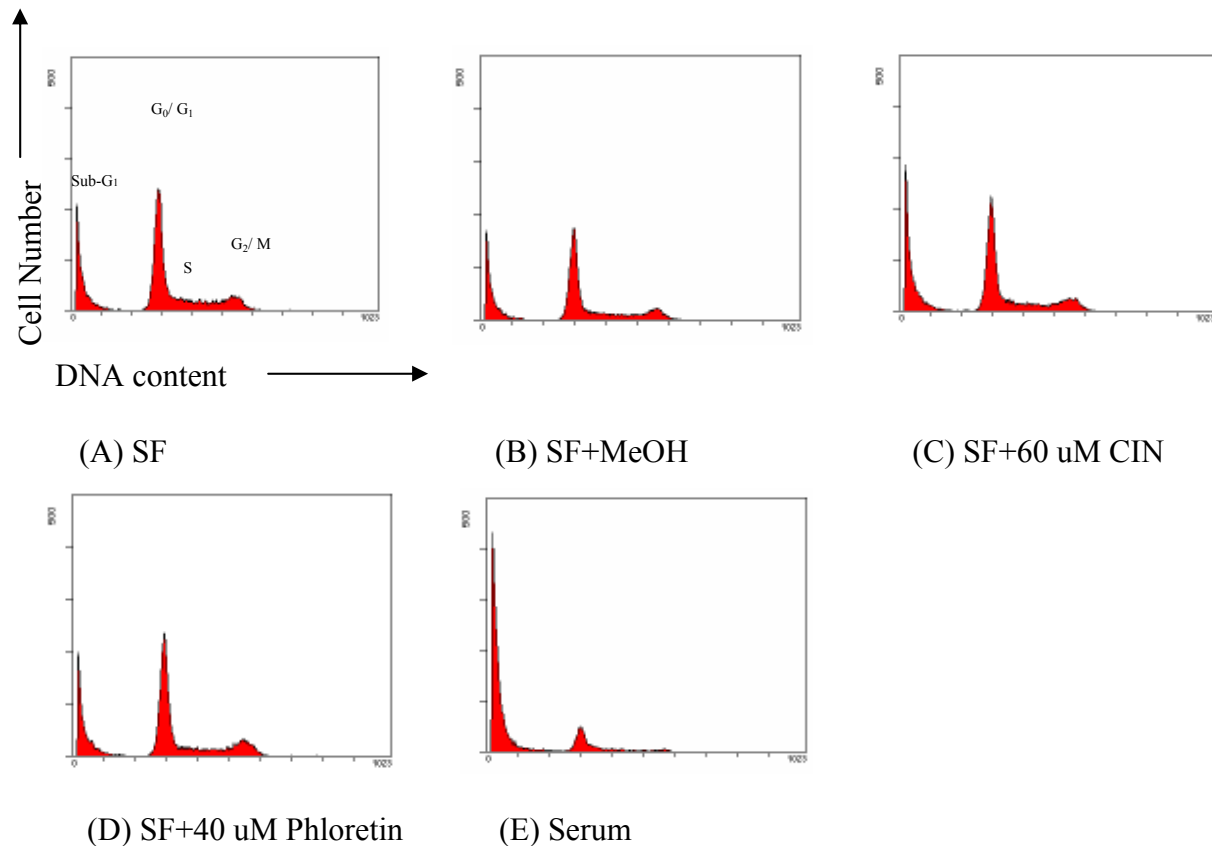
Fig. 36. RGC-5 cells under 24-hour hypoxia conditions with different treatments.

Results from fluorescence-activated cell sorting (FACS) analysis. The life cycle of cells is divided into four stages - Gap (G_0, quiescence and G_1, main period of cell growth); Synthesis (S, DNA replication); G2, preparation for mitosis; Mitosis (M, mitosis and cell division). Growth factor withdrawal is known to cause apoptosis. Apoptotic cells have decreased cell sizes and lowered DNA contents. Serum-free (SF) in (A) is the control. Cells were treated with vehicle for 24 hours (B). Cells were treated with CIN for 24 hours (C). Cells were treated with Phloretin for 24 hours (D). Cells were treated with serum (E) There are no significant differences among these treatments except serum-treated.
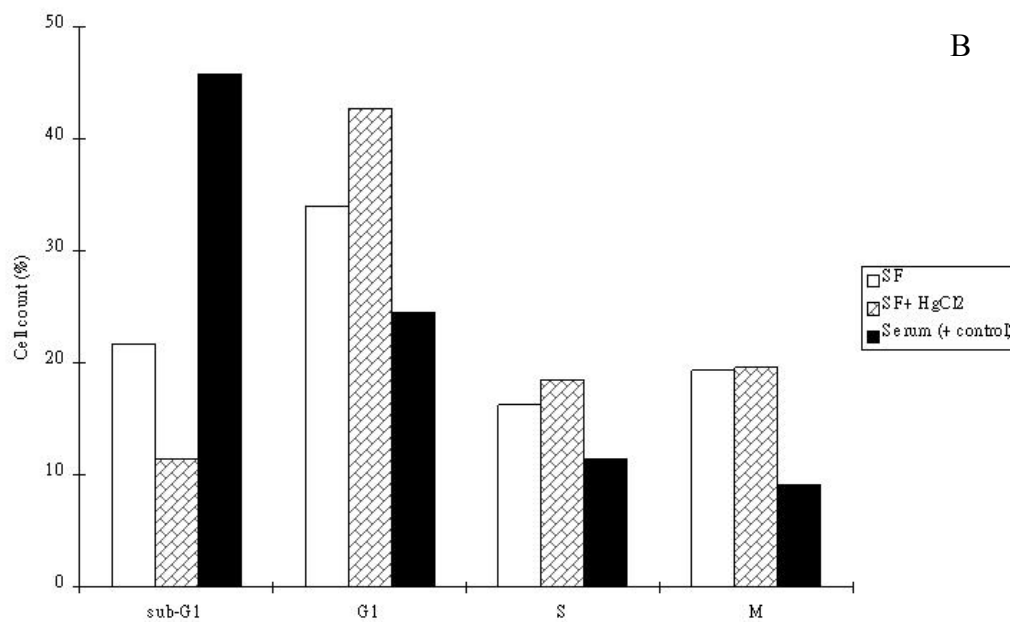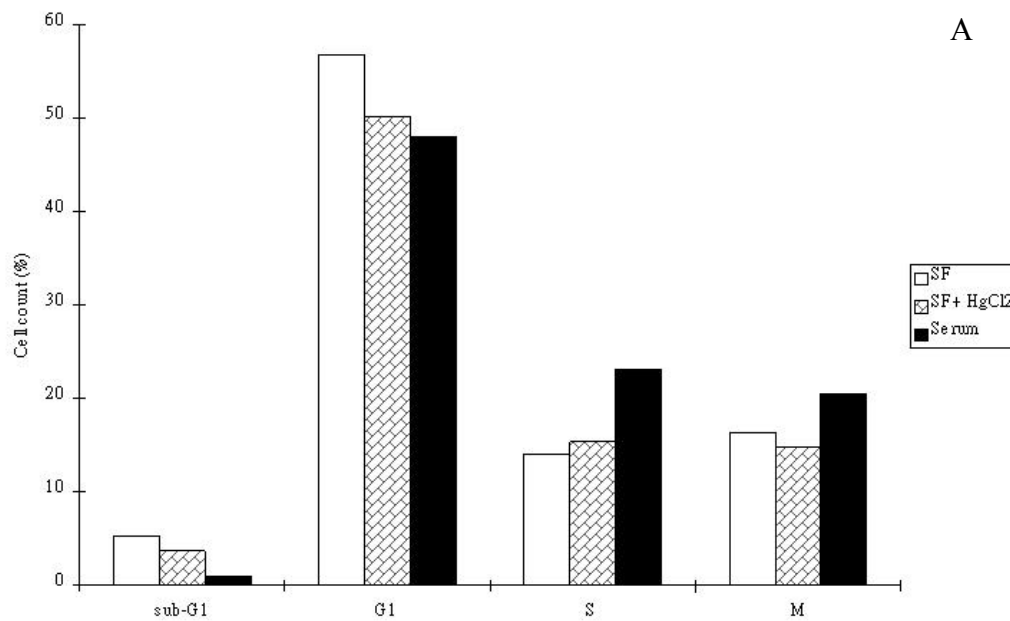
Fig. 37. Results from fluorescence-activated cell sorting (FACS) analysis with

HgCl$_2$.

(A). RGC-5 cell profile under 24-hr normal condition without serum (SF), with aquaporin inhibitor (HgCl$_2$), and with serum. (B). RGC-5 cell profile under 24-hr hypoxia condition without serum (SF), with aquaporin inhibitor (HgCl$_2$), and with serum.
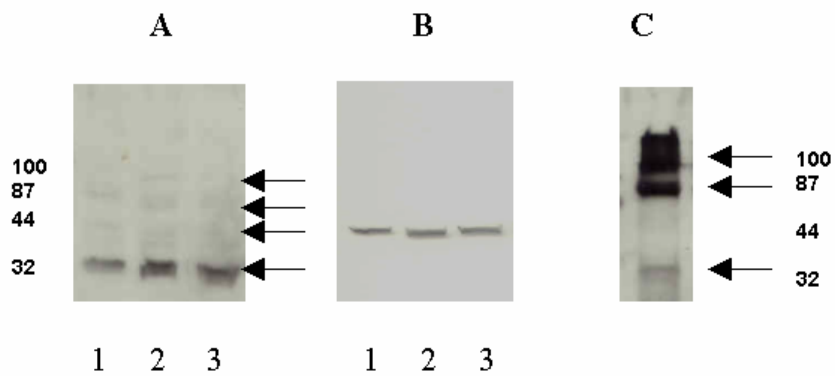
Fig. 38. Mg132, a proteasomal inhibitor, increased AQP4 protein levels.

After incubation with Mg132 for 4 hrs, the cells were processed for Western blotting. (A): Western blotting against AQP4. A dominant protein of 32 kDa and other faint bands (37, 87, 100 kDa) are observed in U373MG. Mg132 increased the 32 kDa isoform significantly (lane 1: con, lane 2: Mg132, and lane 3: lactacystin). (B): The membrane in A was stripped and re-probed with anti α-tubulin antibodies for normalization. (C): affinity purified ubiquitinated proteins are enriched in 87 and 100 kDa proteins that are recognized by AQP4 antibodies.
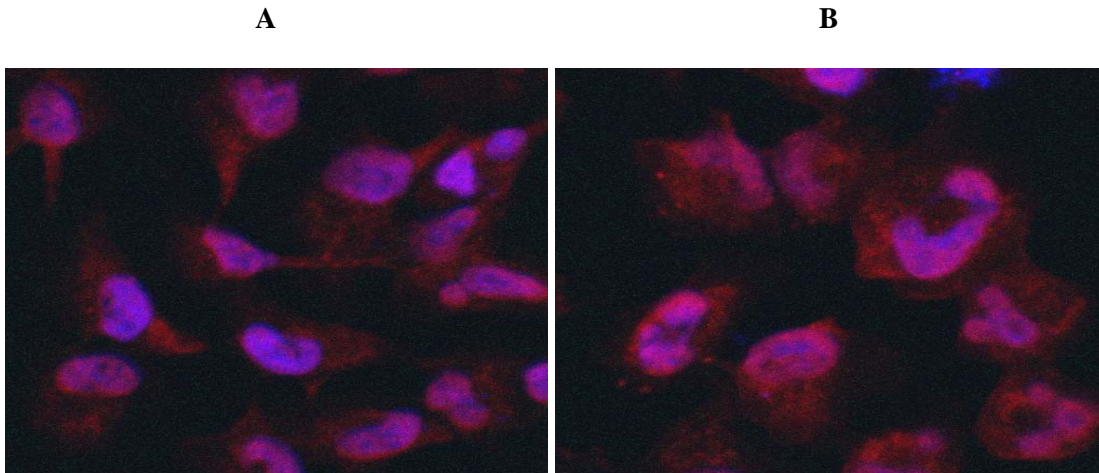
A   **B**

Fig. 39. Mg132, a proteasomal inhibitor, increased AQP4 protein levels as judged

by immunohistochemistry.

Immunofluorescent (IF) staining was used to detect the expression and localization of AQP4 in U373MG astrocytoma cells, which were treated with vehicle (DMSO, A) and 10 μM proteasome inhibitor, MG132 (B), for 6 hours. (Red: aquaporin 4 stained by Alexa 633; blue: nuclei stained by DAPI).
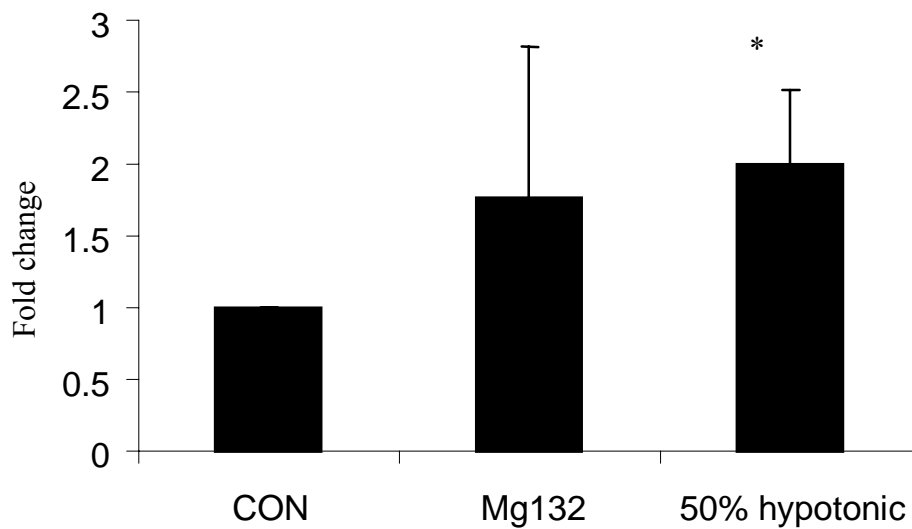
Fig. 40. Mg132, a proteasomal inhibitor, had no significant effect on AQP4 mRNA

levels.

After incubation with Mg132 for the indicated periods (4 hours), cells were processed for Q-PCR. Beta-actin was used as an internal control for these experimental conditions. Hypotonic shock (50%) doubled AQP4 expression whereas Mg132 did not cause significant changes (N=3, *P<0.05 vs. control).
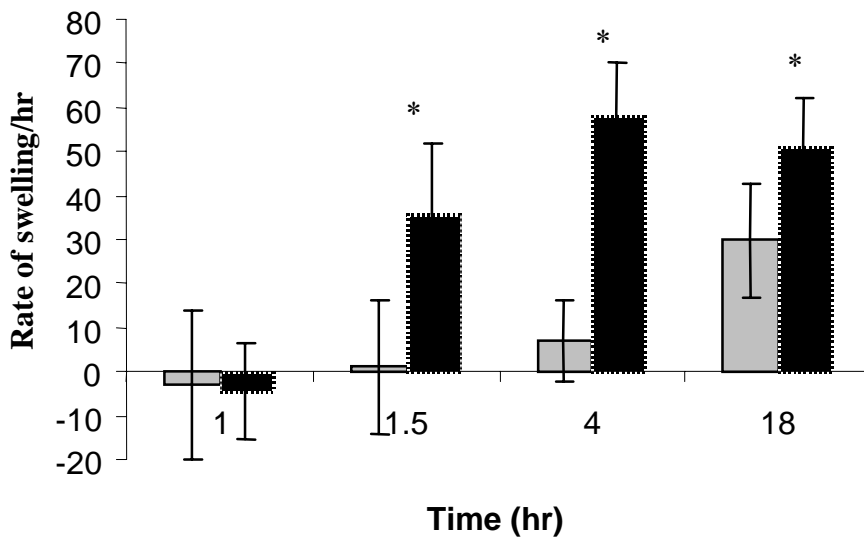
Fig. 41: Mg132, a proteasomal inhibitor, increased rate of cellular swelling upon a

hypotonic shock.

U373MG astrocytoma cells were labeled with fura-2 (3 μM) and pretreated with Mg132 (10 μM) for different time points, and volume changes were followed measuring fluorescence at 360 nm. The rate of swelling was calculated based on the difference of fluorescence readings after shock/time (N=3, P<0.05 vs. DMSO-treated).
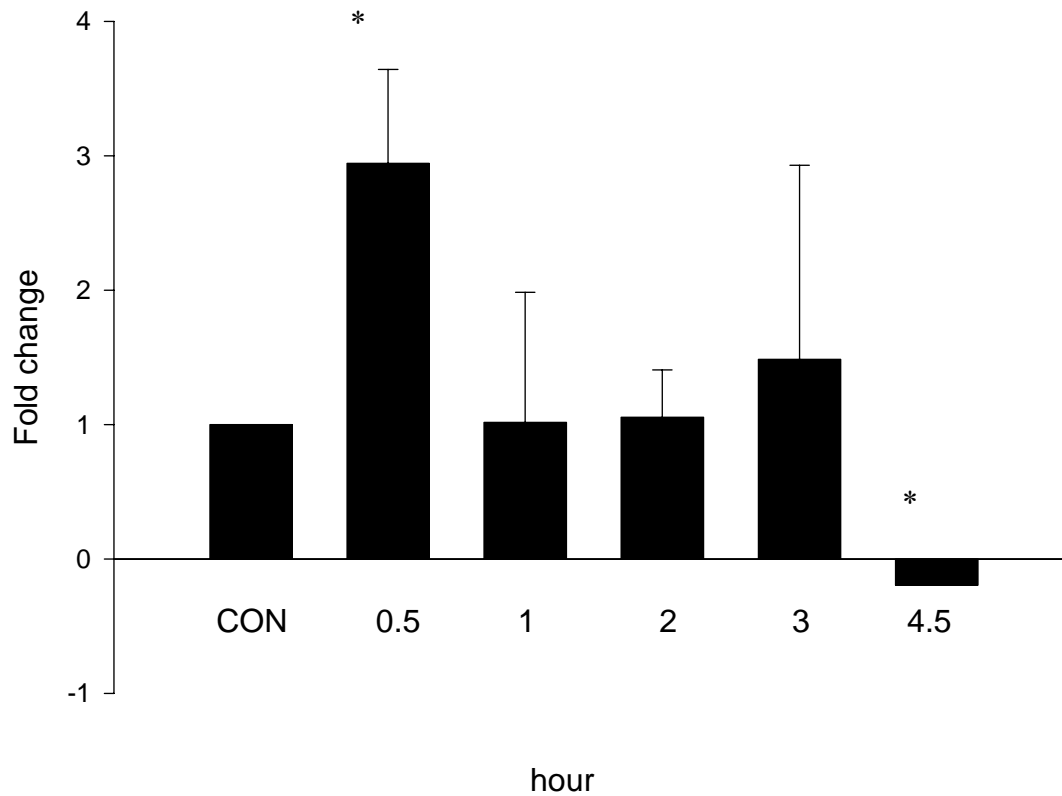
Fig. 42. Effect of hypotonic shock on AQP-9 mRNA in ARPE-19 cells.

After exposure to hypotonic solution for the indicated periods (0.5, 1, 2, 3 or 4.5 hours), cells were processed for RT-PCR. Beta-actin was used as an internal control for these experimental conditions. Hypotonic shock increased AQP9 expression at 0.5 and 3 hour period but decreased at 4.5 hour period ($P<0.05$ vs. control).
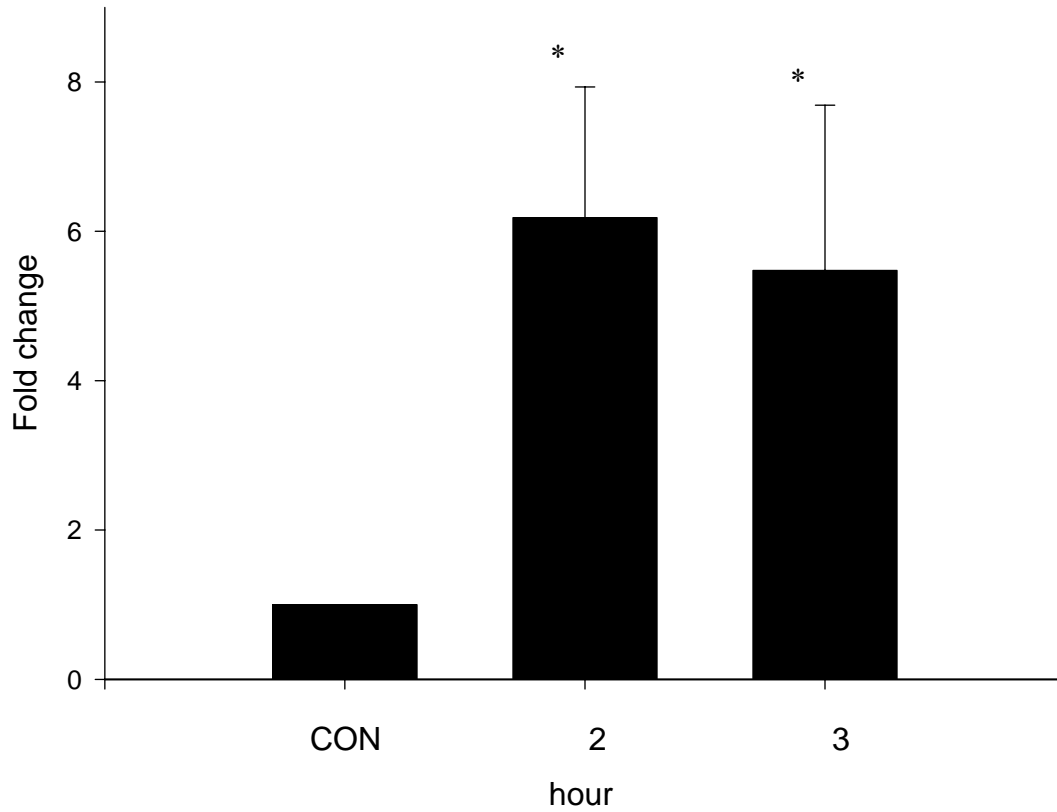
Fig. 43. Effect of hypoxia on AQP-9 mRNA in ARPE-19 cells.

After exposure to hypoxia for the indicated periods (two or three hours), cells were processed for RT-PCR. Beta-actin was used as an internal control for these experimental conditions. Hypoxia increased AQP9 expression. (P<0.05 vs. control)
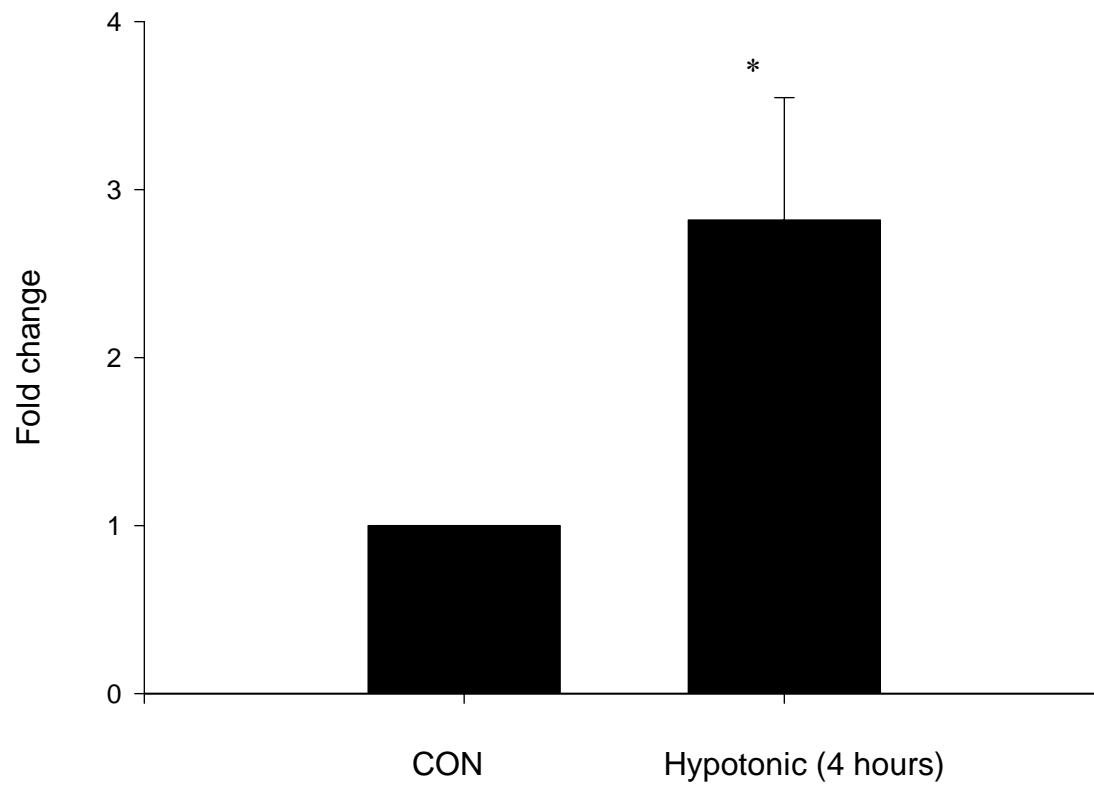
Fig. 44. Effect of hypotonic shock on AQP-9 mRNA in RGC-5 cells.

After exposure to hypotonic solution for four hours, cells were processed for RT-PCR. Beta-actin was used as an internal control for these experimental conditions. Hypotonic shock increased AQP9 expression ($P<0.05$ vs. control).

Table 1. Primer sequences of gene specific forward (sense) and reverse (anti-sense) with corresponding product sizes.

Primers		5'->3'	Sample	Product size (bp)
rAQP9	Sense	CTCAGTCCCAGGCTCTTCAC	Retina	184
	Anti-S	ATGGCTCTGCCTTCATGTCT		
	Sense	TTGGAAGGATGGAGTGGTTC	RGC-5	401
	Anti-S	AGTGAAGAGCCTGGGACTGA		
hAQP9	Sense	AGCCACCTCTGGTCTTGCTA	ARPE19	167
	Anti-S	ATGTAGAGCATCCCCTGGTG		
rAQP4	Sense	CGGTTCATGGAAACCTCACT	Retina	191
	Anti-S	CATGCTGGCTCCGGTATAAT		
hAQP4	Sense	TTGCTTTGGACTCAGCATTG	U373MG	125
	Anti-S	CAATGCTGAGTCCAAAGCAA		
Caspase-3	Sense	ACGGTACGCGAAGAAAAGTGAC	Retina/RGC-5	282
	Anti-S	TCCTGACTTCGTATTTCAGGGC		
Beta-Actin	Sense	TGTGATGGTGGGAATGGGTCAG	Retina/RGC-5	514
	Anti-S	TTTGATGTCACGCACGATTTCC		
S15	Sense	TTCCGCAAGTTCACCTACC	U373MG/ RGC-5/ARPE19	361
	Anti-S	CGGGCCGGCCATGCTTTACG		

Table 2. Optimized running conditions of gene specific primers.

Primer	Sample	Denaturation (°C /sec)	Annealing (°C /sec)	Extension (°C /sec)	Number of cycles
rAQP9	Retina	95/30	60/30	72/60	45
	RGC-5	96/15	57/60	72/60	20
		96/16	60/60	72/60	25
hAQP9	ARPE 19	96/15	60/60	72/60	40
rAQP4	Retina	95/30	60/30	72/60	45
hAQP4	U373MG	96/15	60/30	72/45	40
Caspase-3	Retina	94/30	52/30	72/30	55
	RGC-5	94/30	52/30	72/30	40
Beta-Actin	Retina/RGC-5	95/60	60/60	72/120	25
S15	U373MG/ RGC-5/ARPE19	95/60	60/60	72/120	25

VITA

Personal Background	Ming-Hui Yang Taipei, Taiwan, R.O.C Daughter of Jui-Meng Yang and Yueh-Chu Chou Yang Married Yu-Chang Tyan, April 27, 2002.

Education	Bachelor of Science, Medical Technology, Kaohsiung Medical
	     University, Kaoshiung, 1996
	Bachelor of Science, Chemistry, University of Central
	     Oklahoma, Edmond, 2000
	Master of Science, Chemistry, University of Texas at Dallas,
	     Dallas, 2003
	Doctor of Philosophy, Chemistry, Texas Christian University,
	     Fort Worth, 2007

Experience	Medical Technologist, Po-Jen General Hospital, 1996-1997 Teaching Assistantship, University of Texas at Dallas, 2000-2002 Research Assistantship, National Cheng Kung University, 2003 Teaching Assistantship, Texas Christian University, 2003-2006

Publication

1. Y. C. Tyan, J. D. Liao, S. B. Jong, P. C. Liao, M. H. Yang, Y. W. Chang, R. Klauser, M. Himmelhaus, M. Grunze, *Journal of Biomedical Materials Research* **71A**: 90-97, 2004.
2. Y. C. Tyan, J. D. Liao, S. B. Jong, P. C. Liao, M. H. Yang, Y. W. Chang, R. Klauser, M. Himmelhaus, M. Grunze, *Journal of Materials Science: Materials in Medicine* **16**: 135-142, 2005.
3. Y. C. Tyan, S. B. Jong, J. D. Liao, P. C. Liao, M. H. Yang, C.Y. Liu, R. Klauser, M. Himmelhaus, M. Grunze, *Journal of Proteome Research* **4**: 748-757, 2005.
4. M. H. Yang, M. C. Biewer, *Tetrahedron Letters* **46**:349-351, 2005.
5. M. H. Yang, J. D. Liao, S. B. Jong, P. C. Liao, C. Y. Liu, M. C. Wang, M. Grunze, Y. C. Tyan, *Journal of Medical and Biological Engineering* **25**: 81-86, 2005.
6. Y. C. Tyan, M. H. Yang, P. C. Liao, J.D. Liao, S. B. Jong, C. Y. Liu, M. C. Wang, M. Grunze, *International Journal of Mass Spectrometry* **262**: 67-72, 2007.
7. M. H. Yang, Y. C. Tyan, S. B. Jong, Y. F. Huang, P. C. Liao, M. C. Wang, *Analytical & Bioanalytical Chemistry*, Accepted.
8. A. Dibas, M. H. Yang, J. Bobich, T. Yorio, *Pharmacological Research*, Accepted.

ABSTRACT

A WATER CHANNEL (AQP9) IN RETINAL GANGLION CELL APOPTOSIS AND
GLAUCOMA

By Ming-Hui Yang, Ph.D., 2007
Department of Chemistry
Texas Christian University

Dissertation Advisor: Joseph A. Bobich, Professor of Chemistry

Aquaporin-9 (AQP9) is a neutral channel, permeable to water, glycerol, and a number of solutes. The presence of AQP9 in retinal ganglion cells (RGCs) was confirmed. AQP9 and a number of proteins responded differently to two animal models of glaucoma. Inhibition of AQP9 may protect RGCs under hypoxia conditions. The expression of AQP9 responded to hypotonic shock in a time-dependent matter. Aquaporin in the RGCs and astrocytes may play a role in cell survival or death, depending on the stimulus. Under some conditions, increasing AQP4 may also be protective, such as in vasogenic edema, whereas under cytotoxic edema it becomes detrimental. This work describes possible physiological and pathophysiological roles of AQP9. Aquaporin-4 is expressed in astrocytes, which are considered RGCs supportive cells. AQP4 may be targeted by the proteasome system, so inhibition of this pathway may be protective in vasogenic brain edema.